



Steel Bridge Design Handbook

.....

APPENDIX

Design Example 3: Three-Span
Continuous Horizontally Curved
Composite Steel I-Girder Bridge

February 2022



.....
**Smarter.
Stronger.
Steel.**

© AISC 2022

by

American Institute of Steel Construction

*All rights reserved. This book or any part thereof must not be reproduced in any form without the written permission of the publisher.
The AISC and NSBA logos are registered trademarks of AISC.*

The information presented in this publication has been prepared following recognized principles of design and construction. While it is believed to be accurate, this information should not be used or relied upon for any specific application without competent professional examination and verification of its accuracy, suitability and applicability by a licensed engineer or architect. The publication of this information is not a representation or warranty on the part of the American Institute of Steel Construction, its officers, agents, employees or committee members, or of any other person named herein, that this information is suitable for any general or particular use, or of freedom from infringement of any patent or patents. All representations or warranties, express or implied, other than as stated above, are specifically disclaimed. Anyone making use of the information presented in this publication assumes all liability arising from such use.

Caution must be exercised when relying upon standards and guidelines developed by other bodies and incorporated by reference herein since such material may be modified or amended from time to time subsequent to the printing of this edition. The American Institute of Steel Construction bears no responsibility for such material other than to refer to it and incorporate it by reference at the time of the initial publication of this edition.

Printed in the United States of America

Foreword

The Steel Bridge Design Handbook covers a full range of topics and design examples to provide bridge engineers with the information needed to make knowledgeable decisions regarding the selection, design, fabrication, and construction of steel bridges. The Handbook has a long history, dating back to the 1970s in various forms and publications. The more recent editions of the Handbook were developed and maintained by the Federal Highway Administration (FHWA) Office of Bridges and Structures as FHWA Report No. FHWA-IF-12-052 published in November 2012, and FHWA Report No. FHWA-HIF-16-002 published in December 2015. The previous development and maintenance of the Handbook by the FHWA, their consultants, and their technical reviewers is gratefully appreciated and acknowledged.

This current edition of the Handbook is maintained by the National Steel Bridge Alliance (NSBA), a division of the American Institute of Steel Construction (AISC). This Handbook, published in 2021, has been updated and revised to be consistent with the 9th edition of the AASHTO LRFD Bridge Design Specifications which was released in 2020. The updates and revisions to various chapters and design examples have been performed, as noted, by HDR, M.A. Grubb & Associates, Don White, Ph.D., and NSBA. Furthermore, the updates and revisions have been reviewed independently by Francesco Russo, Ph.D., P.E., Brandon Chavel, Ph.D., P.E., and NSBA.

The Handbook consists of 19 chapters and 6 design examples. The chapters and design examples of the Handbook are published separately for ease of use, and available for free download at the NSBA website, www.aisc.org/nsba.

The users of the Steel Bridge Design Handbook are encouraged to submit ideas and suggestions for enhancements that can be implemented in future editions to the NSBA and AISC at solutions@aisc.org.

TECHNICAL REPORT DOCUMENTATION PAGE

<p>1. Title and Subtitle Steel Bridge Design Handbook, Appendix Design Example 3: Three-Span Continuous Horizontally Curved Composite Steel I-Girder Bridge</p>	<p>2. Report Date February 2022</p>
<p>3. Original Author(s) Julie Rivera, P.E. and Brandon Chavel, Ph.D., P.E. (HDR)</p>	<p>4. Revision Author(s) Michael A. Grubb, P.E (M.A. Grubb & Associates, LLC)</p>
<p>5. Sponsoring Agency Name and Address National Steel Bridge Alliance, a division of the American Institute of Steel Construction 130 E. Randolph, Suite 2000 Chicago, IL 60601</p>	<p>6. Revision Performing Organization Name and Address HDR, Inc. 301 Grant Street, Suite 1700 Pittsburgh, PA 15219</p>
<p>7. Supplementary Notes The previous edition of this Handbook was published as FHWA-HIF-16-002 and was developed to be current with the 7th edition of the AASHTO LRFD Bridge Design Specifications. This edition of the Handbook was updated to be current with the 9th edition of the AASHTO LRFD Bridge Design Specifications, released in 2020.</p>	
<p>8. Abstract Horizontally curved steel bridges present many unique challenges. Despite their challenges, curved girder bridges have become widespread and are commonly used at locations that require complex geometries and have limited right-of-way, such as urban interchanges. Some of the important issues that differentiate curved steel girders from their straight counterparts include the effects of torsion, flange lateral bending, their inherent lack of stability, and special constructability concerns. Also, the complex behavior of horizontally curved bridges necessitates the consideration of system behavior in the analysis.</p> <p>This design example illustrates the design calculations for a curved steel I-girder bridge, considering the Strength, Service, Fatigue and Constructability limit states in accordance with the AASHTO LRFD Bridge Design Specifications. Calculations are provided for design checks at critical girder locations, a bolted field splice design, a cross-frame member design, shear connector design, and a bearing stiffener design.</p>	
<p>9. Keywords Curved I-Girder Bridge, Bridge Design, LRFD, Constructability, Bolted Field Splice, Cross- Frame</p>	<p>10. AISC Publication No. B954-22</p>

Steel Bridge Design Handbook

Design Example 3: Three-Span Continuous Horizontally Curved Composite Steel I-Girder Bridge

Table of Contents

1.0	INTRODUCTION	1
2.0	OVERVIEW OF LRFD ARTICLE 6.10.....	3
3.0	DESIGN PARAMETERS	5
4.0	GENERAL STEEL FRAMING CONSIDERATIONS.....	6
4.1	Span Arrangement	6
4.2	Girder Spacing	6
4.3	Girder Depth	7
4.4	Cross-Section Proportions	8
4.5	Cross-Frames	11
4.6	Field Section Sizes.....	12
5.0	FINAL DESIGN	16
5.1	AASHTO LRFD Limit States.....	16
5.1.1	Service Limit State (Articles 1.3.2.2 and 6.5.2).....	16
5.1.2	Fatigue and Fracture Limit State (Articles 1.3.2.3 and 6.5.3)	16
5.1.3	Strength Limit State (Articles 1.3.2.4 and 6.5.4).....	16
5.1.4	Extreme Event Limit State (Articles 1.3.2.5 and 6.5.5).....	17
5.2	Loads.....	17
5.2.1	Noncomposite Dead Load (DC_1).....	17
5.2.2	Deck Placement Sequence	17
5.2.3	Superimposed Dead Load (DC_2)	18
5.2.4	Future Wearing Surface (DW).....	20
5.2.5	Live Load (LL+IM)	20
5.3	Vehicular Centrifugal Force Computation (CE).....	21
5.4	Load Combinations.....	24
6.0	ANALYSIS.....	28
6.1	Three-Dimensional Finite Element Analysis.....	29

6.1.1	Bearing Orientation.....	30
6.1.2	Live Load Analysis.....	30
6.2	Analysis Results.....	31
7.0	DESIGN.....	41
7.1	General Design Considerations.....	41
7.1.1	Flanges.....	41
7.1.2	Webs.....	42
7.1.3	Shear Connectors.....	42
7.1.4	Details (Fatigue Categories for Stiffeners, Cross-Frame Connection Plates, and Shear Studs).....	43
7.1.5	Wind Loading.....	44
7.1.5.1	Loading.....	44
7.1.5.2	Construction.....	45
7.1.6	Fit and Steel Erection.....	45
7.1.6.1	Fit.....	45
7.1.6.2	Erection.....	47
7.1.7	Deck Placement Sequence.....	47
7.2	Section Properties.....	48
7.2.1	Section G4-1 Properties – Span 1 Positive Moment.....	49
7.2.1.1	Effective Width of Concrete Deck.....	50
7.2.1.2	Elastic Section Properties: Section G4-1.....	50
7.2.1.3	Plastic Moment Neutral Axis: Section G4-1.....	52
7.2.2	Section G4-2 Properties – Support 2 Negative Moment.....	53
7.2.2.1	Elastic Section Properties: Section G4-2.....	53
7.2.3	Check of Minimum Negative Flexure Concrete Deck Reinforcement.....	56
7.3	Girder Check: Section G4-3, Shear at End Support (Article 6.10.9).....	58
7.3.1	Applied Shear.....	58
7.3.2	Shear Resistance.....	58
7.4	Girder Check: Section G4-1, Constructability (Article 6.10.3).....	60
7.4.1	Constructability of Top Flange.....	61
7.4.1.1	Deck Overhang Bracket Load.....	61

7.4.1.2	Curvature Effects	63
7.4.1.3	Top Flange Lateral Bending Amplification.....	64
7.4.1.4	Flexure in Top Flange (Article 6.10.3.2.1).....	67
7.4.2	Constructability of Bottom Flange.....	71
7.4.3	Constructability Shear Strength, Web.....	72
7.4.4	Constructability of the Deck	72
7.5	Girder Check: Section G4-1, Service Limit State (Article 6.10.4).....	73
7.5.1	Permanent Deformations (Article 6.10.4.2).....	73
7.5.2	Web Bend-Buckling.....	75
7.6	Girder Check: Section G4-1, Fatigue Limit State (Article 6.10.5).....	76
7.6.1	Fatigue in Bottom Flange.....	76
7.6.2	Special Fatigue Requirement for Webs	78
7.7	Girder Check: Section G4-1, Strength Limit State (Article 6.10.6)	80
7.7.1	Flexure (Article 6.10.6.2).....	80
7.7.1.1	Strength I Flexural Stress in Top and Bottom Flange.....	81
7.7.1.2	Top Flange Flexural Resistance in Compression.....	83
7.7.1.3	Bottom Flange Flexural Resistance in Tension	83
7.7.2	Web Flexural Resistance.....	85
7.7.3	Concrete Deck Stresses.....	85
7.8	Girder Check: Section G4-2, Constructability (Article 6.10.3).....	86
7.8.1	Constructability of Top Flange	87
7.8.2	Constructability of Bottom Flange.....	88
7.8.2.1	Bottom Flange Lateral Bending Amplification	88
7.8.2.2	Flexure in Bottom Flange (Article 6.10.3.2.1).....	89
7.9	Girder Check: Section G4-2, Service Limit State (Article 6.10.4).....	92
7.9.1	Permanent Deformations (Article 6.10.4.2).....	92
7.9.2	Web Bend-Buckling.....	93
7.10	Girder Check: Section G4-2, Fatigue Limit State (Article 6.10.5).....	96
7.10.1	Fatigue in Top Flange	96
7.10.2	Special Fatigue Requirement for Webs	98
7.11	Girder Check: Section G4-2, Strength Limit State (Article 6.10.6)	100

7.11.1	Flexure (Article 6.10.6.2).....	100
7.11.1.1	Strength I Flexural Stress in Top and Bottom Flange.....	100
7.11.1.2	Top Flange Flexural Resistance in Tension.....	104
7.11.1.3	Bottom Flange Flexural Resistance in Compression.....	105
7.11.2	Web Shear Strength (Article 6.10.9).....	107
7.11.2.1	Applied Shear.....	108
7.11.2.2	Shear Resistance	108
7.12	Bolted Field Splice.....	109
7.12.1	General.....	109
7.12.2	Bolt Resistance Calculation for the Service Limit State and Constructability ...	113
7.12.3	Bolt Resistance Calculations for the Strength Limit State.....	113
7.12.3.1	Bolt Shear Resistance (Article 6.13.2.7).....	114
7.12.3.2	Bearing Resistance of the Connected Material (Article 6.13.2.9)	114
7.12.3.3	Bolt Tensile Resistance (Article 6.13.2.10)	115
7.12.4	Flange Splice Design	116
7.12.4.1	General.....	116
7.12.4.2	Flange Splice Bolts	116
7.12.4.3	Moment Resistance.....	118
7.12.4.4	Flange Splice Plates	119
7.12.4.5	Bearing Resistance Check.....	127
7.12.4.6	Slip Resistance Check.....	129
7.12.4.7	Article 6.10.1.8 – Tension Flanges with Holes.....	131
7.12.5	Web Splice Design.....	131
7.12.5.1	General.....	131
7.12.5.2	Web Splice Bolts.....	132
7.12.5.3	Web Splice Plates	133
7.12.5.4	Bearing Resistance.....	137
7.12.5.5	Slip Resistance	138
7.13	Cross-Frame Member and Connection	139
7.13.1	Cross-Frame Diagonal Design.....	139
7.13.2	Cross-Frame Fatigue Check.....	142

7.13.3	Cross-Frame Welded Connection	144
7.14	Shear Connector Design	146
7.14.1	Shear Connector Design for Strength – Girder G4, Span 1	146
7.14.1.1	End of Span to Maximum Positive Live Load Moment Location....	147
7.14.1.2	Maximum Positive Live Load Moment Location to Adjacent Interior Support	149
7.14.2	Shear Connector Design for Fatigue – Girder G4, Span 1	151
7.14.2.1	Maximum Positive Moment Location	151
7.14.2.2	Interior Support Location (Support 2)	154
7.15	Bearing Stiffener Design.....	157
7.15.1	Minimum Thickness	158
7.15.2	Bearing Resistance.....	158
7.15.3	Axial Resistance.....	159
8.0	SUMMARY OF DESIGN CHECKS AND PERFORMANCE RATIOS.....	162
8.1	Maximum Positive Moment Region, Span 1 (Section G4-1).....	162
8.2	Interior Support, Maximum Negative Moment (Section G4-2)	162
8.3	End Support (Section G4-3).....	163
9.0	REFERENCES	164

LIST OF FIGURES

Figure 1: Typical Bridge Cross-Section	7
Figure 2: Framing Plan	14
Figure 3: Girder Elevation	15
Figure 4: Deck Placement Sequence.....	19
Figure 5: Vehicular Centrifugal Force Wheel-Load Reactions	21
Figure 6: Effects of Superelevation	23
Figure 7: Sketch of I-girder Cross-Section at Section G4-1	50
Figure 8: Sketch of I-girder cross-section at Section G4-2.....	53
Figure 9 Deck Overhang Bracket Loading	62
Figure 10 Bolted Field Splice in Span 2 of G4 – Elevation View.....	111
Figure 11 Bolted Field Splice in Span 2 of G4 – Top Flange.....	112
Figure 12 Bolted Field Splice in Span 2 of G4 – Bottom Flange	112
Figure 13 Bottom Flange Splice – Assumed Block Shear Failure Planes in the Splice Plates ..	123
Figure 14 Bottom Flange Splice – Assumed Block Shear Failure Planes in the Flange on the Right-Hand Side of the Splice	124
Figure 15 Assumed Block Shear Failure Planes for the Web Splice Plates	136

LIST OF TABLES

Table 1 Girder G1 Unfactored Shears by Tenth Point.....	32
Table 2 Girder G2 Unfactored Shears by Tenth Point.....	33
Table 3 Girder G3 Unfactored Shears by Tenth Point.....	34
Table 4 Girder G4 Unfactored Shears by Tenth Point.....	35
Table 5 Girder G1 Unfactored Major-Axis Bending Moments by Tenth Point.....	36
Table 6 Girder G2 Unfactored Major-Axis Bending Moments by Tenth Point.....	37
Table 7 Girder G3 Unfactored Major-Axis Bending Moments by Tenth Point.....	38
Table 8 Girder G4 Unfactored Major-Axis Bending Moments by Tenth Point.....	39
Table 9 Selected Girder G4 Unfactored Major-Axis Bending Moments	40
Table 10 Selected Girder G4 Unfactored Shears by Tenth Point	40
Table 11 Section G4-1: Steel Only Section Properties.....	50
Table 12 Section G4-1: $3n=22.68$ Long-term Composite Section Properties	51
Table 13 Section G4-1: $n=7.56$ Short-term Composite Section Properties.....	51
Table 14 Section G4-2: Steel Only Section Properties.....	54
Table 15 Section G4-2: $3n=22.68$ Composite Section Properties with Transformed Deck	55
Table 16 Section G4-2: $n=7.56$ Composite Section Properties with Transformed Deck	55
Table 17 Section G4-2: Long-term ($3n$) Composite Section Properties with Longitudinal Steel Reinforcement.....	56
Table 18 Section G4-2: Short-term (n) Composite Section Properties with Longitudinal Steel Reinforcement.....	56

1.0 INTRODUCTION

Horizontally curved steel bridges present many unique challenges. Despite these challenges, curved girder bridges have become widespread and are commonly used at locations that require complex geometries and have limited right-of-way, such as urban interchanges. Some of the important issues that differentiate curved steel girders from their straight counterparts include the effects of torsion, flange lateral bending, their inherent lack of stability, and special constructability concerns. Also, the complex behavior of horizontally curved bridges necessitates the consideration of system behavior in the analysis.

Curved steel girder bridges have been built in the United States since the 1950s. Curved girder bridges represent a significant percentage of the total steel bridge market.

Horizontally curved girders typically offer certain advantages over kinked or chorded girders. Some of these advantages include:

- Overall simplification of the structure by allowing curved girders to follow the roadway alignment;
- Use of longer spans and reduced number of intermediate permanent supports;
- Continuity over several spans permitting simplified framing, efficient use of material, increased vertical clearance, and fewer joints;
- Simplified forming of the deck with a constant deck overhang;
- Simpler reinforcing bar schedule; and
- Improved aesthetics.

However, horizontally curved girder bridges require special attention during design and construction. Fabrication can require additional labor or material, and shipping costs may be greater than for a straight girder. Due to torsional behavior during lifting of the girders during erection, additional lifting points and temporary supports may be required, leading to increased costs. Nevertheless, curved girder bridges are typically more economical than kinked or chorded girder bridges that are on a horizontally curved alignment.

Another unique concern for curved girder bridges is the classification of the cross-frames as primary load-carrying members according to the governing design specifications. Also, bottom-flange level lateral bracing, when provided, may need to be considered as primary members. As such, these elements require greater attention during bridge inspections.

Starting with the 2005 Interims to the 3rd Edition, the AASHTO *LRFD Bridge Design Specifications* [1], referred to hereafter as the *AASHTO LRFD BDS*, have provided a unified design approach for both straight and horizontally curved girders within a single design specification. It should be noted that kinked (chorded) girders exhibit similar behavior to horizontally curved girders and should be treated as horizontally curved girders with respect to the AASHTO specifications.

The example calculations provided herein comply with the 9th Edition AASHTO LRFD BDS, but the analysis described herein was not performed as part of this design example. The analysis results

and general superstructure details contained within this design example were taken from the design example published as part of the National Cooperative Highway Research Program (NCHRP) Project 12-52 published in 2005, entitled “AASHTO-LRFD Design Example: Horizontally Curved Steel I-Girder Bridge, Final Report” [2].

2.0 OVERVIEW OF LRFD ARTICLE 6.10

The design of I-section flexural members is covered within Article 6.10 of the *AASHTO LRFD BDS (9th Edition, 2020)*. The provisions of Article 6.10 are organized to correspond to the general flow of the calculations necessary for the design of I-section flexural members. Each of the sub-articles of Article 6.10 are written such that they are largely self-contained, thus minimizing the need for reference to multiple sub-articles to address any of the essential design considerations. The provisions of Article 6.10 are organized as follows:

- 6.10.1 General
- 6.10.2 Cross-Section Proportion Limits
- 6.10.3 Constructability
- 6.10.4 Service Limit State
- 6.10.5 Fatigue and Fracture Limit State
- 6.10.6 Strength Limit State
- 6.10.7 Flexural Resistance - Composite Sections in Positive Flexure
- 6.10.8 Flexural Resistance - Composite Sections in Negative Flexure and Noncomposite Sections
- 6.10.9 Shear Resistance
- 6.10.10 Shear Connectors
- 6.10.11 Web Stiffeners
- 6.10.12 Cover Plates

Section 6 also contains five appendices. Four of these appendices are relevant to the design of flexural members. It should be noted that Appendices A6 and B6 are not applicable to horizontally curved I-girder bridges since they relate to straight I-sections only. The other two appendices are applicable and are as follows:

- Appendix C6 - Basic Steps for Steel Bridge Superstructures
- Appendix D6 - Fundamental Calculations for Flexural Members

Flow charts for flexural design of steel I-girders according to the provisions, along with an outline giving the basic steps for steel-bridge superstructure design, are provided in Appendix C6. Appendix C6 can be a useful reference for horizontally curved I-girder design. Fundamental calculations for flexural members are contained within Appendix D6.

General discussion of Article 6.10 is provided in Example 1 of the *Steel Bridge Design Handbook* for a straight I-girder bridge. This section will highlight several of the provisions of the *AASHTO LRFD BDS* as they relate to horizontally curved I-girder design.

In the *AASHTO LRFD BDS*, flange lateral bending stresses are included in the design checks. The provisions of Articles 6.10 provide a unified approach for consideration of major-axis bending and flange lateral bending for both straight and curved bridges. Flange lateral bending is caused by the torsional behavior of a curved bridge, resulting in cross-frame forces which impart a lateral load on the flanges. Other sources of flange lateral bending are wind loads, temporary support brackets for deck overhangs, and flange level lateral bracing systems.

In addition to providing adequate strength, the constructability provisions of Article 6.10.3 verify that nominal yielding does not occur and that there is no reliance on post-buckling resistance for main load-carrying members during critical stages of construction. The *AASHTO LRFD BDS* specifies that for critical stages of construction, both compression and tension flanges must be investigated, and the effects of flange lateral bending should be considered as appropriate. For noncomposite flanges in compression, constructability design checks verify that the maximum combined stress in the flange will not exceed the specified minimum yield strength, that the member has sufficient strength to resist lateral torsional and flange local buckling, and that theoretical web bend-buckling and web shear buckling will not occur during construction. For noncomposite flanges in tension, constructability design checks make certain that the maximum combined stress will not exceed the specified minimum yield strength of the flanges during construction.

3.0 DESIGN PARAMETERS

The following data apply to this design example:

Specifications:	2020 AASHTO <i>LRFD Bridge Design Specifications</i> [1], Customary U.S. Units, Ninth Edition
Structural Steel:	ASTM A709, Grade 50 steel with $F_y = 50$ ksi, $F_u = 65$ ksi
Concrete:	$f'_c = 4.0$ ksi, $\gamma = 150$ pcf
Slab Reinforcing Steel:	ASTM A615, Grade 60 with $F_y = 60$ ksi

The bridge has spans of 160.0 feet – 210.0 feet – 160.0 feet measured along the centerline of the bridge. Span lengths are arranged to give similar positive dead load moments in the end and center spans and to minimize the chance of uplift occurring at the bearings. The radius of the bridge is 700 feet at the centerline of the bridge. The out-to-out deck width is 40.5 feet, and there are three 12-foot traffic lanes. All supports are radial with respect to the bridge centerline. There are four I-girders in the cross-section.

The total deck thickness is 9.5 inches, with a 0.5-inch integral wearing surface assumed. Therefore, the structural thickness of the concrete deck is taken as 9.0 inches. The deck haunch thickness is taken as 4.0 inches and is measured from the top of the web to the bottom of the deck; that is, the top flange thickness is included in the haunch. The width of the haunch is assumed to be 20 inches for load computation purposes. The haunch thickness is considered in section property computations, but the haunch concrete area is not considered.

Concrete parapets are each assumed to weigh 495 plf. Permanent steel stay-in-place deck forms are used between the girders; the forms are assumed to weigh 15.0 psf since it is assumed concrete will be in the flutes of the deck forms. An allowance for a future wearing surface of 30.0 psf is incorporated in this design example.

The bridge is designed for HL-93 live load in accordance with Article 3.6.1.2. Live load for fatigue is taken as defined in Article 3.6.1.4. The bridge is designed for a 75-year fatigue life, and the projected single-lane average daily truck traffic ($ADTT_{SL}$) in one direction is assumed to be 1,000 trucks per day.

The bridge site is assumed to be located in Seismic Zone 1, so seismic effects are not considered in this design example. Steel erection is not explicitly examined in this example, but sequential placement of the concrete deck is considered.

Bridge underclearance is limited such that the total bridge depth may not exceed 120 inches at the low point on the cross section. The roadway is superelevated 5 percent.

The girders in this example are composite throughout the entire span, including regions of negative flexure since shear connectors are provided along the entire length of each girder. Shear connectors are required throughout the entire length of a curved continuous composite bridge according to the provisions of Article 6.10.10.1.

4.0 GENERAL STEEL FRAMING CONSIDERATIONS

Detailing guidelines can be found in the AASHTO/NSBA Steel Bridge Collaboration standard entitled *Guidelines for Design Details* [3]. Three other detailing references offering guidance are the Texas Steel Quality Council's *Preferred Practices for Steel Bridge Design, Fabrication, and Erection* [4], the Mid-Atlantic States Structural Committee for Economic Fabrication (SCEF) Standards, and the AASHTO/NSBA Steel Bridge Collaboration *Guidelines to Design for Constructability and Fabrication* [5] (hereafter referred to as "the Guidelines").

4.1 Span Arrangement

Careful consideration of the layout of the steel framing is an important part of the design process and involves evaluating alternative span arrangements and their corresponding superstructure and substructure costs to determine the most economical solution. Often, site-specific features will influence the span arrangement required. However, in the absence of these issues, choosing a balanced span arrangement for continuous steel bridges (end spans approximately 80% of the length of the center spans) will provide an efficient design. The span arrangement chosen for this design example has spans of 160-210-160 feet, which is a reasonably balanced span arrangement. Refer to NSBA's *Steel Bridge Handbook Design: Example 1: Three-Span Continuous Straight Composite Steel I-Girder Bridge* [6] for further discussion on span arrangement considerations.

4.2 Girder Spacing

When developing the bridge cross-section, the designer typically evaluates the number of girder lines required relative to the overall cost. Specifically, the total cost of the superstructure is a function of steel quantity, details, and erection costs. Developing an efficient bridge cross-section should also give consideration to providing an efficient deck design, which is generally influenced by girder spacing and overhang dimensions. Specifically, with the exception of an empirical deck design, girder spacing significantly affects the design moments in the deck slab. Larger deck overhangs result in a greater load on the exterior girder. Larger overhangs will increase the bending moment in the deck, caused by the cantilever action of the overhang, resulting in additional deck slab reinforcing for the overhang region of the deck.

In addition, wider deck spans between top flanges can become problematic for several reasons. Some owners have economical deck detail standards that may not be suited, or even permitted, for wider deck spans. At the same time, wider deck spans are progressively more difficult to form and construct.

The bridge cross-section in this design example consists of four I-girders spaced at 11 feet on center with 3.75-foot deck overhangs. The deck overhangs are 34 percent of the adjacent girder spacing. (Note that a somewhat smaller overhang on the order of 1/4 to 1/3 of the girder spacing is currently recommended.) Reducing the girder spacing below 11 feet would lead to an increase in the size of the deck overhangs which would, in turn, lead to larger loading on the exterior girders, particularly the girder on the outside of the curve. Wider girder spacing would increase the deck thickness with a corresponding increase in dead load. The bridge cross-section is shown in Figure 1.

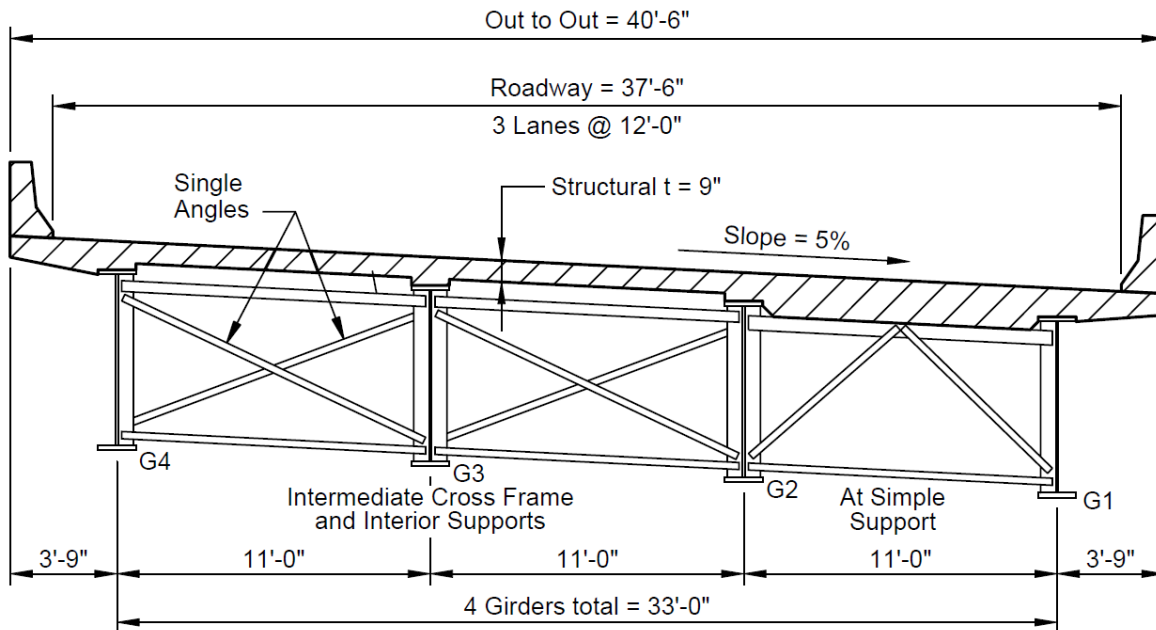


Figure 1: Typical Bridge Cross-Section

4.3 Girder Depth

The proper girder depth is an extremely important consideration affecting the economy and constructability of a steel-girder design. Deeper girders not only lead to a stiffer bridge but result in flanges that meet specified depth-to-width limits and girders that are easier to handle. The chosen depth also dictates the flange sizes. Clearance restrictions or poor span ratios in continuous-span structures can prevent the use of the desired depth. However, in the absence of such restrictions, it is usually desirable to use the near optimum depth for the largest span in the unit if feasible.

In the absence of any depth restrictions, Article 2.5.2.6.3 provides suggested minimum span-to-depth ratios. Unless specified otherwise by the Owner-agency, these are only suggested and not required minimum depths; the Engineer is otherwise permitted to use a depth that is shallower than these suggested minimums, and in some cases, may be forced to do so by other constraints. However, when depths below these suggested minimums must be used, additional attention should be paid to the structure deformations and cross-frame forces. The most important thing to keep in mind is that the optimum depth will typically be larger than the suggested minimum depth.

Article 2.5.2.6.3 recommends a maximum span-to-depth ratio, L_{as}/D , of 25 for curved steel-girder systems in which the specified minimum yield strength of the girder in regions of positive flexure is not greater than 50 ksi and either the specified minimum yield strength of the girder in regions of negative flexure is not greater than 70 ksi or a hybrid section satisfying the provisions of Article 6.10.1.3 is used. *In this case, D represents the depth of the steel girder, and not the total composite section depth.* In checking this requirement, the arc girder length, L_{as} , for spans continuous on both ends is defined as eighty percent of the longest girder in the span (girder length is taken as the arc

length between bearings). The arc girder length of spans continuous on only one end is defined as ninety percent of the longest girder in the span. The longest arc span length (either end or interior span) controls. The maximum arc length occurs at the center span of the outside girder, G4, and is 214.95 feet. Therefore, the recommended girder depth is computed as follows:

$$0.8(214.95)/25 = 6.88 \text{ ft} = 82.5 \text{ in.}$$

For simplicity, it is recommended that the suggested minimum depth be applied to the web depth rather than to the total depth of the girder; therefore, a web depth of 84 inches is selected.

4.4 Cross-Section Proportions

Proportion limits for webs of I-girders are specified in Article 6.10.2.1. Provisions for webs with and without longitudinal stiffeners are presented. For this design example, the need for a longitudinally stiffened web is not anticipated. Therefore, the web plate must be proportioned such that the web plate thickness (t_w) meets the following requirement:

$$\frac{D}{t_w} \leq 150 \quad \text{Eq. (6.10.2.1.1-1)}$$

Rearranging:

$$(t_w)_{\min.} = \frac{D}{150} = \frac{84}{150} = 0.56 \text{ in.}$$

Based on preliminary designs, a web thickness of 0.625 inches is found to be sufficient for a transversely stiffened web and is used in the field sections over the interior piers. A 0.5625-inch-thick web is used in positive-moment regions. Note that the Guidelines recommend a minimum web thickness of 0.5 inches to reduce deformation and the potential for weld defects as well as to provide increased corrosion resistance.

For illustration purposes, the proportions of girder G4 in Span 1 at the maximum positive moment location are checked. These plate sizes are applicable to the section defined later in this example as Section G4-1. The flanges are selected as follows:

Top flange (compression flange): 1.0 in. x 20 in.
Bottom flange (tension flange): 1.625 in. x 21 in.

The flanges must satisfy the provisions of Article 6.10.2.2:

$$\frac{b_f}{2t_f} \leq 12.0 \quad \text{Eq. (6.10.2.2-1)}$$

$$\text{Top flange: } \frac{20}{2(1.0)} = 10.0 < 12.0 \quad \text{Bottom flange: } \frac{21}{2(1.625)} = 6.5 < 12.0 \quad \text{Both flanges}$$

OK

$$b_f \geq \frac{D}{6} \quad \text{Eq. (6.10.2.2-2)}$$

$$\frac{84}{6} = 14 \text{ in.} \quad \text{Both flanges OK}$$

$$t_f \geq 1.1t_w \quad \text{Eq. (6.10.2.2-3)}$$

$$1.0 \text{ in.} \geq 1.1(0.5625) = 0.619 \text{ in.} \quad \text{Both flanges OK}$$

The Guidelines recommend a minimum flange thickness of 0.75 inches for the same reasons discussed previously for webs. Therefore, use $(t_f)_{\min} = 0.75$ inches.

$$0.1 \leq \frac{I_{yc}}{I_{yt}} \leq 10 \quad \text{Eq. (6.10.2.2-4)}$$

$$I_{yc} = \frac{1.0(20)^3}{12} = 666.7 \text{ in.}^4 \quad I_{yt} = \frac{1.625(21)^3}{12} = 1,254 \text{ in.}^4$$

$$0.1 < \frac{666.7}{1,254} = 0.53 < 10 \quad \text{OK}$$

In addition to the flange proportions required by Article 6.10.2.2, Article C6.10.2.2 provides the following additional guideline for the minimum top-flange width, b_{tfs} , within an individual unspliced girder field section. This guideline, which should be considered in conjunction with the flange proportioning limits specified in Article 6.10.2.2, is intended to provide more stable field pieces that are easier to handle during fabrication and erection without the need for special stiffening trusses or falsework:

$$(b_{tfs})_{\min} \geq \frac{L_{fs}}{85} \quad \text{Eq. (C6.10.2.2-1)}$$

where L_{fs} is the length of the unspliced girder field section in feet. This equation is provided as a guideline and is not considered a mandatory requirement, but satisfying this proportional limit is strongly encouraged.

The guideline is applied to the top-flange width because the top flange of each girder field section is subject to compression over its entire length during lifting, erection, and shipping regardless of the final location of the field section in the bridge. The bottom flange is also typically either wider or of the same width as the top flange in most typical field sections. The guideline is also applied

to unspliced girder field sections rather than to girder shipping pieces during the design. It is not intended in the application of this guideline that the Engineer attempt to anticipate how the individual field sections may eventually be assembled or spliced together and/or stabilized or supported for shipping or erection; such concerns should instead be considered the responsibility of the Contractor.

From Figure 3, the length of the longest unspliced girder field section is 129 feet (Field Section 3 of G4). Therefore, applying the guideline for this field section gives:

$$20 \text{ in.} > \frac{129.0(12)}{85} = 18.2 \text{ in. OK}$$

Therefore, all section proportion checks for this location are satisfied. Section proportion checks for the other design locations are not shown. All subsequent sections satisfy these limits. The assumed member sizes for all the girders in the cross-section are shown in Figure 3.

Because the top flange of the outermost girder G4 will be subject to flange lateral bending due to the effects of curvature, eccentric deck overhang loads, and wind loads during construction, top-flange sizes slightly larger than the minimum sizes are assumed in regions of positive flexure. The bottom flange plates in regions of positive flexure in this example are primarily sized based on the flange-stress limitation at the service limit state specified in Article 6.10.4.2.2. However, in the end spans, the size of the larger bottom-flange plate in this region is controlled by the stress-range limitation on a cross-frame connection plate weld to the tension flange at the fatigue and fracture limit state, as will be demonstrated later. The bottom-flange sizes in regions of negative flexure are assumed controlled by either the flange local buckling or lateral torsional buckling resistance at the strength limit state. Top-flange sizes in these regions are assumed controlled by tension-flange yielding at the strength limit state. At this stage, the initial trial plate sizes in regions of negative flexure are primarily educated guesses based on experience and any approximate preliminary design calculations that may have been performed. Because the girder is assumed to be composite throughout, the minimum one-percent longitudinal reinforcement required in Article 6.10.1.7 will be included in the section properties in regions of negative flexure. As a result, a top flange with an area slightly smaller than the area of the bottom flange can be used in these regions.

Because the most economical plate to buy from a mill is between 72 and 96 inches wide, an attempt was made in the design to minimize the number of thicknesses of plate that will be ordered for the flanges. Larger order quantities of plate cost less and minimizing the number of different thicknesses simplifies fabrication and inspection. As recommended in the Guidelines, flange thicknesses should be selected in not less than 1/8-inch increments up to 2½ inches in thickness and ¼-inch increments over 2½ inches in thickness. Note that individual flange widths are kept constant within each field piece, as recommended in the Guidelines; flange widths should be changed instead at bolted field splices. There is little need to maintain a constant flange width among individual field sections. However, some Owners may prefer a constant-width bottom flange along the entire length of the girder for aesthetic reasons should many pedestrians be expected underneath the bridge. Note that top and bottom flange widths within a field section can be, and often are, different. The Guidelines contain more detailed discussion on specific issues pertinent to the sizing of girder flanges as it relates to the ordering of plate and the fabrication of

the flanges. Fabricators can also be consulted regarding these issues and all other fabrication-related issues discussed herein.

Flange transitions, or shop-welded splices, are located based on design considerations, plate length availability and the economics of welding and inspecting a splice compared to the cost of extending a thicker plate. The design plans should consider allowing an option for the Fabricator to eliminate a shop splice by extending a thicker flange plate subject to the approval of the Engineer. When evaluating such a request, the Engineer should consider the effect of the thicker plate on the girder deflections and stresses. Typically, a change in the location of a shop-welded flange thickness transition does not significantly affect deflections as much as the elimination of the transition (and extension of the thicker plate to the end of the field section). Usually, a savings in weight of between 800 to 1000 pounds should be realized to justify the cost of the full penetration flange butt splice required for a shop-welded flange thickness transition. Again, the Guidelines contain more detailed discussion regarding this issue.

In typical cases, no more than two shop splices, or three different flange thicknesses, should be necessary in any one field section of a plate girder, unless the girders are unusually heavy or plate length availability limits dictate the need for additional splices with or without a thickness change. Generally, different flange thicknesses within a field section are more economical in negative-moment region field sections, where the moment gradients are more significant. At flange shop splices, the cross-sectional area of the thinner plate should not be less than one-half the cross-sectional area of the thicker plate to reduce the stress concentration and provide a smooth transition of stress across the splice.

Fabricators will either weld the shop splices in the individual flanges after cutting them to width or utilize slab welding if the necessary crane capacity and hook height are available within the shop. Slab welding is the process of butt-welding wide plates of different thicknesses together from which individual flanges may be nested and stripped. If the use of slab welding is expected, it will be used only within a field section. The process is most often employed for the interior-pier field sections. The process of slab welding is discussed in greater detail in the Guidelines. The Engineer should be aware if and where the fabricator plans to use slab welding, as it can affect the sizing of the flanges. When utilized, the flange widths for an individual girder must be kept constant within the field section. Also, use a common flange thickness within all the girders, or a group of girders depending on which is more practical, across the cross-section for each of the end plates and the center plate of the field section. For curved girders where different demands typically exist for each girder in the cross-section, change the width of the flange plates instead of the thickness for each girder, or group of girders, across the cross-section as needed. Note that this strategy was employed in the sizing of the flanges shown in Figure 3 and can lead to significant savings in the amount of scrap that is generated during fabrication.

4.5 Cross-Frames

The chosen cross-frame spacings of 20 feet in Spans 1 and 3 and 19.09 feet in Span 2 (measured along the centerline of the bridge) are within the maximum spacing allowed by Eq. (6.7.4.2-1) for horizontally curved I-girder bridges and are also less than the prescribed maximum limit of 30 feet. Reduction of the cross-frame spacing reduces cross-frame forces since the load transferred

between girders is a function of the curvature. Reduction of cross-frame spacing also reduces flange lateral bending moments and transverse deck stresses. By reducing flange lateral bending, flange sizes can be reduced, but at the expense of requiring more cross-frames. Refer to *Steel Bridge Handbook Design: Example 1: Three-Span Continuous Straight Composite Steel I-Girder Bridge* [6] for further discussion on the function, layout, and configuration of cross-frames.

In the analytical model used to analyze the bridge, cross-frames are composed of single angles with an area of 5.0 square inches. Cross-frames with an "X" configuration with top and bottom chords are used for intermediate cross-frames and at interior supports. A "K" configuration is assumed at the simple end supports with the diagonals intersecting at the midpoint of the top strut (see Figure 1). The "K" configuration is advantageous at end supports because the top member, typically a channel or W shape, can support the deck edge beam. Also, as support members to the top beam at the midpoint, the diagonals help to distribute the deck load to the bearings. Refer to NSBA's *Steel Bridge Handbook Design: Example 2A: Two-Span Continuous Straight Composite Steel I-Girder Bridge* [7] for illustrations of intermediate and end-support cross-frame designs.

Figure 2 shows the selected framing plan for this design example. Cross-frames are spaced at approximately 20 feet measured along the centerline of the bridge, which results in 8 panels in the end spans and 11 panels in the center span. Critical girder sections are identified in Figure 2. These sections will be referred to frequently in the following narratives, tables, and calculations. Although not shown in Figure 2, transverse stiffeners are provided at three equal spaces between cross-frame locations.

4.6 Field Section Sizes

The lengths of field sections are generally dictated by shipping weight and length restrictions. The choice of field splice locations and the corresponding field section lengths is in many ways project specific. The Engineer is often at a disadvantage in making these determinations since the Fabricator is often not known at design and hence the shipping route that must be taken is also unknown.

Generally, the weight of a single shipping piece is restricted to 200,000 lbs. The piece length is typically limited to a maximum of 140 feet, with an ideal piece length of 120 feet. However, shipping requirements are often dictated by state or local authorities, in which additional restrictions may be placed on piece weight and length. Handling issues during erection and in the fabrication shop also need to be considered as they may govern the length of field sections. Therefore, the Engineer should consult with contractors and fabricators who are expecting to be bidding the work regarding any specific weight and length restrictions that might influence the field section lengths.

Field section lengths should also be determined with consideration given to the number of field splices required as well as the locations of field splices. It is desirable to locate field splices at or near dead load inflection points to reduce the forces that must be carried by the field splice. Field splices located in higher moment regions can become quite large, with cost increasing proportionally to their size. Furthermore, the size of the girder may be controlled by the net section fracture check at the holes in the girder tension flange associated with the splice's bolted

connections. The Engineer must determine what the most cost competitive solution is for the given span arrangement. For complex and longer span bridges, the fabricator's input can be helpful in reaching an economical solution.

The final girder field section lengths for this example are shown in the girder elevation in Figure 3. There is one field splice in each end span and two field splices in the center span, resulting in five field sections in each girder line or 20 field sections for the entire bridge. For this layout, the field sections weigh approximately 30,000 to 45,000 pounds. The longest field section, the center field section of G4, is approximately 129 feet in length. Field sections in this length and weight range can generally be fabricated, shipped, and erected without significant issues.

To verify that the shipping width is practical, the out-to-out width of the flanges taking into account the sweep should be computed. In this example, the shipping width for Field Section 3 (the center field section) of G4 taking into account the sweep is approximately 3 feet, which is reasonable for shipping. Additional field splices may be needed to accommodate the sweep for shipment of more sharply curved members.

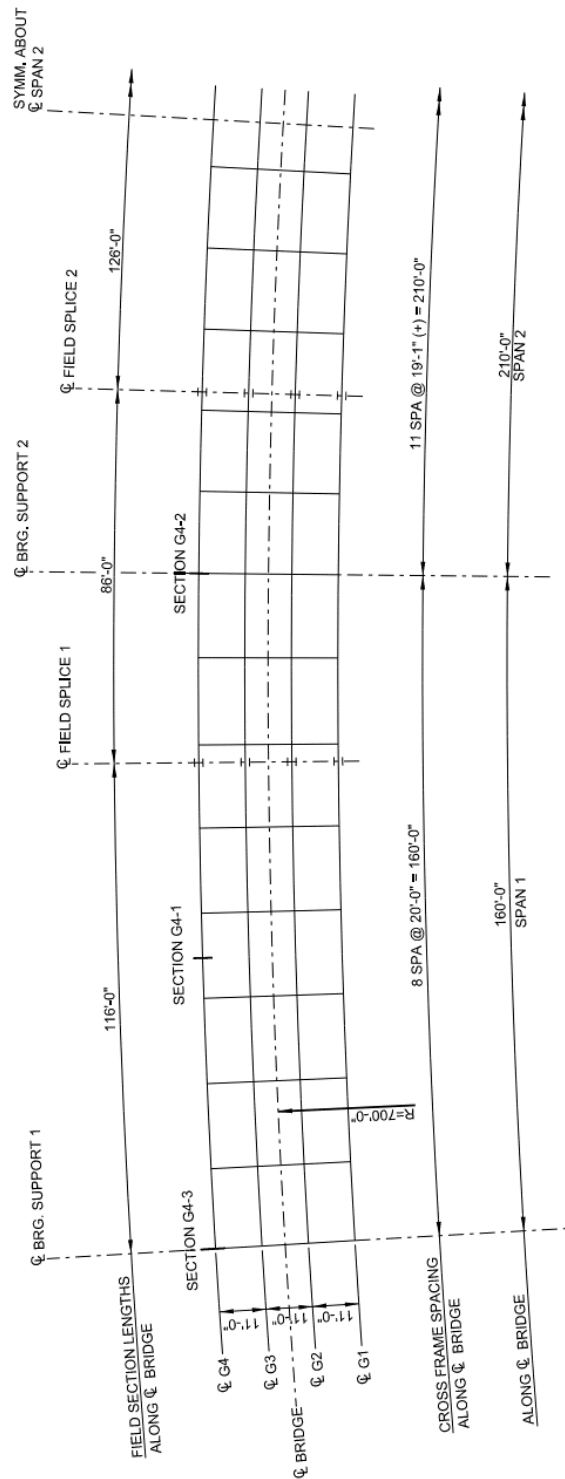
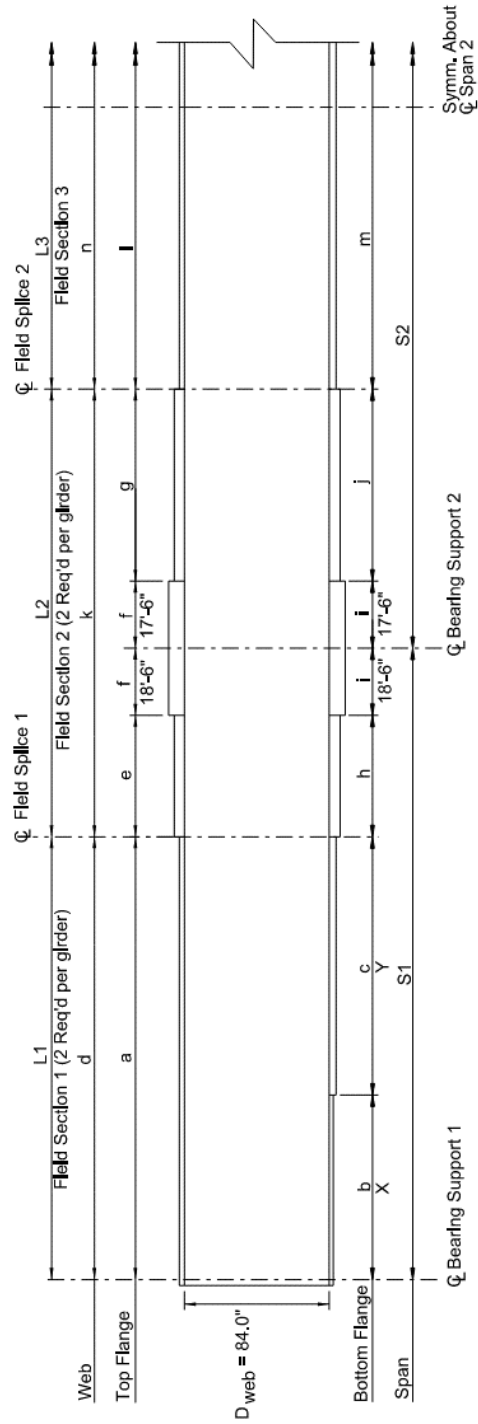


Figure 2: Framing Plan



NOTE:
Transverse stiffeners not shown for clarity.

Dimensions (Shown In feet)

	L1	L2	L3	S1	S2	X	Y
G1	113.0	84.0	123.0	156.2	205.1	0	113.3
G2	115.1	85.3	125.0	158.7	208.4	0	115.1
G3	116.9	86.7	127.0	161.3	211.7	0	116.9
G4	118.7	88.0	129.0	163.8	215.0	33.0	85.7

Member Sizes (Shown In Inches)

	a	b	c	d	e	f	g	h	i	j	k	l	m	n
G1	16X1	n/a	16X1	84x9/16	21x1.25	21x2.5	21x1.25	21x1.50	21x3	21x1.50	84x5/8	18X1	18X1	84x9/16
G2	18X1	n/a	18X1	84x9/16	18x1.25	18x2.5	18x1.25	19x1.50	19x3	19x1.50	84x5/8	18X1	18X1	84x9/16
G3	18X1	n/a	18X1	84x9/16	20x1.25	20x2.5	20x1.25	21x1.50	21x3	21x1.50	84x5/8	18X1	20X1	84x9/16
G4	20X1	21X1	21X1.625	84x9/16	28x1.25	28x2.5	28x1.25	27x1.50	27x3	27x1.50	84x5/8	20X1	21X1.5	84x9/16

5.0 FINAL DESIGN

5.1 AASHTO LRFD Limit States

5.1.1 Service Limit State (Articles 1.3.2.2 and 6.5.2)

To satisfy the service limit state, restrictions on stress and deformation under regular conditions are specified to provide satisfactory performance of the bridge over its service life. As specified in Article 6.10.4.1, optional live load deflection criteria and span-to-depth ratios (Article 2.5.2.6) may be invoked to control deformations.

Steel structures must also satisfy the requirements of Article 6.10.4.2 under the Service II load combination. The intent of the design checks specified in Article 6.10.4.2 is to prevent objectionable permanent deformations caused by localized yielding and potential web bend-buckling under expected severe traffic loadings, which might impair rideability. The live-load portion of the Service II load combination is intended to be the HL-93 design live load specified in Article 3.6.1.1 (discussed in Section 5.2.5). For evaluation of the Service II load combination under Owner-specified special design vehicles and/or evaluation permit vehicles, a reduction in the specified load factor for live load should be considered for this limit-state check.

5.1.2 Fatigue and Fracture Limit State (Articles 1.3.2.3 and 6.5.3)

To satisfy the fatigue limit state, restrictions on stress range under regular service conditions are specified to control crack growth under repetitive loads (Article 6.6.1). Material toughness requirements are specified to satisfy the fracture limit state (Article 6.6.2).

For checking fatigue in steel structures, the fatigue load specified in Article 3.6.1.4 applies, and the Fatigue I or Fatigue II load combination is used, as applicable. Fatigue resistance of details is discussed in Article 6.6. A special fatigue requirement for webs (Article 6.10.3) is also specified to control out-of-plane flexing of the web that might potentially lead to fatigue cracking under repeated live loading.

5.1.3 Strength Limit State (Articles 1.3.2.4 and 6.5.4)

At the strength limit state, it must be verified that adequate strength and stability are provided to resist the statistically significant load combinations the bridge is expected to experience over its design life. The applicable Strength load combinations (discussed later) are used to check the strength limit state.

Although not specified as a separate limit state, constructability is one of the basic design objectives of LRFD. The bridge must be safely erected and have adequate strength and stability during all phases of construction. Specific design provisions are given in Article 6.10.3 of the *AASHTO LRFD BDS* to help verify constructability of steel I-girder bridges, particularly when subject to the specified deck-casting sequence and deck overhang force effects. The constructability checks are typically made on the steel section only under the factored noncomposite dead loads using the appropriate strength load combinations.

5.1.4 Extreme Event Limit State (Articles 1.3.2.5 and 6.5.5)

At the extreme event limit state, structural survival of the bridge must be verified during a major earthquake or flood, or when struck by a vessel, vehicle, or ice flow. Extreme event limit states are not covered in this design example.

5.2 Loads

5.2.1 Noncomposite Dead Load (DC₁)

The steel weight is applied as body forces to the fully erected noncomposite structure in the analysis. The weight of the detail steel such as stiffeners and splices, which were not included in the analysis model, was accounted for in the analysis by increasing the density of the steel (490 pounds per cubic foot) by approximately 7 percent.

The entire concrete deck is assumed to be placed at one time for the strength limit state design checks. The weight of the wet concrete of the deck was applied to the non-composite 3D model with concentrated loads at the nodes representing the tops of the girders. The concrete was assumed to have no stiffness. The concentrated loads applied to each girder top node were determined by the tributary area of deck associated with the distance between girder nodes and the girder spacings. The thickness of the integral wearing surface was considered. The deck overhang tapers (Figure 1) were considered in computing the concentrated loads applied to the exterior girders. The weight of the wet concrete in the deck haunches was included in the concentrated loads applied to each girder. An average deck haunch width of 20 inches and deck haunch thickness of 4 inches was assumed (the reduction in weight due to the concrete displaced by the top flanges was ignored). The unit weight of the concrete was taken equal to 0.150 kcf, which includes an additional 0.005 kcf to account for the weight of the rebars.

The weight of the SIP deck forms was applied directly to the girders of the non-composite 3D model as concentrated loads as done for the deck. The forms exist only between flange edges in the interior bays; thus, the weight of the forms and the concrete in the forms was based on the clear span between the top flanges in the interior bays.

5.2.2 Deck Placement Sequence

The deck was considered placed in the following sequence for the constructability limit state design checks, which is also illustrated in Figure 4. The concrete was assumed first cast from the left abutment to the dead load inflection point in Span 1. The concrete between dead load inflection points in Span 2 was assumed cast second. The concrete beyond the dead load inflection point to the abutment in Span 3 was assumed cast third. Finally, the concrete between the points of dead load contraflexure over the two piers was assumed cast. In the analysis, earlier concrete casts were assumed composite for each subsequent cast.

For the constructability design checks, the noncomposite section is checked for the moments resulting from the deck placement sequence or the moments computed assuming the entire deck is cast at one time, whichever is larger.

The deck load is assumed to be applied through the shear center of the interior girders in the analysis. However, the weight of the fresh concrete on the overhang brackets produces significant lateral force on the flanges of the exterior girders. This eccentric loading and subsequent lateral force on the flanges must be considered in the constructability design checks.

5.2.3 Superimposed Dead Load (DC₂)

The concrete parapet loads were applied as concentrated loads along the edges of the deck elements in the three-dimensional analysis. These superimposed dead loads were applied to the composite structure in the analysis.

The superimposed dead load is considered a permanent load applied to the long-term composite section to account in an approximate fashion for the effects of concrete creep. For computing flexural stresses from permanent loading, the long-term composite section in regions of positive flexure is determined by transforming the concrete deck using a modular ratio of $3n$ (Article 6.10.1.1.1b). In regions of negative flexure, the long-term composite section is assumed to consist of the steel section plus the longitudinal reinforcement within the effective width of the concrete deck (Article 6.10.1.1.1c), except as permitted otherwise for the fatigue and service limit states (see Articles 6.6.1.2.1 and 6.10.4.2.1).

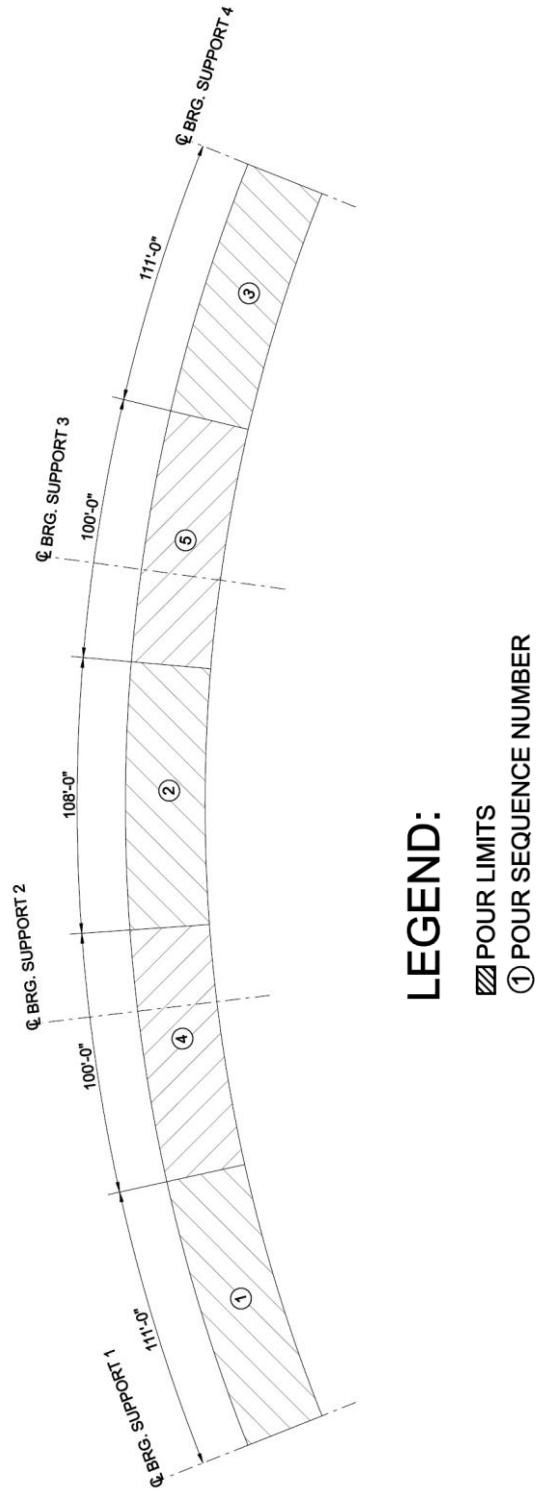


Figure 4: Deck Placement Sequence

5.2.4 Future Wearing Surface (DW)

The future wearing surface was applied uniformly over the deck area and was applied to the composite structure. The future wearing surface load was applied to the composite 3D model by applying an artificial increased density of the hardened concrete deck to the deck elements extending over the approximate width of the roadway.

The future wearing surface is considered a permanent load applied to the long-term composite section. Flexural stresses are computed in the same manner as described previously for the superimposed dead load.

5.2.5 Live Load (LL+IM)

Live loads are assumed to consist of gravity loads (vehicular live loads, rail transit loads and pedestrian loads), the dynamic load allowance, centrifugal forces, braking forces and vehicular collision forces. Live loads illustrated in this example include the HL-93 vehicular live load and a fatigue load, which include the appropriate dynamic load allowance and centrifugal force (see Section 5.3) effects.

Influence surfaces were utilized to determine the live load force effects in this design example. More details regarding influence surfaces and the live load analysis associated with the 3D analysis model are provided in Section 6.1.2 of this example.

Live loads are treated as transient loads applied to the short-term composite section. For computing flexural stresses from transient loading, the short-term composite section in regions of positive flexure is determined by transforming the concrete deck using a modular ratio of n (Article 6.10.1.1.1b). In regions of negative flexure, the short-term composite section is assumed to consist of the steel section plus the longitudinal reinforcement within the effective width of the concrete deck (Article 6.10.1.1.1c), except as permitted otherwise for the fatigue and service limit states (see Articles 6.6.1.2.1 and 6.10.4.2.1).

When computing longitudinal flexural stresses in the concrete deck (see Article 6.10.1.1.1d), due to permanent and transient loads, the short-term composite section should be used.

Design Vehicular Live Load (Article 3.6.1.2)

The design vehicular live load is designated as HL-93 and consists of a combination of the following placed within each design lane:

- a design truck *or* design tandem, and
- a design lane load.

The design vehicular live load is discussed in more detail in Design Example 1 of the NSBA Steel Bridge Design Handbook.

Fatigue Load (Article 3.6.1.4)

The vehicular live load for checking fatigue consists of a single design truck (without the lane load) with a constant rear-axle spacing of 30 feet (Article 3.6.1.4.1). The fatigue live load is discussed in greater detail in Design Example 1 of the NSBA Steel Bridge Design Handbook.

5.3 Vehicular Centrifugal Force Computation (CE)

The vehicular centrifugal force is determined according to Article 3.6.3. The centrifugal force has two components, the radial force and the associated overturning moment. The radial component of the centrifugal force is assumed to be transmitted from the deck through the support cross-frames or diaphragms to the bearings and the substructure.

The overturning component of centrifugal force occurs because the radial force is applied at a distance above the top of the deck. The center of gravity of the design truck is assumed to be 6 feet above the roadway surface according to the provisions of Article 3.6.3. The transverse spacing of the wheels is 6 feet per Figure 3.6.1.2.2-1. The overturning component causes the exterior (with respect to curvature) wheel line to apply more than half the weight of the truck and the interior wheel line to apply less than half the weight of the truck by the same amount. Thus, the outside of the bridge is more heavily loaded with live load. Article 3.6.3 permits the effect of superelevation, which reduces the overturning effect of centrifugal force, to be considered. Figure 5 shows the geometric relationship between the centrifugal force and the superelevation. The dimensions denoted by s and h in Figure 5 are both equal to 6 feet.

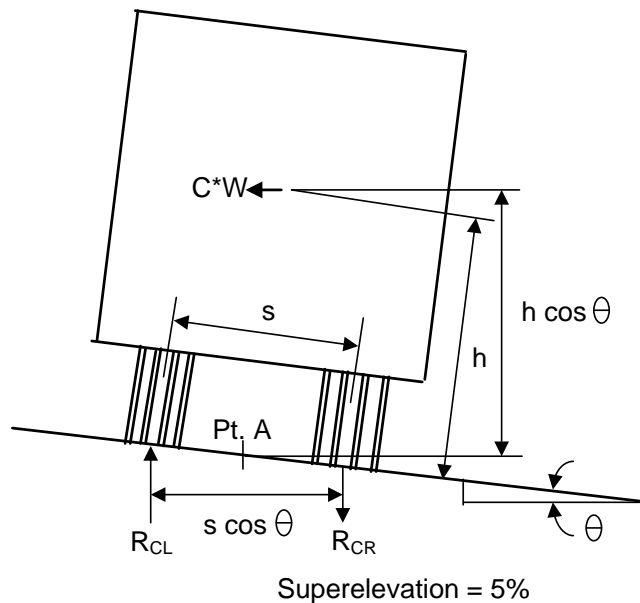


Figure 5: Vehicular Centrifugal Force Wheel-Load Reactions

Article 3.6.3 states that the centrifugal force is to be taken as the product of the axle weights of the design truck or tandem and the factor C , taken as:

$$C = f \frac{v^2}{gR} \quad \text{Eq. (3.6.3-1)}$$

where: $f = 4/3$ for load combinations other than fatigue and 1.0 for fatigue

v = highway design speed (ft/sec)

g = gravitational acceleration: 32.2 ft/sec²

R = radius of curvature of the traffic lane (ft)

Use the average bridge radius, $R = 700$ ft in this case. For this design example, the design speed is assumed to be 35 mph = 51.3 ft/sec. Therefore, for the strength and service limit states:

$$C = \frac{4}{3} \left[\frac{51.3^2}{(32.2)(700)} \right] = 0.156$$

For the fatigue limit state, the 4/3 factor is changed to 1.0. The factor C is applied to the axle weights. Per Figure 3.6.1.2.2-1, the total weight of the design truck axles is 72 kips.

The radial force is computed as follows:

$$\text{Truck in one lane} = 1.2(0.156)(72) = 13.48 \text{ kips}$$

$$\text{Truck in two lanes} = 1.0(0.156)(72)(2) = 22.46 \text{ kips}$$

$$\text{Truck in three lanes} = 0.85(0.156)(72)(3) = 28.64 \text{ kips}$$

All three cases have been adjusted by the appropriate multiple presence factor given in Table 3.6.1.1.2-1. The centrifugal force due to trucks in two lanes is used since the two-lanes loaded case controls for major-axis bending. The force will be applied to the deck in the radial direction. The force is resisted by the shear strength of the deck and is transferred to the bearings through the cross-frames at the bearings.

The overturning force is computed by taking the sum of the moments about the outside (left) wheel and setting the sum equal to zero. For a 5% cross slope (i.e., superelevation), the angle θ is equal to:

$$\theta = \arctan\left(\frac{5}{100}\right) = 2.862^\circ$$

First, the wheel-load reactions, R_{CL} and R_{CR} , due to centrifugal force effects are computed. Since the wheel spacing, s , and the height the radial force is applied above the deck, h , are both equal to 6.0 feet, the equal and opposite wheel-load reactions, R_{CL} and $-R_{CR}$, are simply equal to C multiplied by W . Referring to Figure 5, R_{CL} and R_{CR} are computed as follows:

$$R_{CL} = -R_{CR} = (C * W) \frac{h \cos \theta}{2 \left[\frac{s}{2} \cos \theta \right]} = C * W = 0.156W$$

This represents an upward reaction for the left (outside) wheel and an equal and opposite downward reaction for the right (inside) wheel.

As mentioned previously, superelevation helps to offset the effects of the overturning moment due to the centrifugal force. This beneficial effect may be considered to adjust the wheel-load reactions, as shown in Figure 6:

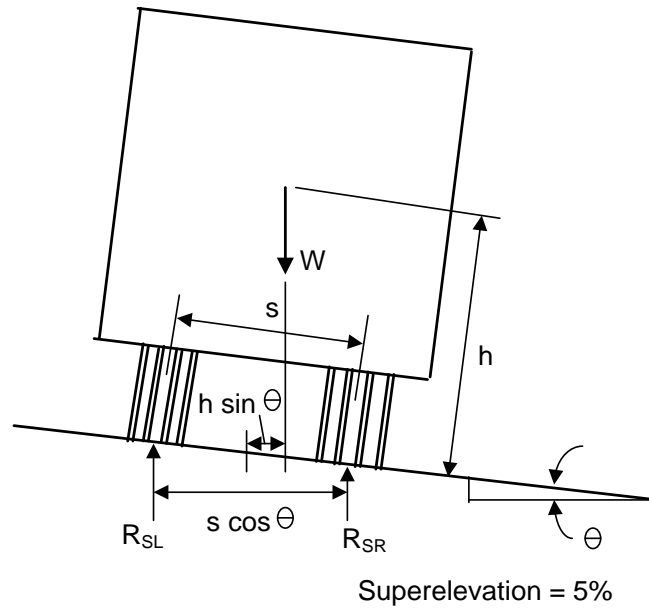


Figure 6: Effects of Superelevation

Referring to Figure 6, the wheel-load reactions, R_{SL} and R_{SR} , due to superelevation are computed by summing moments about the outside (left) wheel, as follows:

$$R_{SR} = \frac{\left[\frac{s}{2} \cos \theta + h \sin \theta \right] * W}{s \cos \theta} = \frac{\left[\frac{6 \text{ ft}}{2} \cos(2.862^\circ) + (6 \text{ ft}) \sin(2.862^\circ) \right] * W}{(6 \text{ ft}) \cos(2.862^\circ)} = 0.550W$$

$$R_{SL} = 1.0 - R_{SR} = 0.450W$$

If the superelevation is significant, the Engineer may wish to consider its effect for the case with no centrifugal force effects included (that is, a stationary vehicle), since the superelevation will cause an increase in the vertical wheel loads toward the inside of the bridge and an unloading of the vertical wheel loads toward the outside of the bridge, which may potentially be a more critical case for the interior girders.

For the refined analysis, unit wheel-load factors, F_L and F_R , can be computed based on the sum of the wheel-load reactions due to the centrifugal force and superelevation effects, as follows:

$$F_L = 2.0 \frac{R_{CL} + R_{SL}}{W} = 2.0 \frac{0.156W + 0.450W}{W} = 1.212$$

$$F_R = 2.0 \frac{R_{CR} + R_{SR}}{W} = 2.0 \frac{-0.156W + 0.550W}{W} = 0.788$$

F_L and F_R represent the factors that must be multiplied by the left wheel load and the right wheel load, respectively, to account for the combined effects of both centrifugal force and superelevation. F_L and F_R are unitless, and their sum is always equal to 2.0.

If no centrifugal force and no superelevation are present, then both F_L and F_R equal 1.0. That is, both the left wheel load and the right wheel load are simply 1.0 times the weight of the wheel. The sum of F_L and F_R is again equal to 2.0.

Therefore, for this example, the wheel loads of the design truck and tandem in each lane that were applied to the influence surfaces were adjusted by a factor of 1.212 applied to the outside wheels and 0.788 applied to the inside wheels of each axle to account for centrifugal force effects at the strength and service limit state. Separate unit wheel-load factors were similarly calculated for application to the fatigue live load for determination of the force effects at the fatigue limit state. The result was that the outermost girder generally received slightly higher load and the innermost girder generally received slightly lower load. The force effects in each member or component with the centrifugal force effects included were compared to the case with no centrifugal force effects included and the worst case was selected.

Article C3.6.3 indicates that centrifugal force effects need not be applied to the design lane load since the spacing of vehicles at high speeds is assumed to be large, resulting in a low density of vehicles following and/or preceding the design truck. The design lane load is still considered, as applicable, even though the centrifugal force is not applied to the load.

5.4 Load Combinations

For each limit state described previously in Section 5.1, the following basic equation (Article 1.3.2.1) must be satisfied:

$$\sum \eta_i \gamma_i Q_i \leq \phi R_n = R_r \quad \text{Eq. (1.3.2.1-1)}$$

where: η_i = load modifier related to ductility, redundancy and operational importance
 γ_i = load factor, a statistically based multiplier applied to force effects
 ϕ = resistance factor, a statistically based multiplier applied to nominal resistance
 Q_i = force effect
 R_n = nominal resistance
 R_r = factored resistance

The load factors are specified in Tables 3.4.1-1 and 3.4.1-2 of the specifications. For steel structures, the resistance factors are specified in Article 6.5.4.2.

As evident from the above equation, in the LRFD specifications, redundancy, ductility, and operational importance are considered more explicitly in the design. Ductility and redundancy relate directly to the strength of the bridge, while the operational importance relates directly to the consequences of the bridge being out of service. The grouping of these three effects on the load side of the above equation through the use of the load modifier η_i represents an initial attempt at their codification. Improved quantification of these effects may be possible in the future. For loads for which a maximum value of γ_i is appropriate:

$$\eta_i = \eta_D \eta_R \eta_I \geq 0.95 \quad \text{Eq. (1.3.2.1-2)}$$

where: η_D = ductility factor specified in Article 1.3.3
 η_R = redundancy factor specified in Article 1.3.4
 η_I = operational importance factor specified in Article 1.3.5

For loads for which a minimum value of γ_i is appropriate:

$$\eta_i = \frac{1}{\eta_D \eta_R \eta_I} \leq 1.0 \quad \text{Eq. (1.3.2.1-3)}$$

Eq. (1.3.2.1-3) is only applicable for the calculation of the load modifier when dead- and live-load force effects are of opposite sign and the minimum load factor specified in Table 3.4.1-2 is applied to the dead-load force effects (e.g., when investigating for uplift at a support or when designing bolted field splices located near points of permanent load contraflexure); otherwise, Eq. (1.3.2.1-2) is to be used.

For typical bridges for which additional ductility-enhancing measures have not been provided beyond those required by the specifications, and/or for which exceptional levels of redundancy are not provided, the η_D and η_R factors have default values of 1.0 specified at the strength limit state. The value of the load modifier for operational importance η_I should be chosen with input from the Owner-agency. In the absence of such input, the load modifier for operational importance at the strength limit state should be taken as 1.0. At all other limit states, all three η factors must be taken equal to 1.0. For this example, η_i will be taken equal to 1.0 at all limit states.

Table 3.4.1-1 is used to determine load combinations for strength. The Strength I load combination is to be used for checking the strength of a member or component under normal use in the absence of wind. Load Combinations Strength III and V from Table 3.4.1-1 are checked for temperature and wind loadings in combination with vertical loading.

Service I relates to normal operational use of the bridge in combination with a 70-mph wind with all loads taken at their nominal values and would be used primarily for crack control in reinforced concrete structures. However, the live-load portion of the Service I load combination is used for checking live-load deflection in steel bridges. Service II is used only for steel structures to control permanent deformations due to local yielding and slip of slip-critical connections under vehicular live load.

Two Fatigue load combinations are given in Table 3.4.1-1. The Fatigue I load combination is to be used when designing a detail or component for infinite fatigue life, and the Fatigue II load combination is to be used when designing a detail or component for finite fatigue life.

The following load combinations and load factors are typically checked in girder designs similar to this design example. For this example, it has been assumed that the Strength I load combination governs for the strength limit state, so only Strength I loads are checked in the sample calculations for the strength limit state included herein. In some design instances, other load cases may be critical, but for this example, these other load cases are assumed not to apply. Refer to Design Example 1 of the NSBA Steel Bridge Design Handbook for further detail on all of the load combinations specified in Table 3.4.1-1.

From Table 3.4.1-1 (minimum load factors of Table 3.4.1-2 are not considered here):

Strength I	$\eta \times [1.25(\text{DC}) + 1.5(\text{DW}) + 1.75((\text{LL} + \text{IM}) + \text{CE} + \text{BR}) + 1.2(\text{TU})]$
Strength III	$\eta \times [1.25(\text{DC}) + 1.5(\text{DW}) + 1.0(\text{WS}) + 1.2(\text{TU})]$
Strength V	$\eta \times [1.25(\text{DC}) + 1.5(\text{DW}) + 1.35((\text{LL} + \text{IM}) + \text{CE} + \text{BR}) + 1.0(\text{WS}) + 1.0(\text{WL}) + 1.2(\text{TU})]$
Service I	$\eta \times [\text{DC} + \text{DW} + ((\text{LL} + \text{IM}) + \text{CE} + \text{BR}) + 1.0(\text{WS}) + 1.0(\text{WL}) + 1.2(\text{TU})]$
Service II	$\eta \times [\text{DC} + \text{DW} + 1.3((\text{LL} + \text{IM}) + \text{CE} + \text{BR}) + 1.2(\text{TU})]$
Fatigue I	$\eta \times [1.75((\text{LL} + \text{IM}) + \text{CE})]$
Fatigue II	$\eta \times [0.80((\text{LL} + \text{IM}) + \text{CE})]$

where:

η	= Load modifier specified in Article 1.3.2
DC	= Dead load: components and attachments
DW	= Dead load: wearing surface and utilities
LL	= Vehicular live load
IM	= Vehicular dynamic load allowance
CE	= Vehicular centrifugal force
WS	= Wind load on structure
WL	= Wind on live load
TU	= Uniform temperature
BR	= Vehicular braking force

When evaluating the strength of the structure for the maximum force effects during construction, the load factor for construction loads, for equipment and for dynamic effects (i.e., temporary dead and/or live loads that act on the structure only during construction) is not to be taken less than 1.5 in the Strength I load combination (Article 3.4.2.1). Also, the load factors for the weight of the structure and appurtenances, DC and DW, are not to be taken less than 1.25 when evaluating the construction condition. The load factor for wind load when evaluating the Strength III load combination during construction is to be specified by the Owner-agency (Article 3.4.2.1). Any applicable construction loads are to be included with a load factor not less than 1.25. Also, the load factors for the weight of the structure and appurtenances, DC and DW, are not to be taken less than

1.25 when evaluating the construction condition. The Strength II, IV, and V load combinations are not applicable to the investigation of construction stages.

Article 3.4.2.1 further states that unless otherwise specified by the Owner, primary steel superstructure components are to be investigated for maximum force effects during construction for an additional load combination consisting of the applicable DC loads and any construction loads that are applied to the fully erected steelwork. For this additional load combination, the load factor for DC and construction loads including dynamic effects (if applicable) is not to be taken less than 1.4. For steel superstructures, the use of higher-strength steels, composite construction, and limit-states design approaches in which smaller factors are applied to dead load force effects than in previous service-load design approaches, have generally resulted in lighter members overall. To provide adequate stability and strength of primary steel superstructure components during construction, an additional strength limit state load combination is specified for the investigation of loads applied to the fully erected steelwork (i.e., for investigation of the deck placement sequence and deck overhang effects).

Construction: Strength I:	$\eta \times [1.25(D) + 1.5(C)]$
Strength III:	$\eta \times [1.25D + \text{Owner-specified load factor} * (WC)]$
Special Load Combination:	$\eta \times [1.4(D + C)]$

where:

D = Dead load
C = Construction loads
WC = Wind load for construction conditions

In this design example, it has been assumed that there is no equipment on the bridge during construction and wind load is not considered during construction or in the final condition. Refer to Design Example 1 of the NSBA Steel Bridge Design Handbook for an illustration of these wind-load checks. Thermal loads and vehicular braking forces are also not considered.

6.0 ANALYSIS

Article 4.4 of the *AASHTO LRFD BDS* requires that the analysis be performed using a method that satisfies the requirements of equilibrium and compatibility and utilizes stress-strain relationships for the proposed materials. Article 4.6.1.2 provides additional guidelines for structures that are curved in plan. The moments, shears, and other force effects required to proportion the superstructure components are to be based on a rational analysis of the entire superstructure. Equilibrium of horizontally curved I-girders is developed by the transfer of load between the girders, thus the analysis must recognize the integrated behavior of structural components.

Furthermore, in accordance with Article 4.6.1.2, the entire superstructure, including bearings, is to be considered as an integral structural unit in the analysis. Boundary conditions should represent the articulations provided by the bearings and/or integral connections used in the design.

In most cases, small deflection elastic theory is acceptable for the analysis of horizontally curved steel-girder bridges. However, curved girders, especially I-girders, are prone to deflect laterally when the girders are insufficiently braced during erection, and this behavior may not be appropriately recognized in some cases by small deflection theory.

In general, three levels of analysis exist for horizontally curved girder bridges: approximate methods of analysis, 2D (two-dimensional) methods of analysis, and 3D (three-dimensional) methods of analysis. The V-load method is an approximate analysis method that may be used to analyze curved I-girder bridges. This statics-based method was developed based on the understanding of the distribution of forces through the curved bridge system. The two primary types of 2D analysis models are the traditional grid (or grillage) model and the plate and eccentric beam model. In a traditional 2D grid model, the girders and cross-frames are modeled using beam elements, with nodes in a single horizontal plane. In a plate and eccentric beam model, the girders and cross-frames are modeled using beam elements, with nodes in a single horizontal plane, and the deck is modeled with plate or shell elements offset a vertical distance from the steel superstructure elements. A 3D model recognizes the depth of the superstructure. In a 3D model, the girders are typically modeled using beam elements for the flanges and plate or shell elements for the webs. The deck is typically modeled using plate or shell elements. Truss-type cross-frame members are typically modeled using beam or truss-type elements; solid web diaphragms are typically modeled using plate or shell elements, sometimes with beam elements used to model the diaphragm flanges. Two planes of nodes are typically used on each girder, one in the plane of the top flange and the second in the plane of the bottom flange. Further details regarding these methods of analysis can be found in the NSBA's *Steel Bridge Handbook Design: Structural Analysis* [8] and in the FHWA *Manual for Refined Analysis in Bridge Design and Evaluation* [9].

It should be noted that when an I-girder bridge satisfies the requirements of Article 4.6.1.2.4b, the effects of curvature may be ignored in the analysis for determining the major-axis bending moments and shears. If the requirements of Article 4.6.1.2.4b are satisfied, the I-girders may be analyzed as individual straight girders with a span length equal to the arc length. Cross-frame or diaphragm spacing is to be set to limit flange lateral bending effects in the girder, which may be determined from an appropriate approximation. The cross-frame or diaphragm spacing must also satisfy Eq. (6.7.4.2-1). Cross-frames or diaphragms and their connections are to be designed in

accordance with the applicable provisions of Articles 6.7.4.2 and 6.13. At a minimum, cross-frame or diaphragms are to be designed to transfer wind loads according to the provisions of Article 4.6.2.7 and to meet all applicable slenderness requirements specified in Articles 6.8.4 or 6.9.3, as applicable. Although not currently required by AASHTO, it is recommended that cross-frames for such bridges also be designed to satisfy the stability bracing strength and stiffness requirements specified in AISC Specification Appendix 6 (Article 6.3.2a). Consult the NSBA's *Steel Bridge Handbook Design: Bracing System Design* [10] and *National Cooperative Highway Research Project Report 962: Proposed Modification to AASHTO Cross-Frame Analysis and Design* for further information on these requirements [11]

6.1 Three-Dimensional Finite Element Analysis

A three-dimensional finite element analysis was used to analyze the superstructure in this design example. The girder webs were modeled using plate elements. The top and bottom flanges were modeled with beam elements. The girder elements were connected to nodes that were placed in two horizontal planes, one plane at the top flange and one plane at the bottom flange. The horizontal curvature of the girders was represented by straight elements that have small kinks at the nodes, rather than by curved elements. Nodes were placed at the top and bottom flanges along the girders at each cross-frame location and typically at the third points along the length of the girders between cross-frame locations.

The composite deck was modeled using a series of eight-node solid elements attached to the girder top flanges with beam elements, which represented the shear studs.

Bearings were modeled with dimensionless elements called “foundation elements.” These dimensionless elements can provide six different stiffnesses, with three for translation and three for rotation. If a guided bearing is to be modeled and is oriented along the tangential axis of a girder, a stiffness of zero is assigned to the stiffness in the tangential direction. The stiffness of the bearing, and supporting structure if not explicitly modeled, is assigned to the direction orthogonal to the tangential axis.

Cross-frame members were modeled with individual truss elements connected to the nodes at the top and bottom flanges of the girders. Article 4.6.3.3.4 specifies that the influence of end-connection eccentricities is to be considered in the calculation of the equivalent axial stiffness of single-angle and flange-connected tee-section cross-frame members in the analysis. In lieu of a more accurate analysis, Article C4.6.3.3.4 recommends that a stiffness reduction factor of 0.65 be applied to the axial stiffness, AE , of the cross-frame members in a 3D analysis, or when computing the equivalent beam stiffness of the cross-frame members in a 2D analysis, to account for the influence of the end-connection eccentricities. Although this reduction factor was not applied in the analysis originally performed for this design example, the use of this stiffness reduction factor is strongly encouraged.

6.1.1 Bearing Orientation

The orientation and horizontal restraint of the bearings affects the behavior of most girder bridges for most load conditions (and particularly for horizontal loads). This is especially true for curved and skewed girder bridges.

In the analyses to determine the cross-frame forces and the horizontal bearing reactions in this example, the bearings at the piers are assumed fixed against translation in both the radial and tangential directions. The bearings at the abutments are assumed fixed against radial movement but are assumed free in the tangential direction (i.e., no horizontal restraint). The pier stiffness in the tangential direction at the fixed bearings is considered and is simulated in the analysis by using a spring with a spring constant based on the computed stiffness of the pier in the tangential direction. In the radial direction, the piers and abutments are assumed to be perfectly rigid. Section 2.2 of the *Reference Manual for NHI Course 130095, Analysis and Design of Skewed and Curved Steel Bridges with LRFD* [12] discusses various strategies for the orientation of bearings and their constraints and the effect of pier flexibility on bearing constraint in skewed and curved steel-girder bridges in greater detail.

The tangential restraints resist the elastic lengthening of the girders due to bending. The result is large tangential bearing forces, which in turn cause an arching effect on the girders that reduces the apparent bending moments due to gravity loads. If the reduced moments were used in the girder design, the bearings would have to function as assumed for the life of the bridge to prevent possible overstress in the girders. To avoid this situation, the horizontal bearing restraints described above are assumed free for the gravity load analyses used to design the girders; only the restraint necessary to provide overall stability to the system is provided in the analysis. However, the proper horizontal bearing restraints (described above) are assumed in the analyses to determine cross-frame forces and the horizontal bearing reactions for the design of the bearings for horizontal loads (e.g., wind and thermal loads).

6.1.2 Live Load Analysis

The use of live load distribution factors is typically not appropriate for horizontally curved steel I-girder bridges because these structures are most appropriately analyzed as a system. Therefore, influence surfaces are most often utilized to more accurately determine the live-load force effects in curved girder bridges. Influence surfaces are an extension of influence lines, in that an influence surface not only considers the longitudinal position of the live loads but also the transverse position.

Influence surfaces provide influence ordinates over the entire deck. The influence ordinates are determined by applying a series of unit vertical loads, one at a time, at each node on the bridge deck surface. The magnitude of the member response under consideration for each unit vertical load is the magnitude of the ordinate of the influence surface at the point on the deck where the load is applied. The entire influence surface is created by curve fitting between calculated ordinates. Specified live loads are then placed on the surface, mathematically, at the critical locations (maximum and minimum effects), as allowed by the governing specification. The actual live load effect is determined by multiplying the live load by the corresponding ordinate. In the

case of an HL-93 truck or tandem load, a different ordinate will probably exist for each wheel load. The total HL-93 truck or tandem live load effect is the summation of all the wheel loads times their respective ordinates. For the design lane load portion of the HL-93 loading, the live load force effect is determined by multiplying the magnitude of the uniform load by the area of the influence surface covered by the load.

The fatigue load, which consists of a single design truck without a lane load, is analyzed in a similar manner as the HL-93 truck load.

In curved girder bridges, influence surfaces are generally needed for all force results, such as major-axis bending moments, flange lateral bending moments, girder shears, reactions, torques, deflections, cross-frame forces, lateral-bracing forces, etc.

Unless noted otherwise, all live load force effects in this example were computed using influence surfaces developed using the three-dimensional analysis. The dynamic load allowance (impact) was applied to the force effects in accordance with Article 3.6.2 for strength, service, and fatigue as required. Multiple presence factors were also appropriately applied to the force effects from the analysis. Also, as appropriate, centrifugal force effects were considered in the analysis by applying adjustment factors to the wheel loads as described in Section 6.3 of this design example.

6.2 Analysis Results

This section shows the results from the three-dimensional analysis of the superstructure. Analysis results are provided for the moments and shears for all four girders. All analysis results are unfactored. The reported live load results include multiple presence factors, dynamic load allowance (impact), and centrifugal force effects.

NOTE: *The analysis results shown herein, including the results of the deck-placement analysis shown in Table 9 and Table 10, apply to an example girder designed using earlier versions of the AASHTO LRFD BDS (i.e., prior to the 8th Edition). Revisions to the load factors for the Fatigue I and Fatigue II load combinations that appeared in the 8th Edition specification necessitated an increase in some of the plate sizes in this example design. Other flange sizes were revised slightly from the original design to satisfy the $L_{fs}/85$ guideline described previously. While it is nearly always desirable to perform a new analysis whenever plate sizes are revised, the effect on the analysis results in this case was felt to be relatively minor and so new analyses were not performed. The primary intent of this example is to illustrate the proper application of the AASHTO LRFD BDS provisions to the design of a continuous horizontally curved composite steel I-girder bridge with no skew. However, this also illustrates that a designer should always be aware of specification changes and how they may affect a design and perhaps future load ratings.*

Table 1 Girder G1 Unfactored Shears by Tenth Point

Girder G1 Unfactored Shears									
10th Point	Span Length (ft)	Dead Load				LL+I		Fatigue LL+I	
		DC1 _{STEEL} (kip)	DC1 _{CONC} (kip)	DC2 (kip)	DW (kip)	Pos. (kip)	Neg. (kip)	Pos. (kip)	Neg. (kip)
0	0.00	14	66	17	13	109	-31	45	-11
1	15.62	9	45	6	9	87	-21	33	-5
2	31.25	5	26	2	5	69	-27	27	-8
3	46.87	1	9	2	2	55	-36	23	-12
4	62.49	-2	-9	0	-1	43	-46	19	-16
5	78.11	-5	-29	-4	-5	34	-58	13	-20
6	93.74	-9	-49	-8	-9	27	-73	9	-27
7	109.36	-14	-70	-12	-13	25	-89	8	-33
8	124.98	-20	-98	-14	-18	22	-106	8	-37
9	140.61	-28	-127	-23	-24	20	-125	7	-41
10	156.23	-40	-159	-35	-30	12	-146	4	-48
10	0.00	41	159	35	31	148	-12	49	-4
11	20.50	25	116	22	23	124	-24	39	-7
12	41.01	17	83	11	15	104	-31	36	-9
13	61.51	10	50	8	9	83	-33	29	-9
14	82.02	4	24	4	4	66	-37	24	-12
15	102.52	0	0	0	0	51	-52	19	-19
16	123.03	-5	-25	-4	-4	41	-66	15	-24
17	143.53	-10	-51	-7	-10	33	-81	11	-29
18	164.04	-16	-80	-12	-15	29	-102	9	-36
19	184.54	-26	-119	-21	-23	25	-121	7	-40
20	205.05	-41	-160	-36	-31	12	-152	4	-51
20	0.00	40	158	35	31	154	-11	52	-4
21	15.62	28	126	24	23	121	-18	43	-5
22	31.25	20	96	16	17	107	-21	39	-5
23	46.87	14	72	10	14	91	-25	33	-8
24	62.49	9	50	7	9	75	-30	28	-11
25	78.11	6	30	4	6	62	-34	24	-15
26	93.74	1	9	1	2	48	-44	17	-19
27	109.36	-1	-8	-1	-1	38	-55	13	-23
28	124.98	-5	-26	-3	-6	31	-69	9	-27
29	140.61	-9	-45	-7	-9	24	-86	8	-33
30	156.23	-14	-66	-17	-13	29	-108	9	-45

Note: Live load results include multiple presence factors, dynamic load allowance (impact), and centrifugal force effects.

Table 2 Girder G2 Unfactored Shears by Tenth Point

Girder G2 Unfactored Shears									
10th Point	Span Length (ft)	Dead Load				LL+I		Fatigue LL+I	
		DC1 _{STEEL}	DC1 _{CONC}	DC2	DW	Pos.	Neg.	Pos.	Neg.
		(kip)	(kip)	(kip)	(kip)	(kip)	(kip)	(kip)	(kip)
0	0.00	16	71	7	15	109	-12	41	-3
1	15.87	10	47	8	9	73	-13	23	-3
2	31.75	6	26	7	5	59	-24	19	-7
3	47.62	1	9	0	2	49	-33	15	-9
4	63.50	-2	-11	-2	-2	39	-42	12	-12
5	79.37	-6	-30	-4	-5	32	-52	12	-15
6	95.25	-10	-51	-7	-9	25	-63	9	-19
7	111.12	-15	-71	-10	-13	17	-75	5	-21
8	126.99	-21	-92	-15	-18	8	-89	1	-25
9	142.87	-28	-116	-16	-24	1	-108	0	-31
10	158.74	-37	-139	-16	-29	4	-138	1	-44
10	0.00	37	139	16	30	138	-4	44	-1
11	20.83	24	109	15	22	101	-9	28	-3
12	41.67	17	78	14	16	84	-22	20	-5
13	62.50	11	52	8	9	70	-27	20	-8
14	83.34	5	26	3	5	58	-33	16	-9
15	104.17	0	0	0	0	45	-46	12	-13
16	125.01	-6	-26	-3	-5	34	-56	11	-16
17	145.84	-11	-51	-8	-10	28	-68	8	-20
18	166.68	-17	-79	-12	-15	19	-84	5	-23
19	187.51	-26	-109	-17	-22	12	-97	4	-25
20	208.35	-37	-139	-15	-30	4	-148	1	-47
20	0.00	37	139	15	30	148	-4	47	-1
21	15.87	28	117	16	23	101	-7	31	-1
22	31.75	21	93	13	19	89	-14	27	-4
23	47.62	15	71	11	13	77	-21	23	-7
24	63.50	10	50	8	9	66	-27	20	-9
25	79.37	7	31	5	5	56	-34	17	-12
26	95.25	2	11	1	2	47	-42	13	-13
27	111.12	-1	-7	-2	-1	38	-51	11	-16
28	126.99	-6	-27	-5	-6	29	-60	8	-20
29	142.87	-10	-48	-7	-9	20	-76	5	-24
30	158.74	-16	-71	-7	-15	12	-111	3	-43

Note: Live load results include multiple presence factors, dynamic load allowance (impact), and centrifugal force effects.

Table 3 Girder G3 Unfactored Shears by Tenth Point

Girder G3 Unfactored Shears									
10th Point	Span Length (ft)	Dead Load				LL+I		Fatigue LL+I	
		DC1 _{STEEL}	DC1 _{CONC}	DC2	DW	Pos.	Neg.	Pos.	Neg.
		(kip)	(kip)	(kip)	(kip)	(kip)	(kip)	(kip)	(kip)
0	0.00	18	78	8	16	113	-17	40	-4
1	16.13	12	53	9	10	84	-18	23	-3
2	32.25	7	29	6	6	64	-28	19	-7
3	48.38	1	8	0	1	51	-37	15	-9
4	64.50	-3	-12	-2	-2	41	-45	12	-12
5	80.63	-7	-34	-5	-6	32	-54	11	-15
6	96.75	-12	-56	-8	-9	26	-67	8	-19
7	112.88	-17	-77	-10	-15	19	-81	5	-21
8	129.01	-23	-98	-17	-18	11	-95	3	-25
9	145.13	-31	-123	-17	-25	3	-114	0	-31
10	161.26	-42	-151	-17	-31	6	-143	1	-44
10	0.00	42	150	17	32	143	-6	44	-1
11	21.16	28	114	16	24	109	-14	28	-4
12	42.33	19	84	16	15	90	-24	20	-7
13	63.49	13	56	8	11	75	-27	20	-7
14	84.66	6	28	4	4	60	-34	16	-9
15	105.82	0	0	0	0	46	-47	12	-13
16	126.99	-6	-28	-4	-5	36	-60	11	-16
17	148.15	-13	-56	-9	-11	28	-73	8	-19
18	169.32	-19	-84	-13	-17	20	-90	5	-23
19	190.48	-29	-115	-17	-25	16	-103	4	-27
20	211.65	-42	-150	-17	-31	6	-153	1	-47
20	0.00	42	151	17	31	153	-6	47	-1
21	16.13	31	124	17	25	108	-6	31	-3
22	32.25	23	99	15	20	95	-15	27	-5
23	48.38	17	77	12	15	83	-22	23	-7
24	64.50	12	55	9	10	69	-28	20	-9
25	80.63	8	35	5	7	57	-35	17	-12
26	96.75	3	13	1	3	48	-42	13	-13
27	112.88	-1	-7	-2	-1	39	-52	11	-16
28	129.01	-6	-29	-5	-5	30	-65	8	-19
29	145.13	-12	-53	-8	-11	23	-84	5	-24
30	161.26	-18	-77	-8	-16	17	-112	4	-41

Note: Live load results include multiple presence factors, dynamic load allowance (impact), and centrifugal force effects.

Table 4 Girder G4 Unfactored Shears by Tenth Point

Girder G4 Unfactored Shears									
10th Point	Span Length (ft)	Dead Load				LL+I		Fatigue LL+I	
		DC1 _{STEEL}	DC1 _{CONC}	DC2	DW	Pos.	Neg.	Pos.	Neg.
		(kip)	(kip)	(kip)	(kip)	(kip)	(kip)	(kip)	(kip)
0	0.00	23	92	23	18	143	-37	53	-11
1	16.38	16	69	11	13	119	-33	41	-9
2	32.75	11	44	5	10	99	-33	36	-8
3	49.13	3	10	3	2	79	-42	29	-11
4	65.51	-4	-19	-2	-3	58	-58	21	-19
5	81.89	-10	-47	-7	-9	40	-77	16	-25
6	98.26	-18	-74	-13	-14	25	-96	9	-33
7	114.64	-24	-101	-18	-18	17	-114	4	-40
8	131.02	-30	-121	-20	-23	14	-132	3	-45
9	147.39	-36	-134	-26	-27	13	-148	3	-49
10	163.77	-45	-144	-36	-28	9	-159	3	-55
10	0.00	44	142	36	29	159	-9	55	-3
11	21.49	33	131	27	27	150	-24	47	-5
12	42.99	25	107	17	21	137	-26	45	-7
13	64.48	18	77	12	15	114	-30	37	-8
14	85.98	9	38	7	7	90	-41	31	-13
15	107.47	0	-1	0	0	65	-65	23	-23
16	128.97	-9	-38	-7	-7	45	-88	15	-31
17	150.46	-17	-76	-12	-15	35	-110	9	-36
18	171.96	-26	-109	-18	-21	27	-132	7	-44
19	193.45	-33	-127	-26	-25	24	-146	5	-48
20	214.95	-44	-141	-36	-29	7	-159	3	-56
20*	0.00	45	144	36	28	169	-7	60	-3
21*	16.38	36	134	28	25	140	-15	49	-3
22*	32.75	30	121	22	21	130	-15	47	-3
23*	49.13	24	101	17	19	116	-17	41	-5
24*	65.51	18	74	12	15	98	-26	35	-9
25*	81.89	10	47	8	8	81	-40	29	-16
26*	98.26	4	19	3	2	59	-57	21	-21
27*	114.64	-3	-10	-1	-4	45	-78	13	-29
28*	131.02	-11	-44	-7	-8	36	-98	8	-36
29*	147.39	-16	-69	-12	-12	30	-117	8	-43
30*	163.77	-23	-92	-23	-18	36	-142	9	-53

Note: Live load results include multiple presence factors, dynamic load allowance (impact), and centrifugal force effects.

* Exact analysis results for DC₁ shears in Span 3 of Girder 4 are not provided in the NCHRP example referenced by this design example. For this design example, DC₁ shears in Span 3 of Girder 4 are based on Span 1 Girder 4 shears, as the bridge is symmetrical.

Table 5 Girder G1 Unfactored Major-Axis Bending Moments by Tenth Point

Girder G1 Unfactored Major-Axis Bending Moments									
10th Point	Span Length (ft)	Dead Load				LL+I		Fatigue LL+I	
		DC1 _{STEEL}	DC1 _{CONC}	DC2	DW	Pos.	Neg.	Pos.	Neg.
		(kip-ft)	(kip-ft)	(kip-ft)	(kip-ft)	(kip-ft)	(kip-ft)	(kip-ft)	(kip-ft)
0	0.00	0	0	0	0	0	0	0	0
1	15.62	178	889	184	188	1415	-381	529	-116
2	31.25	295	1478	288	311	2409	-718	873	-200
3	46.87	351	1767	327	375	3003	-1006	1049	-252
4	62.49	348	1754	316	373	3249	-1245	1103	-291
5	78.11	284	1438	260	313	3192	-1448	1067	-327
6	93.74	156	804	161	189	2875	-1605	955	-412
7	109.36	-42	-184	6	-6	2201	-2003	741	-512
8	124.98	-322	-1553	-229	-274	1465	-2569	463	-621
9	140.61	-716	-3348	-564	-619	770	-3305	181	-764
10	156.23	-1333	-5897	-1169	-1167	883	-5274	185	-991
10	0.00	-1333	-5897	-1169	-1167	883	-5274	185	-991
11	20.50	-569	-2719	-447	-505	842	-2755	232	-624
12	41.01	-123	-648	-78	-94	1694	-1796	588	-484
13	61.51	157	709	141	176	2655	-1485	917	-369
14	82.02	331	1554	293	347	3273	-1481	1085	-329
15	102.52	384	1812	335	400	3498	-1462	1144	-360
16	123.03	323	1513	272	338	3297	-1488	1089	-327
17	143.53	159	717	150	182	2678	-1528	924	-371
18	164.04	-131	-688	-87	-103	1705	-1871	597	-497
19	184.54	-575	-2733	-433	-489	906	-2700	261	-620
20	205.05	-1302	-5781	-1124	-1130	885	-5113	180	-956
20	0.00	-1302	-5781	-1124	-1130	885	-5113	180	-956
21	15.62	-726	-3371	-560	-617	776	-3236	191	-744
22	31.25	-323	-1555	-237	-277	1464	-2544	468	-612
23	46.87	-42	-187	0	-5	2196	-1980	744	-505
24	62.49	154	797	160	187	2866	-1567	956	-405
25	78.11	283	1433	262	313	3186	-1420	1068	-323
26	93.74	347	1750	315	373	3247	-1222	1107	-284
27	109.36	350	1761	323	372	3003	-988	1052	-251
28	124.98	294	1473	282	309	2420	-706	880	-204
29	140.61	177	881	183	184	1436	-376	543	-112
30	156.23	0	0	0	0	0	0	0	0

Note: Live load results include multiple presence factors, dynamic load allowance (impact), and centrifugal force effects.

Table 6 Girder G2 Unfactored Major-Axis Bending Moments by Tenth Point

Girder G2 Unfactored Major-Axis Bending Moments									
10th Point	Span Length (ft)	Dead Load				LL+I		Fatigue LL+I	
		DC1 _{STEEL} (kip-ft)	DC1 _{CONC} (kip-ft)	DC2 (kip-ft)	DW (kip-ft)	Pos. (kip-ft)	Neg. (kip-ft)	Pos. (kip-ft)	Neg. (kip-ft)
0	0.00	0	0	0	0	0	0	0	0
1	15.87	206	962	139	201	1210	-185	373	-43
2	31.75	340	1585	247	330	1996	-376	581	-87
3	47.62	404	1875	312	392	2444	-570	681	-132
4	63.50	397	1840	322	389	2632	-772	715	-179
5	79.37	322	1488	271	321	2582	-986	695	-228
6	95.25	177	820	149	189	2325	-1196	631	-280
7	111.12	-38	-182	-23	-17	1813	-1635	507	-335
8	126.99	-334	-1533	-247	-291	1203	-2146	331	-391
9	142.87	-733	-3262	-494	-644	605	-2683	148	-455
10	158.74	-1324	-5605	-817	-1186	556	-4053	112	-560
10	0.00	-1324	-5605	-817	-1186	556	-4053	112	-560
11	20.83	-597	-2681	-419	-526	652	-2177	167	-369
12	41.67	-143	-676	-95	-109	1351	-1347	400	-301
13	62.50	159	700	145	173	2070	-931	591	-241
14	83.34	355	1600	284	355	2505	-760	703	-184
15	104.17	416	1879	333	410	2668	-664	739	-143
16	125.01	347	1550	293	344	2521	-764	703	-185
17	145.84	162	714	139	178	2060	-927	585	-243
18	166.68	-150	-708	-106	-120	1355	-1375	396	-308
19	187.51	-602	-2690	-412	-513	688	-2142	179	-364
20	208.35	-1297	-5504	-811	-1151	552	-3942	109	-549
20	0.00	-1297	-5504	-811	-1151	552	-3942	109	-549
21	15.87	-742	-3274	-495	-640	649	-2644	164	-447
22	31.75	-336	-1539	-248	-295	1236	-2139	339	-387
23	47.62	-39	-185	-25	-14	1835	-1640	509	-332
24	63.50	176	816	148	187	2344	-1214	633	-279
25	79.37	321	1485	264	320	2600	-992	699	-228
26	95.25	395	1833	318	388	2650	-775	719	-177
27	111.12	403	1865	314	389	2458	-572	685	-131
28	126.99	338	1575	248	328	2017	-379	588	-87
29	142.87	203	950	135	196	1240	-189	383	-43
30	158.74	0	0	0	0	0	0	0	0

Note: Live load results include multiple presence factors, dynamic load allowance (impact), and centrifugal force effects.

Table 7 Girder G3 Unfactored Major-Axis Bending Moments by Tenth Point

Girder G3 Unfactored Major-Axis Bending Moments									
10th Point	Span Length (ft)	Dead Load				LL+I		Fatigue LL+I	
		DC1 _{STEEL}	DC1 _{CONC}	DC2	DW	Pos.	Neg.	Pos.	Neg.
		(kip-ft)	(kip-ft)	(kip-ft)	(kip-ft)	(kip-ft)	(kip-ft)	(kip-ft)	(kip-ft)
0	0.00	0	0	0	0	0	0	0	0
1	16.13	248	1090	163	226	1388	-301	389	-71
2	32.25	406	1775	281	366	2296	-581	600	-133
3	48.38	478	2080	349	429	2814	-845	700	-195
4	64.50	468	2024	355	422	3038	-1105	733	-256
5	80.63	379	1622	294	345	2993	-1365	708	-316
6	96.75	206	873	156	196	2703	-1628	639	-381
7	112.88	-48	-237	-44	-20	2143	-2126	508	-452
8	129.01	-388	-1708	-292	-326	1435	-2711	339	-525
9	145.13	-842	-3570	-568	-702	727	-3254	169	-608
10	161.26	-1517	-6112	-931	-1283	750	-4594	209	-732
10	0.00	-1517	-6112	-931	-1283	750	-4594	209	-732
11	21.16	-694	-2960	-485	-578	699	-2517	173	-421
12	42.33	-183	-803	-122	-129	1454	-1560	371	-344
13	63.49	164	708	149	179	2255	-1160	541	-272
14	84.66	390	1696	307	377	2837	-1015	659	-207
15	105.82	461	2006	362	439	3026	-914	696	-160
16	126.99	380	1646	317	367	2851	-1020	657	-209
17	148.15	167	721	145	183	2259	-1165	535	-276
18	169.32	-191	-832	-134	-140	1459	-1591	368	-352
19	190.48	-700	-2965	-476	-562	727	-2461	184	-419
20	211.65	-1486	-5999	-923	-1244	733	-4458	203	-711
20	0.00	-1486	-5999	-923	-1244	733	-4458	203	-711
21	16.13	-852	-3586	-569	-698	747	-3200	183	-595
22	32.25	-389	-1714	-293	-330	1450	-2685	345	-519
23	48.38	-47	-240	-40	-27	2153	-2120	511	-448
24	64.50	206	870	155	195	2711	-1623	641	-377
25	80.63	378	1619	287	344	3002	-1360	711	-313
26	96.75	468	2017	352	420	3044	-1100	735	-253
27	112.88	476	2065	350	426	2811	-837	697	-192
28	129.01	403	1759	281	362	2299	-572	599	-132
29	145.13	244	1071	156	220	1408	-298	395	-68
30	161.26	0	0	0	0	0	0	0	0

Note: Live load results include multiple presence factors, dynamic load allowance (impact), and centrifugal force effects.

Table 8 Girder G4 Unfactored Major-Axis Bending Moments by Tenth Point

Girder G4 Unfactored Major-Axis Bending Moments									
10th Point	Span Length (ft)	Dead Load				LL+I		Fatigue LL+I	
		DC1 _{STEEL}	DC1 _{CONC}	DC2	DW	Pos.	Neg.	Pos.	Neg.
		(kip-ft)	(kip-ft)	(kip-ft)	(kip-ft)	(kip-ft)	(kip-ft)	(kip-ft)	(kip-ft)
0	0.00	0	0	0	0	0	0	0	0
1	16.38	328	1364	287	288	2009	-529	695	-143
2	32.75	558	2305	463	483	3570	-1059	1192	-289
3	49.13	678	2775	542	586	4636	-1582	1497	-436
4	65.51	675	2744	527	586	5134	-2076	1611	-580
5	81.89	546	2192	425	479	5084	-2546	1560	-715
6	98.26	293	1136	241	269	4575	-2966	1396	-843
7	114.64	-69	-374	-24	-32	3498	-3745	1072	-957
8	131.02	-532	-2263	-375	-411	2286	-4502	657	-1060
9	147.39	-1108	-4482	-814	-846	1135	-5092	249	-1161
10	163.77	-1917	-7272	-1537	-1478	1368	-6726	351	-1315
10	0.00	-1917	-7272	-1537	-1478	1368	-6726	351	-1315
11	21.49	-940	-3811	-675	-713	1078	-3926	280	-852
12	42.99	-277	-1151	-155	-165	2307	-2610	749	-737
13	64.48	208	881	214	257	3687	-2110	1207	-620
14	85.98	531	2224	474	537	4842	-1924	1484	-495
15	107.47	635	2658	554	629	5192	-1768	1579	-395
16	128.97	518	2173	452	526	4832	-1940	1487	-500
17	150.46	210	888	225	260	3765	-2147	1225	-631
18	171.96	-284	-1174	-163	-177	2337	-2377	767	-759
19	193.45	-945	-3805	-648	-689	1130	-3812	317	-844
20	214.95	-1871	-7126	-1474	-1432	1309	-6519	336	-1259
20*	0.00	-1871	-7126	-1474	-1432	1309	-6519	336	-1259
21*	16.38	-1108	-4482	-806	-854	1140	-4897	271	-1124
22*	32.75	-532	-2263	-381	-405	2272	-4379	665	-1032
23*	49.13	-69	-374	-24	-32	3470	-3676	1069	-937
24*	65.51	293	1136	243	267	4553	-2915	1393	-827
25*	81.89	546	2192	429	475	5070	-2505	1560	-703
26*	98.26	675	2744	529	584	5127	-2044	1612	-569
27*	114.64	678	2755	540	588	4643	-1557	1503	-428
28*	131.02	558	2305	460	486	3607	-1051	1209	-285
29*	147.39	328	1364	286	289	2054	-531	716	-144
30*	163.77	0	0	0	0	0	0	0	0

Note: Live load results include multiple presence factors, dynamic load allowance (impact), and centrifugal force effects.

*Exact analysis results for DC₁ moments in Span 3 of Girder 4 are not provided in the NCHRP example referenced by this design example. For this design example, DC₁ moments in Span 3 of Girder 4 are based on Span 1 Girder 4 moments, as the bridge is symmetrical.

Table 9 Selected Girder G4 Unfactored Major-Axis Bending Moments

Girder G4 Unfactored Moments Used in Example Calculations*											
Location	10th Point	Dead Load				LL+I		Fatigue LL+I		Concrete Casts	
		DC1 _{STEEL}	DC1 _{CONC}	DC2	DW	Pos.	Neg.	Pos.	Neg.	#1	#2
		(kip-ft)	(kip-ft)	(kip-ft)	(kip-ft)	(kip-ft)	(kip-ft)	(kip-ft)	(kip-ft)	(kip-ft)	(kip-ft)
Section G4-1	4.2	661	2682	510	583	5125	-	1603	-603	3932	-3035
Section G4-2	10	-1917	-7272	-1537	-1478	-	-6726	351	-1315	-	-
Field Splice 2	11.8**	-382	-1585	-250	-237	2054	-2772	664	-759	-1910	-169

* Values not shown are not critical and/or are not used in the example calculations.

** Actual Field Splice 2 location is at 10th Point 12, but the values at 10th Point 11.8 are conservatively used for design.

Table 10 Selected Girder G4 Unfactored Shears by Tenth Point

Girder G4 Unfactored Shears Used in Example Calculations ⁽¹⁾											
Location	10th Point	Dead Load				LL+I		Fatigue LL+I		Concrete Casts	
		DC1 _{STEEL}	DC1 _{CONC}	DC2	DW	Pos.	Neg.	Pos.	Neg.	#1	#2
		(kip)	(kip)	(kip)	(kip)	(kip)	(kip)	(kip)	(kip)	(kip)	(kip)
Section G4-1	4.2	-5	-23.8	-4	-2.9	-	-61.3	20	-20	-	-
Section G4-2	10	-45	-144	-36	-28	-	-159	3	-55	-	-
Section G4-3	0	23	92	23	19	143	-	-	-	-	-
Field Splice 2	11.8 ⁽²⁾	27	112	19	22	139	-	-	-	7	92

(1) Values not shown are not critical and/or are not used in the example calculations.

(2) Actual Field Splice 2 location is at 10th Point 12, but the values at 10th Point 11.8 are conservatively used for design.

7.0 DESIGN

7.1 General Design Considerations

7.1.1 Flanges

The size of curved I-girder flanges is a function of girder depth, girder radius, cross-frame spacing, and the minimum specified yield stress of the flange.

According to Article 6.10.6.2.3, sections in negative flexure in kinked (chorded) continuous or horizontally curved steel girder bridges are to be proportioned at the strength limit state according to the provisions specified in Article 6.10.8. That is, the sections must always be treated as slender-web sections regardless of the web slenderness meaning that the provisions of Appendix A6 may not be used. In regions of negative flexure, the bottom (compression) flange is a discretely braced compression flange and must be checked for local and lateral torsional buckling under the combined major-axis bending and flange lateral bending stress (Article 6.10.8.1.1). The top (tension) flange in regions of negative flexure is considered to be continuously braced by the composite concrete deck at the strength limit state. Continuously braced flanges in tension must be checked for nominal yielding under only the major-axis bending stress at the strength limit state (Article 6.10.8.1.3). Any flange lateral bending stresses need not be considered once the flange is continuously braced (Article C6.10.1.6).

The smaller flange plate should be used to compute the nominal lateral torsional buckling resistance of a discretely braced compression flange between brace points when the flange size changes within a panel, unless the transition to the smaller section is located at a distance less than or equal to 20 percent of the unbraced length from the brace point with the smaller moment, and the lateral moment of inertia of the flange of the smaller section is equal to or larger than one-half the corresponding value in the larger section, in which case the flange transition may be ignored (Article 6.10.8.2.3). Otherwise, the smaller section within the panel is used to compute the nominal lateral torsional buckling resistance. For checking the lateral torsional buckling resistance, the largest major-axis bending stress within the unbraced length is to be used in conjunction with the largest flange lateral bending stress (Article 6.10.1.6). For checking the local buckling resistance, the major-axis bending and flange lateral bending stress at the section under consideration may be used.

According to Article 6.10.6.2.2, at the strength limit state, composite sections in positive flexure in kinked (chorded) continuous or horizontally curved steel girder bridges are to be considered as noncompact sections designed according to the requirements of Article 6.10.7.2. For noncompact sections, the nominal flexural resistance is not permitted to exceed the moment at first yield. The nominal flexural resistance in these cases is therefore more appropriately expressed in terms of the elastically computed flange stress. The major-axis bending stress in compression flanges of noncompact composite sections in positive flexure is not permitted to exceed the flange yield stress at the strength limit state. For composite sections in positive flexure, lateral bending does not need to be considered in the compression flange at the strength limit state because the flange is continuously supported by the concrete deck. The combined major-axis bending and flange lateral bending stress in tension flanges of noncompact composite sections in positive flexure is also not

permitted to exceed the flange yield stress (Article 6.10.7.2.1). Article 6.10.1.6 specifies that for design checks where the flexural resistance is based on nominal yielding, the major-axis bending and flange lateral bending stresses may be determined as the stresses at the section under consideration.

For constructability, Article 6.10.3 requires that noncomposite top flanges in regions of positive flexure be designed as discretely braced compression flanges prior to hardening of the concrete deck to verify that no local or lateral torsional buckling occurs under the combined major-axis bending and flange lateral bending stresses during the deck placement, which tends to lead to the use of wider top flanges in these regions.

7.1.2 Webs

According to the *AASHTO LRFD BDS*, webs are investigated for elastic bend-buckling at the service limit state and for constructability without consideration of post-buckling shear or bending strength (Articles 6.10.4.2.2 and 6.10.3.2.1, respectively). Bend-buckling must be considered for both the noncomposite and composite cases since the effective slenderness changes when the neutral axis shifts. Webs are also investigated for shear to determine whether transverse stiffeners are required (Article 6.10.9). A special fatigue requirement for webs must also be checked to prevent significant elastic flexing of the web due to shear at the fatigue limit state by limiting the shear in the web to a level that will not result in shear buckling under the combined effects of permanent load and the repetitive fatigue live load (Article 6.10.5.3). This permits the member to sustain an infinite number of smaller loadings without fatigue cracking due to this effect.

7.1.3 Shear Connectors

Shear connectors are to be provided throughout the entire length of the bridge in curved continuous structures according to Article 6.10.10.1. The required pitch of the shear connectors is determined for fatigue and checked for strength. Three 7/8-inch diameter by 6-inch shear studs per row are assumed in the design. The fatigue resistance specified in Article 6.10.10.2 is used for the design of the shear connectors.

The design major-axis bending (longitudinal) fatigue shear range in each stud is computed for a single passage of the factored fatigue truck. The analysis is made assuming that the heavy wheel of the truck is applied to both the positive and negative shear sides of the influence surface. This computation implicitly assumes that the truck direction is reversed. In addition to major-axis bending shear range, Article 6.10.10.1.2 requires that the radial fatigue shear range due to curvature or radial fatigue shear range due to causes other than curvature (whichever is larger) be added vectorially to the major-axis bending shear range for the fatigue check. The deck in the regions in-between points of dead load contraflexure in adjacent spans is considered fully effective in computing the first moment for determining the required pitch for fatigue. This assumption requires tighter shear connector spacing in these regions than if only the longitudinal reinforcing is assumed effective, as is sometimes done for straight bridges. There are several reasons the concrete is assumed effective. First, known field measurements indicate that the concrete deck is effective in tension at service loads. Second, the horizontal shear force in the deck is considered effective in the analysis and the deck must be sufficiently connected to the steel girders to be

consistent with this assumption. Third, maximum shear range occurs when the truck is placed on each side of the point under consideration. Most often this produces positive bending so that the deck is in compression, even when the location is in-between the point of dead load contraflexure and the pier. The point of dead load contraflexure is obviously a poor indicator of positive or negative bending when moving loads are considered.

The strength limit state check for shear connectors (Article 6.10.10.4) requires that a radial shear force due to curvature be considered and be added vectorially to the appropriate specified longitudinal shear force in the concrete deck. In regions between the point of maximum live load moment and each adjacent point of zero moment, the longitudinal force is taken as the specified total longitudinal force in the concrete deck at the point of maximum live load moment. In the regions between the point of maximum live load moment and the centerline of an adjacent interior support, the longitudinal force is conservatively taken as the sum of the specified longitudinal tension force in the concrete deck over an interior support and the specified total longitudinal force in the deck at the point of maximum live load moment in order to provide adequate shear resistance for any live load position. Since there is no point in this region where the live-load moment always changes sign, many shear connectors resist reversing action in the concrete deck depending on the live load position.

For both fatigue and strength checks, the parameters used in the equations are determined using the deck within the effective flange width.

7.1.4 Details (Fatigue Categories for Stiffeners, Cross-Frame Connection Plates, and Shear Studs)

In this example, there are intermediate transverse web stiffeners at three even spaces between cross-frame locations. Intermediate stiffeners are typically fillet welded to the web and to the compression flange. Article 6.10.11.1.1 states that single-sided stiffeners on horizontally curved girders should be attached to both flanges. In this example, the intermediate stiffeners are assumed fillet welded to the tension flange. The termination of the stiffener-to-web weld adjacent to the tension flange is typically stopped a distance of $4t_w$ from the flange-to-web weld. The base metal adjacent to the stiffener weld to the tension flange is checked for fatigue. Condition 4.1 from Table 6.6.1.2.3-1 applies, which corresponds to the base metal at the toe of transverse stiffener-to-flange fillet welds, and Category C' is the indicated fatigue category. Where the stiffener is fillet welded to the compression flange and the flange undergoes a net tension, the flange must also be checked for Category C' . When the girder is curved, the flange lateral bending creates an additional stress at the tip of the stiffener-to-flange weld away from the web. Thus, the total stress range is computed from the sum of the lateral and major-axis bending stress ranges.

Transverse web stiffeners used as connection plates at cross-frames must be positively attached to both flanges (Article 6.6.1.3.1). Typically, the connection plates are fillet welded to the top and bottom flange. When the flanges are subjected to a net tensile stress, fatigue must be checked at these points. This detail is also Condition 4.1 from Table 6.6.1.2.3-1, so the applicable fatigue category is Category C' .

Base metal at the shear stud connector welds to the top flange must be checked for fatigue whenever the flange is subjected to a net tensile stress. Condition 9.1 from Table 6.6.1.2.3-1 relates to the base metal at stud-type shear connectors that are attached by fillet or automatic stud welding, and Category C is the indicated fatigue category.

In this design example, cross-frame angles are assumed to be fillet welded to gusset plates. Condition 7.2 from Table 6.6.1.2.3-1 applies. The assembled cross-frames are then subsequently assumed to be bolted to the connection plates in the field.

7.1.5 Wind Loading

7.1.5.1 Loading

Article 3.8 provides the wind loading to be used for design. Article 3.8.1 requires that various wind directions be examined to determine the extreme force effects in the various elements of the structure. The governing wind force on the curved bridge in this example equals the wind intensity times the projected area of the bridge; in other words, the wind is applied along the chord length. It should be noted that the total force along the chord length is less than that computed if the wind were assumed to be applied perpendicular to the bridge along the arc length. Depending on how the analysis model is set up, the wind force at each node may need to be separated into a transverse and longitudinal component. For simplicity, many designers choose to apply the wind force perpendicular to the girder at each node, which is a conservative approach.

Since there are nodes at the top and bottom of the girder, it is possible to divide the wind force between the top and bottom flange. For the final condition after construction is completed, the tributary area for the top of the windward girder equals half of the girder depth plus the height of the exposed deck and railing concrete times the average spacing to each adjacent node. The tributary area for the bottom of the girder is simply half of the girder depth times the average spacing to each adjacent node.

Since the bridge is superelevated, the girders on the inside of the curve extend below the bottom of girder G4. Each successive girder extends approximately 6 inches lower. This exposed area is included in the load computation if the wind is applied from the G4 side of the bridge. If wind is applied from the G1 side of the bridge, an additional upward projection due to superelevation is manifest in the railing on the opposite side near G4 and is used in computing the wind loading.

When the girders are being erected, wind load may be applied across the ends of the girders, which are temporarily exposed. An analysis of wind load during erection is not included in this example. Further guidance on checking wind load during erection is provided in the *AASHTO Guide Specifications for Wind Loads on Bridges During Construction* [13]. A wind load analysis for the final condition after construction is completed is also not included; refer to NSBA Steel Bridge Design Handbook Design Example 1 for further information on the design for wind loads for the bridge in its final constructed condition.

7.1.5.2 Construction

The need for wind bracing during each critical phase of construction must also be examined as specified by Article 4.6.2.7.3. When investigating wind loads during construction, the load factor to be used for the wind load in the Strength III load combination is to specified by the Owner (Article 3.4.2.1). Wind load acting on the fully erected noncomposite structure prior to placement of the concrete deck (i.e., the “inactive work zone” case) and during the placement of the deck (i.e., the “active work zone” case) should be investigated. An analysis of wind load during these two construction cases is not included in this example. Refer to NSBA Steel Bridge Design Handbook Design Example 1 for further information on the design for wind loads for these two construction cases.

7.1.6 Fit and Steel Erection

7.1.6.1 Fit

Article 6.7.2 indicates that the contract documents should state the fit condition for which the cross-frames or diaphragms are to be detailed for horizontally curved I-girder bridges with or without skewed supports and with a maximum L/R greater than 0.03. The intent of this provision is to provide for the preferences of the Owner and Engineer regarding the fit condition to be clearly conveyed to those involved in the fabrication and construction of the bridge. Early communication between all parties can help to verify that a reasonable and proper fit decision is made for a particular bridge project.

To account for the effects of the twisting that occurs in skewed and curved I-bridges and achieve a desired geometry in the field, a fit condition should be specified for the detailing of the cross-frames in these bridges that is appropriate for the situation at hand. The fit condition of an I-girder bridge refers to the deflected girder geometry associated with a targeted dead load condition for which the cross-frames are detailed to connect to the girders. The girder geometry used by the Detailer to detail the cross-frames or diaphragms in these bridges is based on the deflections provided by the Engineer in the contract documents that are associated with the targeted dead load condition. In addition to the desired fit condition, this is all that the Engineer need provide.

A fit decision must always be made for these bridge types so that the Fabricator and Detailer can complete the shop drawings and fabricate the bridge components in a way that allows the Erector to assemble the steel and achieve a desired geometry in the field. The fit decision also influences the rotation demands on the bearings, as well as the internal forces for which the cross-frames and girders must be designed. Since the fit decision directly influences the cross-frame fabricated geometry, as well as the bridge constructability and subsequent internal forces, the fit condition should ideally be selected by the Engineer, who knows the loads and capacities of the structural members. To facilitate an informed decision regarding detailing and constructability, the engineer can consult with experienced fabricators, and/or erectors prior to completing the contract documents.

The three most common fit conditions are No-Load Fit (NLF), Steel Dead Load Fit (SDLF), and Total Dead Load Fit (TDLF). Refer to Article C6.7.2 and the two NSBA documents *Skewed and*

Curved Steel I-Girder Bridge Fit: Stand-Alone Summary [14] and *Skewed and Curved Steel I-Girder Bridge Fit: Guide Document* [15], which are available from the NSBA website at www.aisc.org/nsba, for further information on these fit conditions. Included in both NSBA documents are tables of recommended fit conditions that can assist the Engineer with the selection of the appropriate fit condition for a given situation. These documents also include information on effects of twisting girders as well as detailing of cross-frames and diaphragms when differential deflection is present in the I-girders.

Horizontally curved I-girders generally exhibit significant coupling between their major-axis bending displacements and their torsional rotations. Major-axis bending of curved girders cannot occur without also inducing twisting of the girders and vice versa. This behavior can exacerbate fit-up problems in curved girder bridges since it is more difficult to adjust the twist of the girders to connect them with the cross-frames. In horizontally curved bridges built with either SDLF or TDLF detailing, the lack-of-fit fabricated into the cross-frames twists the girders back an additional amount in the direction opposite from the twist rotations of the bridge cross-section. As such, both SDLF and TDLF detailing tend to increase the cross-frame forces in curved girder bridges, particularly the forces in the cross-frame diagonals. That is, unlike straight skewed bridges in which the locked-in forces that result due to the lack-of-fit detailed between the cross-frames and the girders in the base no-load geometry tend to be reduced substantially or to be substantially offset by the dead load effects, the locked-in cross-frame forces associated with SDLF and TDLF detailing tend to be additive with the general dead load effects in the cross-frames in horizontally curved bridges.

Fortunately, for SDLF detailing, the additional forces usually are not particularly large. As such, it is common that the cross-frame installation can be completed successfully. This fact has been demonstrated extensively in practice, since SDLF is the most common detailing practice used for curved bridges. For the case of TDLF detailing of curved bridges with $(L/R)_{\max}$ greater than 0.03, the additional forces required to twist the girders back in the opposite direction from which they and the bridge cross-section want to roll, and the resulting additive locked-in force effects, can be more substantial. This is because TDLF aims to overcome the rotations caused by the total dead load. Also, the total dead load is not yet in place on the structure when the steel is being erected. Practice and research (White et al., 2015) [16] have demonstrated that the use of a TDLF in such cases can potentially render the bridge unconstructable. As such, TDLF detailing should not be specified for curved bridges unless the supports are skewed, the spans are relatively small, and the horizontal curvature is minor.

Horizontally curved bridges with $(L/R)_{\max}$ greater than 0.03 should be detailed for a SDLF (a NLF is also acceptable), unless the maximum L/R is greater than or equal to 0.2, which is the case in this example; i.e., $(L/R)_{\max} = (210/700) = 0.3$. In this case, either the bridge should be detailed for a NLF, or the additive locked-in force effects associated with the SDLF detailing should be considered.

Should it be desired to detail such bridges for a SDLF, the larger NSBA guideline document on fit provides an approximate approach for estimating the additional locked-in force effects if these effects are not determined as part of a refined analysis; further consideration of these locked-in force effects may show in some cases that they are small enough to be neglected. For bridges with

a maximum L/R smaller than 0.2 that are detailed for a SDLF, the research showed that the horizontal curvature effects are smaller, and hence the additive locked-in force effects are also smaller and may be neglected (White et al., 2015) [16].

Detailing curved I-girder bridges with or without skew and with a maximum L/R greater than or equal to 0.2 for a NLF avoids the introduction of additional locked-in force effects. Hence, for simplicity in this design example, a NLF is assumed and any locked-in force effects are therefore neglected in the subsequent computations.

7.1.6.2 Erection

Erection is one of the most significant issues pertaining to curved girder bridges. A curved I-girder bridge often requires more temporary intermediate vertical support than a straight I-girder bridge of the same span. The support, typically via holding cranes or temporary shoring at critical stages of erection, is needed to provide stability and deflection control. Erection of girders in this design example is assumed to be performed by assembling and lifting pairs of girders with the cross-frames between the girders bolted into place.

The first lift is composed of two pairs of girders, G1-G2 and G3-G4, in Span 1. The positive moment sections of each pair are spliced to the corresponding pier sections before lifting. Prior to erection, each pair of girders is fit up with cross-frames and the bolts are tightened. These assemblies are assumed to be accomplished while the girders are fully supported, which simulates the no-load condition that was used in the fabrication shop, so that strain due to self-weight is negligible. Each girder pair is then erected. With the girder pair held in its approximate no-load position, cross-frames between girders G2 and G3 are then erected and their bolts are tightened. This procedure is repeated in Span 3. The sections in Span 2 are similarly fit up in pairs and erected. Finally, the bolts in the splices in Span 2 are installed and tightened and the cross-frames between girders G2 and G3 in Span 2 are installed.

According to the provisions of Article 2.5.3, one feasible erection sequence should be defined in the contract documents when the designer has assumed a particular sequence that induces certain stresses under dead load or when the bridge is of unusual complexity. A curved girder bridge is a good candidate for including an erection sequence in the contract documents. Although it is not the responsibility of the designer to consider all potential conditions during the construction of the bridge, sufficient conditions should be considered during a study of the erection scheme to illustrate that it is feasible. A detailed steel erection analysis is not included in this example. Refer to the AASHTO/NSBA Steel Bridge Collaboration document entitled *Steel Bridge Erection Guide Specification* [17] for further information regarding erection analyses and the development of erection plans.

7.1.7 Deck Placement Sequence

The deck is assumed to be placed in five casts. The first cast is in Span 1 commencing at the abutment and ending at the point of dead load contraflexure. The second cast is in Span 2 between points of dead load contraflexure. The third cast is in Span 3 from the point of dead load

contraflexure to the abutment. The fourth cast is over Support 2 and the fifth cast is over Support 3. The deck placement sequence is illustrated in Figure 4. The concrete deck is cast in the positive moment regions prior to casting concrete deck in the negative moment regions. This is common practice when the deck placement includes both positive and negative moment regions to minimize cracking at the top of the slab in the negative moment regions.

The unfactored moments from the deck staging analysis are presented in Table 9. DC_{1STEEL} moments are due to the steel weight based on the assumption that it was placed at one time. DC_{1CONC} moments are due to the deck weight assumed to be placed on the bridge at one time. The concrete cast moments are due to the particular deck cast. DC_2 and DW are superimposed dead loads placed on the fully composite bridge. Included in the DC_1 and concrete cast moments are the moments due to the deck haunch and the stay-in-place forms. Reactions are accumulated sequentially in the analysis so that uplift can be checked at each stage. Accumulated deflections by stage are also computed. If the contractor chooses an alternate deck placement sequence from that specified in the contract plans, it needs to be coordinated and investigated as well before the actual concrete placement, as the change can affect the accumulated deflections and subsequent vertical camber.

In each analysis stage of the deck placement, prior casts are assumed to be composite. The modular ratio for the deck is assumed to be $3n$ to account for creep. A smaller modular ratio may be desirable for the staging analyses since full creep usually takes approximately three years to occur (note that one State DOT has found a composite stiffness calculated using $1.4n$ to be appropriate based on an assumed E_c during construction of $0.7E_c$ at 28 days). A modular ratio of n should be used to check the deck stresses.

7.2 Section Properties

The calculation of the section properties for Sections G4-1 and G4-2 is illustrated in this section. In computing the composite section properties, the structural slab thickness, or total thickness minus the thickness of the integral wearing surface, should be used. In this example, the total slab thickness is 9.5 inches with a 0.5-inch integral wearing surface; therefore, the structural thickness of the deck slab is 9.0 inches.

For all section property calculations, the haunch depth of 4.0 inches is considered in computing the section properties, but the area of the haunch concrete is not included. Since the actual depth of the haunch concrete may vary from its theoretical value to account for construction tolerances, many designers ignore the haunch concrete depth in all calculations. For composite section properties including only longitudinal reinforcement, a haunch depth is considered when determining the vertical position of the reinforcement relative to the steel girder. For the purposes of the section property calculations in this example, a longitudinal reinforcement steel area equal to 8.0 in.^2 per girder placed 4.0 inches from the bottom of the deck is assumed (see Section 7.2.3).

The composite section must consist of the steel section and the transformed area of the effective width of the concrete deck. Therefore, compute the modular ratio n (Article 6.10.1.1.1b):

$$n = \frac{E}{E_c} \quad \text{Eq. (6.10.1.1.1b-1)}$$

where E_c is the modulus of elasticity of the concrete determined as specified in Article 5.4.2.4. A unit weight of 0.150 kcf is used for the concrete in the calculation of the modular ratio, which is more conservative than the value given in Table 3.5.1-1 since it includes an additional 0.005 kcf to account for the weight of the reinforcement. The correction factor for source of aggregate, K_1 , is taken as 1.0. The traditional equation for E_c for normal-weight concrete given in Article C5.4.2.4 is used in this example.

$$E_c = 33,000 K_1 w_c^{1.5} \sqrt{f'_c} \quad \text{Eq. (C5.4.2.4-2)}$$

$$E_c = 33,000 (1.0) (0.150)^{1.5} \sqrt{4.0} = 3,834 \text{ ksi}$$

$$n = \frac{29,000}{3,834} = 7.56$$

$n = 7.56$ will be used in all subsequent computations in this design example.

7.2.1 Section G4-1 Properties – Span 1 Positive Moment

Section G4-1 is located near the mid-span of Span 1 and is as shown in Figure 7. For this section, the longitudinal reinforcement is conservatively neglected in computing the composite section properties as is typically assumed in design.

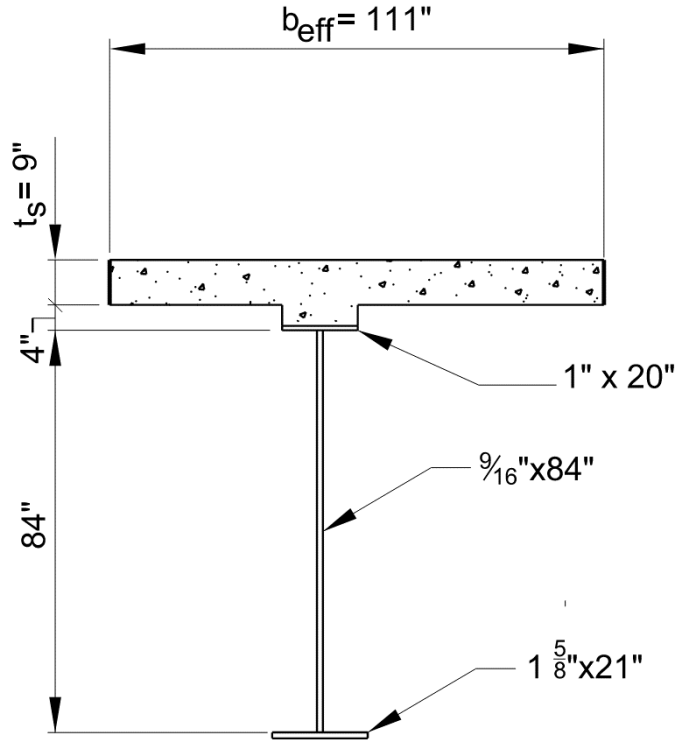


Figure 7: Sketch of I-girder Cross-Section at Section G4-1

7.2.1.1 Effective Width of Concrete Deck

As specified in Article 6.10.1.1.1e, the effective flange width is to be determined as specified in Article 4.6.2.6. According to Article 4.6.2.6, the deck slab effective width for an interior composite girder may be taken as the tributary width of the deck over the girder equal to taken as the sum of one-half the distances to the adjacent girder on each side of the component; and for an exterior girder it may be taken as one-half the distance to the adjacent girder plus the full overhang width. Therefore, the deck slab effective width, b_{eff} , for Girder G4 is:

$$b_{eff} = \frac{11.0}{2} + 3.75 = 9.25 \text{ ft} = 111 \text{ in.}$$

7.2.1.2 Elastic Section Properties: Section G4-1

In the calculation of the section properties that follow in Table 11 to Table 13, d is measured vertically from a horizontal axis through the mid-depth of the web to the centroid of each element of the I-girder. Section properties are calculated for the noncomposite (steel only) section, composite section using $3n$, and composite section using n .

Table 11 Section G4-1: Steel Only Section Properties

Component	A	d	Ad	Ad ²	I _o	I
Top Flange (1" x 20")	20.00	42.50	850.0	36,125	1.67	36,127
Web (9/16" x 84")	47.25				27,783	27,783

Component	A	d	Ad	Ad ²	I _o	I
Bottom Flange (1-5/8" x 21")	34.13	-42.81	-1,461	62,550	7.51	62,557
Σ	101.4		-611.0			126,467

$$-6.03(611.0) = \underline{-3,684}$$

$$I_{NA} = 122,783 \text{ in.}^4$$

$$d_s = \frac{-611.0}{101.4} = -6.03 \text{ in.}$$

$$d_{\text{Top of Steel}} = 43.00 + 6.03 = 49.03 \text{ in.}$$

$$d_{\text{Bot of Steel}} = 43.625 - 6.03 = 37.595 \text{ in.}$$

$$S_{\text{Top of Steel}} = \frac{122,783}{49.03} = 2,504 \text{ in.}^3$$

$$S_{\text{Bot of Steel}} = \frac{122,783}{37.595} = 3,266 \text{ in.}^3$$

Table 12 Section G4-1: 3n=22.68 Long-term Composite Section Properties

Component	A	d	Ad	Ad ²	I _o	I
Steel Section	101.4		-611.0			126,467
Concrete Slab (9" x 111")/22.68	44.05	50.50	2,225	112,339	297.3	112,636
Σ	145.45		1,614			239,103

$$-11.10(1,614) = \underline{-17,915}$$

$$I_{NA} = 221,188 \text{ in.}^4$$

$$d_{3n} = \frac{1,614}{145.45} = 11.10 \text{ in.}$$

$$d_{\text{Top of Steel}} = 43.00 - 11.10 = 31.90 \text{ in.}$$

$$d_{\text{Bot of Steel}} = 43.625 + 11.10 = 54.725 \text{ in.}$$

$$S_{\text{Top of Steel}} = \frac{221,188}{31.90} = 6,934 \text{ in.}^3$$

$$S_{\text{Bot of Steel}} = \frac{221,188}{54.725} = 4,042 \text{ in.}^3$$

Table 13 Section G4-1: n=7.56 Short-term Composite Section Properties

Component	A	d	Ad	Ad ²	I _o	I
Steel Section	101.4		-611.0			126,467
Concrete Slab (9" x 111")/7.56	132.14	50.50	6,673	336,990	892.0	337,882
Σ	233.54		6,062			464,349

$$-25.96(6,062) = \underline{-157,370}$$

$$I_{NA} = 306,979 \text{ in.}^4$$

$$d_n = \frac{6,062}{233.54} = 25.96 \text{ in.}$$

$$d_{\text{Top of Steel}} = 43.00 - 25.96 = 17.04 \text{ in.}$$

$$d_{\text{Bot of Steel}} = 43.625 + 25.96 = 69.585 \text{ in.}$$

$$S_{\text{Top of Steel}} = \frac{306,979}{17.04} = 18,015 \text{ in.}^3$$

$$S_{\text{Bot of Steel}} = \frac{306,979}{69.585} = 4,412 \text{ in.}^3$$

7.2.1.3 Plastic Moment Neutral Axis: Section G4-1

Per Article 6.10.6.2.2 for sections in positive flexure, the ductility requirements of Article 6.10.7.3 must be satisfied for compact and noncompact sections to protect the concrete deck from premature crushing. This requires the computation of the plastic neutral axis in accordance with Article D6.1. The longitudinal deck reinforcement is conservatively neglected. The location of the plastic neutral axis for the I-girder is computed as follows:

$$\begin{aligned} P_t &= F_{yt} b_t t_t &= (50)(21.0)(1.625) &= 1,706 \text{ kips} \\ P_w &= F_{yw} D t_w &= (50)(84.0)(0.5625) &= 2,363 \text{ kips} \\ P_c &= F_{yc} b_c t_c &= (50)(20.0)(1.0) &= 1,000 \text{ kips} \\ P_s &= 0.85 f'_c b_{\text{eff}} t_s &= (0.85)(4.0)(111)(9.0) &= 3,397 \text{ kips} \\ P_{rb} &= P_{rt} = 0 \text{ kips} \end{aligned}$$

$$\begin{aligned} P_t + P_w + P_c &> P_s + P_{rb} + P_{rt} \\ 1,706 + 2,363 + 1,000 &= 5,069 \text{ kips} > 3,397 \text{ kips} \end{aligned}$$

Therefore, the plastic neutral axis (PNA) is in the top flange per Case II of Table D6-1. Compute the PNA in accordance with Case II:

$$\bar{Y} = \frac{t_c}{2} \left[\frac{P_w + P_t - P_s - P_{rt} - P_{rb}}{P_c} + 1 \right]$$

$$\bar{Y} = \frac{1.0}{2} \left[\frac{2,363 + 1,706 - 3,397 - 0 - 0}{1,000} + 1 \right]$$

$\bar{Y} = 0.84$ in. downward from the top of the top flange (PNA location)

7.2.2 Section G4-2 Properties – Support 2 Negative Moment

Section G4-2 is located at Support 2 and is as shown in Figure 8.

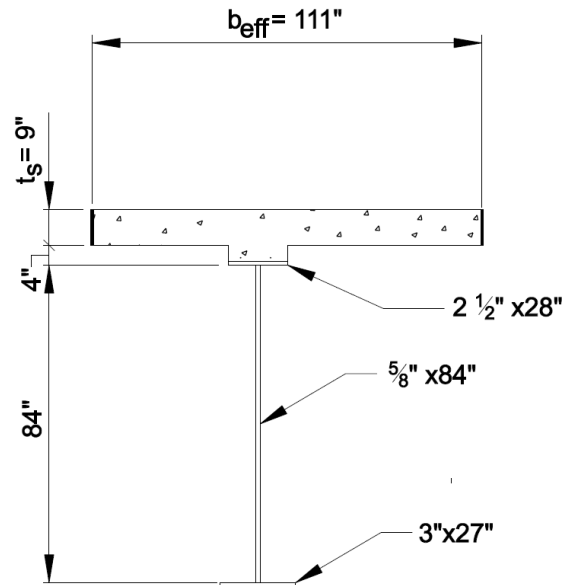


Figure 8: Sketch of I-girder cross-section at Section G4-2

The effective width of concrete deck is the same for Section G4-2 as calculated for Section G4-1, $b_{eff} = 111$ in.

7.2.2.1 Elastic Section Properties: Section G4-2

For members with shear connectors provided throughout their entire length that also satisfy the provisions of Article 6.10.1.7, Articles 6.6.1.2.1 and 6.10.4.2.1 permit the concrete deck to be considered effective for negative flexure when computing stress ranges and flexural stresses acting on the composite section at the fatigue and service limit states, respectively. Therefore, section properties for the long-term ($3n$) and short-term (n) composite section, including the concrete deck, are determined in Table 15 and Table 16, respectively, for later use in the calculations for Section G4-2 at these limits states. Longitudinal reinforcement could have been included in these section property calculations but was ignored due to its minimal effect on the moment of inertia. The

concrete deck should not be considered effective for negative flexure at the strength limit state. For this scenario, longitudinal reinforcement but not the concrete is used to compute the section properties as shown in Table 17 and Table 18.

For stress calculations involving the application of long-term loads to the composite section in regions of negative flexure in this example, the area of the longitudinal reinforcement is conservatively adjusted for the effects of concrete creep. Creep effects are accounted for by dividing the area of longitudinal reinforcement by 3 (i.e., $8.00 \text{ in.}^2/3 = 2.67 \text{ in.}^2$) as shown in Table 17 for the long-term ($3n$) composite section properties of the steel section with longitudinal reinforcement. The concrete is assumed to transfer the force from the longitudinal deck reinforcement to the rest of the cross-section, and concrete creep acts to reduce that force over time. It should be stressed that this is a conservative assumption that was employed in this particular design example and is not required by the *AASHTO LRFD BDS*. Therefore, it is not recommended that this assumption be employed in normal design practice. The short-term (n) composite section properties, as shown in Table 18, consider the full area of longitudinal reinforcement. The concrete is assumed to be cracked in tension in both Table 17 and Table 18 and therefore is not included. The centroid of the longitudinal steel reinforcement is assumed to be located 4.0 inches from the bottom of the deck slab.

In the calculation of the section properties that follow in Table 14 to Table 18, d is measured vertically from a horizontal axis through the mid-depth of the web to the centroid of each element of the I-girder.

Table 14 Section G4-2: Steel Only Section Properties

Component	A	d	Ad	Ad ²	I _o	I
Top Flange (2.5" x 28")	70.00	43.25	3,028	130,939	36.46	130,975
Web (5/8" x 84")	52.50	0.00			30,870	30,870
Bottom Flange (3.0" x 27")	81.00	-43.50	-3,524	153,272	60.75	153,333
	203.50		-496			315,178
					$-(-2.44)(-496) =$	$\frac{-1,210}{313,968 \text{ in.}^4}$
					$I_{NA} =$	
		$d_s = \frac{-496}{203.50} = -2.44 \text{ in.}$				
		$d_{\text{TOPOFSTEEL}} = 2.50 + \frac{84}{2} - (-2.44) = 46.94 \text{ in.}$				
		$d_{\text{BOTOFSTEEL}} = 3.0 + \frac{84}{2} + (-2.44) = 42.56 \text{ in.}$				
		$S_{\text{TOPOFSTEEL}} = \frac{313,968}{46.94} = 6,689 \text{ in.}^3$				
		$S_{\text{BOTOFSTEEL}} = \frac{313,968}{42.56} = 7,377 \text{ in.}^3$				

Table 15 Section G4-2: 3n=22.68 Composite Section Properties with Transformed Deck

Component	A	d	Ad	Ad ²	I _o	I
Steel Section	203.50		-496			315,178
Concrete Slab (9" x 111")/22.68	44.05	50.50	2,225	112,339	297	112,636
	247.55		1,729			427,814
					-6.98(1,729) =	-12,068
					I _{NA} =	415,746 in. ⁴

$d_{3n} = \frac{1,729}{247.55} = 6.98 \text{ in.}$

$d_{\text{TOPOFSTEEL}} = 2.50 + \frac{84}{2} - 6.98 = 37.52 \text{ in.}$

$S_{\text{TOPOFSTEEL}} = \frac{415,746}{37.52} = 11,081 \text{ in.}^3$

$d_{\text{BOTOFSTEEL}} = 3.0 + \frac{84}{2} + 6.98 = 51.98 \text{ in.}$

$S_{\text{BOTOFSTEEL}} = \frac{415,746}{51.98} = 7,998 \text{ in.}^3$

Table 16 Section G4-2: n=7.56 Composite Section Properties with Transformed Deck

Component	A	d	Ad	Ad ²	I _o	I
Steel Section	203.50		-496			315,178
Concrete Slab (9" x 111")/7.56	132.14	50.50	6,673	336,990	892	337,882
	335.64		6,177			653,060
					-18.40(6,177) =	-113,657
					I _{NA} =	539,403 in. ⁴

$d_n = \frac{6,177}{335.64} = 18.40 \text{ in.}$

$d_{\text{TOPOFSTEEL}} = 2.50 + \frac{84}{2} - 18.40 = 26.10 \text{ in.}$

$S_{\text{TOPOFSTEEL}} = \frac{539,403}{26.10} = 20,667 \text{ in.}^3$

$d_{\text{BOTOFSTEEL}} = 3.0 + \frac{84}{2} + 18.40 = 63.40 \text{ in.}$

$S_{\text{BOTOFSTEEL}} = \frac{539,403}{63.40} = 8,508 \text{ in.}^3$

Table 17 Section G4-2: Long-term (3n) Composite Section Properties with Longitudinal Steel Reinforcement

Component	A	d	Ad	Ad ²	I _o	I
Steel Section	203.50		-496			315,178
Longitudinal Reinforcement	2.67	50.00	134	6,675		6,675
	206.17		-362			321,853
					$-(-1.76)(-362) = -637$	
					$I_{NA} = \frac{-637}{321,216 \text{ in.}^4}$	
$d_{3n} = \frac{-362}{206.17} = -1.76 \text{ in.}$						
$d_{\text{TOPOFSTEEL}} = 2.50 + \frac{84}{2} - (-1.76) = 46.26 \text{ in.}$						
$d_{\text{BOTOFSTEEL}} = 3.0 + \frac{84}{2} + (-1.76) = 43.24 \text{ in.}$						
$S_{\text{TOPOFSTEEL}} = \frac{321,216}{46.26} = 6,944 \text{ in.}^3$						
$S_{\text{BOTOFSTEEL}} = \frac{321,216}{43.24} = 7,429 \text{ in.}^3$						

Table 18 Section G4-2: Short-term (n) Composite Section Properties with Longitudinal Steel Reinforcement

Component	A	d	Ad	Ad ²	I _o	I
Steel Section	203.50		-496			315,178
Longitudinal Reinforcement	8.00	50.00	400	20,000		20,000
	211.50		-96			335,178
					$-(-0.45)(-96) = -43$	
					$I_{NA} = \frac{-43}{335,135 \text{ in.}^4}$	
$d_n = \frac{-96}{211.50} = -0.45 \text{ in.}$						
$d_{\text{TOPOFSTEEL}} = 2.50 + \frac{84}{2} - (-0.45) = 44.95 \text{ in.}$						
$d_{\text{BOTOFSTEEL}} = 3.0 + \frac{84}{2} + (-0.45) = 44.55 \text{ in.}$						
$S_{\text{TOPOFSTEEL}} = \frac{335,135}{44.95} = 7,146 \text{ in.}^3$						
$S_{\text{BOTOFSTEEL}} = \frac{335,135}{44.55} = 7,523 \text{ in.}^3$						

7.2.3 Check of Minimum Negative Flexure Concrete Deck Reinforcement

To control concrete deck cracking in regions of negative flexure, Article 6.10.1.7 specifies that the total cross-sectional area of the longitudinal reinforcement must not be less than 1 percent of the total cross-sectional area of the deck. The minimum longitudinal reinforcement must be provided wherever the longitudinal tensile stress in the concrete deck due to either the factored construction loads or Load Combination Service II exceeds ϕf_r . ϕ is to be taken as 0.9 and f_r is to be taken as the modulus of rupture of the concrete determined as follows:

- For normal weight concrete: $f_r = 0.24\sqrt{f'_c}$
- For lightweight concrete: f_r is calculated as specified in Article 5.4.2.6.

It is further specified that the reinforcement is to have a specified minimum yield strength not less than 60 ksi and a size that should not exceed No. 6 bars. The reinforcement should be placed in two layers uniformly distributed across the deck width, and two-thirds should be placed in the top layer. The individual bars should be spaced at intervals not exceeding 12 inches.

Article 6.10.1.1.1c states that for calculating stresses in composite sections subjected to negative flexure at the strength limit state, the composite section for both short-term and long-term moments is to consist of the steel section and the longitudinal reinforcement within the effective width of the concrete deck. Referring to the cross-section shown in Figure 1:

$$A_{\text{deck}} = (\text{entire width of 9" thick deck}) + (\text{triangular portion of overhang})$$

$$A_{\text{deck}} = \frac{9.0}{12}(40.5) + 2 \left[\frac{1}{2} \left(\frac{4.0}{12} \right) \left(3.75 - \frac{28}{12} \right) \right] = 31.24 \text{ ft}^2 = 4,498 \text{ in.}^2$$

$$0.01(4,498) = 44.98 \text{ in.}^2$$

$$\frac{44.98}{40.5} = 1.11 \text{ in.}^2/\text{ft} = 0.093 \text{ in.}^2/\text{in.}$$

$$0.093(111) = 10.32 \text{ in.}^2 \text{ per exterior girder}$$

Therefore, the assumption of 8.00 in.² of longitudinal deck reinforcement, which was assumed in the original design example (see Section 7.2), is conservative for the purpose of section property calculations and is left as shown in Table 17 and Table 18. When the reinforcement is actually detailed, #6 bars at 6 inches placed in the top layer and #4 bars spaced at 6" in the bottom layer should be specified. Therefore, the total area of deck reinforcement steel in the given effective width of concrete deck would be:

$$A_s = (0.44 + 0.44 + 0.20 + 0.20) \left(\frac{111}{12} \right) = 11.84 \text{ in.}^2 > 10.32 \text{ in.}^2$$

Also, approximately two-thirds of the reinforcement is in the top layer: $\frac{0.44 + 0.44}{1.28} = 0.69 \approx \frac{2}{3}$.

The use of the longitudinal reinforcement computed above is also addressed within the deck constructability checks shown later in this design example. It should be noted that the area of longitudinal reinforcement shown above is required to be extended into the "positive moment region" and even at the location of maximum positive moment in the case of this example because of the presence of negative moment at these locations during the placement of the deck.

7.3 Girder Check: Section G4-3, Shear at End Support (Article 6.10.9)

According to the provisions of Article 6.10.9.1, at the strength limit state, straight and curved web panels are to satisfy:

$$V_u \leq \phi_v V_n \quad \text{Eq. (6.10.9.1-1)}$$

where:

- ϕ_v = resistance factor for shear = 1.0 (Article 6.5.4.2)
- V_n = nominal shear resistance determined as specified in Articles 6.10.9.2 and 6.10.9.3 for unstiffened and stiffened webs, respectively
- V_u = factored shear in the web at the section under consideration

In this example, the web is being designed as a stiffened web, so Article 6.10.9.3 will apply. Since the web at Support 1 is an end panel, the transverse stiffener spacing cannot exceed 1.5D for the end panel to qualify as stiffened. Article 6.10.9.3.3 applies, and the nominal shear resistance is to be taken as:

$$V_n = V_{cr} = CV_p \quad \text{Eq. (6.10.9.3.3-1)}$$

where: C = ratio of the shear-buckling resistance to the shear yield strength

V_{cr} = shear-buckling resistance

V_p = plastic shear force

7.3.1 Applied Shear

The unfactored shears for G4 at Support 1 are shown below. These results are directly from the three-dimensional analysis as reported in Table 10.

Steel Dead Load:	$V_{DC1-STEEL}$	= 23 kips
Concrete Deck Dead Load:	$V_{DC1-CONC}$	= 92 kips
Composite Dead Load:	V_{DC2}	= 23 kips
Future Wearing Surface Dead Load:	V_{DW}	= 19 kips
Live Load (including IM + CF):	V_{LL+IM}	= 143 kips

The maximum Strength I factored shear is computed as:

$$V_u = 1.25(23 + 92 + 23) + 1.50(19) + 1.75(143) = 451 \text{ kips}$$

7.3.2 Shear Resistance

Compute the plastic shear force:

$$V_p = 0.58F_{yw}Dt_w \quad \text{Eq. (6.10.9.3.3-2)}$$

$$= 0.58(50)(84)(0.5625) = 1,370 \text{ kips}$$

To determine the ratio C , the shear-buckling coefficient must first be computed as follows:

$$k = 5 + \frac{5}{\left(\frac{d_o}{D}\right)^2} \quad \text{Eq. (6.10.9.3.2-7)}$$

At this particular location, the transverse stiffener spacing is assumed to be 82 inches. Therefore, $d_o = 82$ in.

$$k = 5 + \frac{5}{\left[\frac{82}{84}\right]^2} = 10.2$$

Note that the stiffener spacing of 82 inches does not exceed $1.5D$ ($D = 84$ inches, $1.5D = 126$ inches) as prescribed in Article 6.10.9.1 for stiffened end panels. Check the following relationship in order to select the appropriate equation for computing C :

$$\frac{D}{t_w} = \frac{84}{0.5625} = 149.3 > 1.40 \sqrt{\frac{Ek}{F_{yw}}} = 1.40 \sqrt{\frac{29,000(10.2)}{50}} = 108$$

Since the above relation is true, the ratio C is computed using Eq. (6.10.9.3.2-6) as follows:

$$C = \frac{1.57}{\left(\frac{D}{t_w}\right)^2} \left(\frac{Ek}{F_{yw}}\right) \quad \text{Eq. (6.10.9.3.2-6)}$$

$$C = \frac{1.57}{\left(\frac{84}{0.5625}\right)^2} \left(\frac{29,000(10.2)}{50}\right) = 0.416$$

The nominal shear resistance is then computed in accordance with Eq. (6.10.9.3.3-1):

$$V_n = V_{cr} = (0.416)(1,370) = 570 \text{ kips}$$

Note that post-buckling tension field action is not permitted in end panels in order to allow end panels to provide an anchor for the tension field in the adjacent interior panel.

Using the above results, check the requirement of Article 6.10.9.1, $V_u \leq \phi_v V_n$:

$$V_u = 451 \text{ kips} < \phi_v V_n = (1.0)(570) = 570 \text{ kips} \quad \text{OK (Ratio} = 0.791)$$

Therefore, the web is satisfactory for shear at Support 1. It should be noted that the sample calculation shown above is for a web end panel, but for interior web panels, the provisions of Article 6.10.9.3.2 apply. End web panels are defined as web panels adjacent to the discontinuous end of a girder, whereas interior web panels are defined as web panels not adjacent to the discontinuous end of a girder. Also note that for webs without longitudinal stiffeners, the transverse stiffener spacing in interior web panels cannot exceed $3D$ for the web to qualify as stiffened.

7.4 Girder Check: Section G4-1, Constructability (Article 6.10.3)

For critical stages of construction, the provisions of Articles 6.10.3.2.1 through 6.10.3.2.3 are to be applied to the flanges of the girder. However, in many cases, such as in this design example, 6.10.3.2.3 does not apply since neither flange is continuously braced during construction. Web shear is to be checked in accordance with Article 6.10.3.3.

As specified in Article 6.10.3.4.1, sections in positive flexure that are composite in the final condition, but noncomposite during construction, are to be investigated during the various stages of deck placement. The effects of forces from deck overhang brackets acting on the fascia girders are also to be considered. Wind load effects on the noncomposite structure prior to and during the deck placement are also an important consideration during construction. The presence of construction equipment may also need to be considered. Lastly, potential uplift at bearings should be investigated at each critical construction stage. For this design example, the effects of wind load on the noncomposite structure during construction and the presence of construction equipment are not considered.

Calculate the maximum flexural stresses in the flanges of the steel section due to the factored loads resulting from the application of steel self-weight and Cast #1 of the deck placement sequence. Cast #1 yields the maximum positive moment for the noncomposite Section G4-1. As specified in Article 6.10.1.6, for design checks where the flexural resistance is based on lateral torsional buckling, f_{bu} is to be determined as the largest value of the compressive stress throughout the unbraced length in the flange under consideration, calculated without consideration of flange lateral bending. For design checks where the flexural resistance is based on yielding, flange local buckling or web bend-buckling, f_{bu} may be determined as the corresponding stress values at the section under consideration. From Figure 2, brace points adjacent to Section G4-1 are located at intervals of approximately 20 feet, and the largest stress occurs at a section within this unbraced length.

In accordance with Article 3.4.2.1, when investigating Strength I and III during construction, load factors for the weight of the structure and appurtenances, DC and DW, and any applicable construction loads in the case of the Strength III load combination only, are not to be taken to be less than 1.25. Construction loads including dynamic effects, if applicable, are to be added in

Strength I load combination with a load factor not less than 1.5 when investigating for maximum force effects, unless otherwise specified by the Owner. Also, as discussed previously, the η factor is taken equal to 1.0 in this example. As shown in Table 9, the unfactored moments due to steel self-weight and Cast #1 are 661 kip-ft and 3,932 kip-ft, respectively, for a total of 4,593 kip-ft. Therefore,

For the Strength I Load Combination:

$$\text{General: } f_{bu} = \frac{\eta \gamma M_{DC}}{S_{nc}}$$

$$\text{Top Flange: } f_{bu} = \frac{1.0(1.25)(4,593)(12)}{2,504} = -27.51 \text{ ksi}$$

$$\text{Bot. Flange: } f_{bu} = \frac{1.0(1.25)(4,593)(12)}{3,266} = 21.09 \text{ ksi}$$

For the Special Load Combination specified in Article 3.4.2.1:

$$\text{Top Flange: } f_{bu} = \frac{1.0(1.4)(4,593)(12)}{2,504} = -30.82 \text{ ksi}$$

$$\text{Bot. Flange: } f_{bu} = \frac{1.0(1.4)(4,593)(12)}{3,266} = 23.63 \text{ ksi}$$

The Special Load Combination controls in this case.

Section G4-1 must be checked for steel weight and for Cast #1 of the concrete deck on the noncomposite section as discussed above. The factored steel stresses during the sequential placement of the concrete deck are not to exceed the nominal resistances specified in Article 6.10.3.2.1 for compression flanges and Article 6.10.3.2.2 for tension flanges. The effect of the overhang brackets on the flanges must also be considered according to Article 6.10.3.4.1 since G4 is an exterior girder.

7.4.1 Constructability of Top Flange

7.4.1.1 Deck Overhang Bracket Load

During construction, the weight of the deck overhang wet concrete is resisted by the deck overhang brackets. Other loads supported by the overhang bracket during construction include the formwork, screed rail, railing, worker walkway, and the deck finishing machine.

The deck overhang construction loads are typically applied to the noncomposite section and removed once the concrete deck has become composite with the steel girders. The deck overhang bracket imparts a lateral force on the top and bottom flanges, resulting in lateral bending of the flanges. The lateral bending of both flanges must be considered as part of the constructability check.

Since G4 is an exterior girder, half of the overhang weight is assumed placed on the girder and the other half is assumed placed on the overhang brackets. The overhang bracket loading is shown in Figure 9.

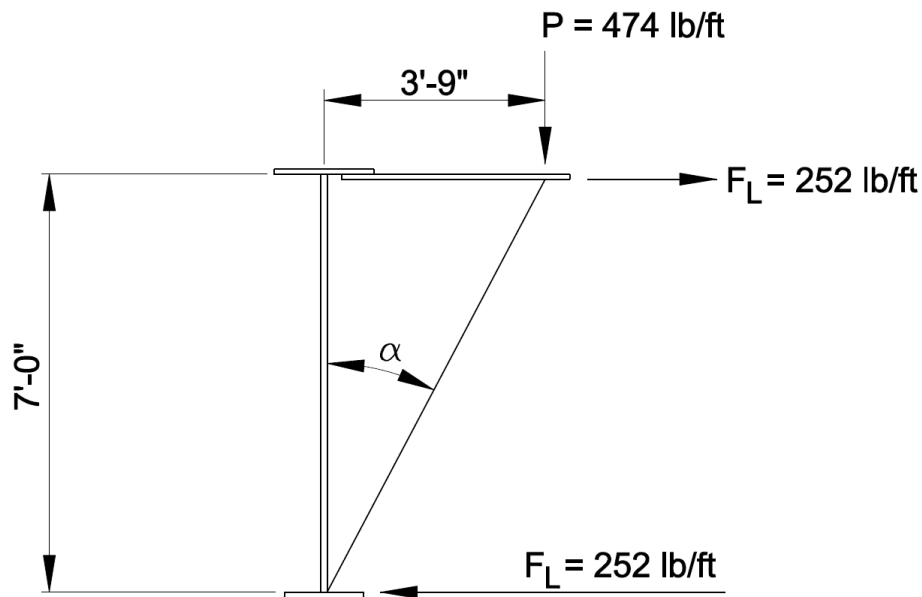


Figure 9 Deck Overhang Bracket Loading

The bracket loads are assumed to be applied uniformly although the brackets are actually spaced at about 3 feet along the girder.

The unbraced length, L_b , of the top flange of G4 is 20.47 feet. Assume that the average deck thickness in the overhang is 10 inches. The weight of the deck finishing machine is not considered in this example. However, designers may wish to consider the live load from traditional finishing machines as also being part of the loads acting on overhang brackets. These machines can transmit reactions over a relatively short distance. (See Example 4 of the Steel Bridge Design Handbook for an example considering the finishing machine load.)

Compute the vertical load on the overhang brackets.

$$\text{Deck} = \frac{1}{2}(3.75)\left(\frac{10}{12}\right)(150) = 234 \text{ lb/ft}$$

Deck forms + screed rail = 240 lb/ft (assumed)

Uniform load on brackets = 234 + 240 = 474 lb/ft

Compute the lateral force on the flange due to the overhang brackets.

$$\alpha = \arctan(3.75 \text{ ft}/7.00 \text{ ft}) = 28^\circ$$

$$F_\ell = \frac{474 \tan(28^\circ)}{1000} = 0.252 \text{ kips/ft}$$

The lateral force, F_ℓ , is used to compute the flange lateral bending moment on top flange due to the deck overhang bracket. The flange lateral moment at the brace points due to the overhang forces is negative in the top flange of girder G4 on the outside of the curve because the stress due to the lateral moment is compressive on the convex side of the flange at the brace points. The opposite would be true on the convex side of the girder G1 top flange on the inside of the curve at the brace points. In the absence of a more refined analysis, the equations given in Article C6.10.3.4.1 may be used to estimate the maximum flange lateral bending moments in the discretely braced compression flange due to the lateral forces from the brackets. Assuming the flange is continuous with the adjacent unbraced lengths that are approximately equal, the flange lateral bending moment due to a statically equivalent uniformly distributed lateral bracket force may be estimated as:

$$M_\ell = \frac{F_\ell L_b^2}{12} \tag{Eq. (C6.10.3.4.1-1)}$$

$$= -\left[\frac{0.252(20.47)^2}{12}\right] = -8.8 \text{ kip-ft (unfactored)}$$

Typically, major-axis bending moments due to construction dead loads (i.e., formwork, walkways, brackets, etc.) and construction live loads (i.e., finishing machine loads and construction worker live loads) are considered in at least an approximate manner and appropriately combined with the noncomposite dead loads associated with the self-weight of the structural steel and the weight of the wet concrete deck. Some Owner-Agencies prescribe standard values for these loading effects, or alternatively, guidance for estimating these loading effects can be found in [18]. For simplicity, the values of the construction dead load and live load major-axis bending moments are not considered in this example.

7.4.1.2 Curvature Effects

In addition to the lateral bending moment due to the overhang brackets, lateral bending due to curvature must also be considered, which can either be taken from the analysis results or estimated

by the approximate V-load equation given in Article C4.6.1.2.4b. In this example, in lieu of using the lateral moments taken directly from the refined analysis results (which are typically less conservative), the use of the approximate V-load equation to obtain a conservative estimate of the lateral bending moments due to curvature will be demonstrated.

The V-load equation assumes the presence of a cross-frame at the point under investigation and a constant major-axis moment over the distance between the brace points. Although the use of the V-load equation is not theoretically pure for locations between brace points, it may conservatively be used. Note that throughout this example, the web depth, D , is conservatively used in this equation. Referring to Table 9, the major-axis bending moment due to the steel weight plus Cast #1 is used for M : $661 + 3,932 = 4,593$ kip-ft.

$$M_{\text{lat}} = \frac{M\ell^2}{NRD} \quad \text{Eq. (C4.6.1.2.4b-1)}$$

where: M = major-axis bending moment (kip-ft)

ℓ = unbraced length (ft)

N = a constant taken as 10 or 12 in past practice (the constant of 12 is generally recommended for use and will be used in this example)

R = girder radius (ft)

D = web depth (ft)

Therefore,

$$M_{\text{lat}} = \frac{(4,593)(20.47)^2}{12(716.5)(7.0)} = -32.0 \text{ kip-ft}$$

The flange lateral moment at the brace points due to curvature is negative in the top flange of all four girders whenever the top flange is subjected to compression because the stress due to the lateral moment is compressive on the convex side of the flange at the brace points. The opposite is true whenever the top flange is subjected to tension. Therefore, for the girder on the outside of the curve, the flange lateral moments due to the overhang brackets are of the same sign as the flange lateral moments due to curvature in regions of positive flexure. The opposite is true for the girder on the inside of the curve.

The total factored lateral bending moment due to the combination of overhang brackets and curvature in regions of positive flexure is therefore (the Special Load Combination specified in Article 3.4.2.1 controls by inspection):

$$M_{\text{tot_lat}} = (1.4)[-8.8 + (-32.0)] = -57.1 \text{ kip-ft (factored)}$$

7.4.1.3 Top Flange Lateral Bending Amplification

According to Article 6.10.1.6, lateral bending stresses determined from a first-order analysis may be used in discretely braced compression flanges for which:

$$L_b \leq 1.2L_p \sqrt{\frac{C_b R_b}{f_{bu}/F_{yc}}} \quad \text{Eq. (6.10.1.6-2)}$$

L_p is the limiting unbraced length specified in Article 6.10.8.2.3 determined as:

$$L_p = 1.0r_t \sqrt{\frac{E}{F_{yc}}} \quad \text{Eq. (6.10.8.2.3-4)}$$

where r_t is the effective radius of gyration for lateral torsional buckling specified in Article 6.10.8.2.3 determined as:

$$r_t = \frac{b_{fc}}{\sqrt{12 \left(1 + \frac{1 D_c t_w}{3 b_{fc} t_{fc}} \right)}} = \frac{20}{\sqrt{12 \left[1 + \frac{1 \cdot 48.03(0.5625)}{20(1.0)} \right]}} = 4.79 \text{ in.} \quad \text{Eq. (6.10.8.2.3-9)}$$

Therefore,

$$L_p = 1.0r_t \sqrt{\frac{E}{F_{yc}}} = \frac{1.0(4.79) \sqrt{\frac{29,000}{50}}}{12} = 9.61 \text{ ft}$$

Since the stresses remain reasonably constant over the section, the moment gradient modifier, C_b , is taken as 1.0. Article C6.10.1.10.2 indicates that the web load-shedding factor, R_b , is to be taken as 1.0 for constructability.

Check the relationship given in Eq. (6.10.1.6-2). The Strength I top-flange compressive stress, f_{bu} , controls in this computation:

$$L_b = 20.47 \text{ ft} > 1.2(9.61) \sqrt{\frac{1.0(1.0)}{|-27.51|/50}} = 15.55 \text{ ft}$$

Because Eq. (6.10.1.6-2) is not satisfied, Article 6.10.1.6 requires that second-order elastic compression-flange lateral bending stresses be determined. The second-order compression-flange lateral bending stresses may be determined by amplifying the first-order values. First compute the first-order compression-flange lateral bending stress acting at the tip of the flange:

$$S_{\text{top_flange}} = \frac{1.0(20)^2}{6} = 66.7 \text{ in.}^3$$

$$f_{t1} = \frac{M_{\text{tot_lat}}}{S_{\text{top flange}}} = \frac{-57.1(12)}{66.7} = -10.27 \text{ ksi (factored)}$$

The first-order values are amplified as follows:

$$f_{\ell} = \left(\frac{0.85}{1 - \frac{f_{bu}}{F_{cr}}} \right) f_{\ell 1} \geq f_{\ell 1} \quad (\text{second - order analysis}) \quad \text{Eq. (6.10.1.6-4)}$$

where: f_{bu} = top flange stress calculated without consideration of flange lateral bending
 F_{cr} = elastic lateral torsional buckling stress for the flange under consideration determined using Eq. (6.10.8.2.3-8)

$$F_{cr} = \frac{C_b R_b \pi^2 E}{\left(\frac{L_b}{r_t} \right)^2} = \frac{(1.0)(1.0)\pi^2 (29,000)}{\left(\frac{20.47(12)}{4.79} \right)^2} = 109 \text{ ksi} \quad \text{Eq. (6.10.8.2.3-8)}$$

The amplification factor (AF) is then determined as follows:

$$AF = \left(\frac{0.85}{1 - \frac{|-30.82|}{109}} \right) = 1.19 > 1.0 \text{ OK}$$

Therefore, the total flange stress due to lateral bending, including the amplification factor, is:

$$f_{\ell} = (AF)(f_{\ell 1}) = (1.19)(-10.27) = -12.22 \text{ ksi}$$

7.4.1.4 Flexure in Top Flange (Article 6.10.3.2.1)

During construction, the top flange at Section G4-1 is a discretely based compression flange, so the provisions of Article 6.10.3.2.1 apply. The article indicates that if the section has a slender web, Eq. (6.10.3.2.1-1) is not checked when f_{ℓ} is zero, and for sections with compact or noncompact webs, Eq. (6.10.3.2.1-3) is not checked. In this case, the web is slender (as demonstrated later) and f_{ℓ} is not zero, so all three equations must be checked.

$$f_{bu} + f_{\ell} \leq \phi_f R_h F_{yc} \quad \text{Eq. (6.10.3.2.1-1)}$$

$$f_{bu} + \frac{1}{3} f_{\ell} \leq \phi_f F_{nc} \quad \text{Eq. (6.10.3.2.1-2)}$$

$$f_{bu} \leq \phi_f F_{crw} \quad \text{Eq. (6.10.3.2.1-3)}$$

where: ϕ_f = resistance factor for flexure = 1.0 (Article 6.5.4.2)

- R_h = hybrid factor specified in Article 6.10.1.10.1 (1.0 at homogeneous Section G4-1)
 F_{crw} = nominal elastic bend-buckling resistance for webs determined as specified in Article 6.10.1.9
 F_{nc} = nominal flexural resistance of the compression flange determined as specified in Article 6.10.8.2 (i.e., local or lateral torsional buckling resistance, whichever controls). The provisions of Article A6.3.3 are not to be used to determine the lateral torsional buckling resistance of sections in curved I-girder bridges, per Article 6.10.3.2.1.

First, check Eq. (6.10.3.2.1-1), using the previously calculated values of flange stresses:

$$f_{bu} + f_\ell = |-30.82| + |-12.22| = 43.04 \text{ ksi} < \phi_f R_h F_{yc} = 1.0(1.0)(50) = 50 \text{ ksi OK}$$

(Ratio = 0.861)

Secondly, check Eq. (6.10.3.2.1-2). The equation must be satisfied for both local buckling and lateral torsional buckling using the appropriate value of the nominal flexural resistance, F_{nc} , for local buckling (Article 6.10.8.2.2) or for lateral torsional buckling (Article 6.10.8.2.3), as applicable.

Determine the local buckling resistance of the compression flange. First, check the flange slenderness.

$$\lambda_f = \frac{b_{fc}}{2t_{fc}} = \frac{20}{2(1)} = 10 \quad \text{Eq. (6.10.8.2.2-3)}$$

$$\lambda_{pf} = 0.38 \sqrt{\frac{E}{F_{yc}}} = 0.38 \sqrt{\frac{29,000}{50}} = 9.15 \quad \text{Eq. (6.10.8.2.2-4)}$$

$$\lambda_{rf} = 0.56 \sqrt{\frac{E}{F_{yr}}} = 0.56 \sqrt{\frac{29,000}{0.7(50)}} = 16.12 \quad \text{Eq. (6.10.8.2.2-5)}$$

Since $\lambda_{pf} < \lambda_f < \lambda_{rf}$, the flange is noncompact and the nominal flexural resistance is determined using Eq. (6.10.8.2.2-2).

R_b is taken as 1.0 for constructability checks per Article 6.10.3.2.1, and R_h is taken as 1.0 per Article 6.10.1.10.1. Therefore, F_{nc} for the local buckling resistance is calculated as:

$$F_{nc} = \left[1 - \left(1 - \frac{F_{yr}}{R_h F_{yc}} \right) \left(\frac{\lambda_f - \lambda_{pf}}{\lambda_{rf} - \lambda_{pf}} \right) \right] R_b R_h F_{yc} \quad \text{Eq. (6.10.8.2.2-2)}$$

$$= \left[1 - \left[1 - \frac{0.7(50)}{1.0(50)} \right] \left(\frac{10 - 9.15}{16.12 - 9.15} \right) \right] (1.0)(1.0)(50) = 48.17 \text{ ksi}$$

Determine the lateral torsional buckling resistance of the compression flange. First, compare the unbraced length, L_b , to the limiting unbraced lengths L_p and L_r .

$$L_b = 20.47 \text{ ft} = \text{unbraced length}$$

$$L_p = 9.61 \text{ ft (calculated previously in top flange lateral bending amplification calculation)}$$

L_r is the limiting unbraced length to achieve the onset of nominal yielding in either flange under uniform bending with consideration of compression-flange residual stress effects and is determined as follows:

$$L_r = \pi r_t \sqrt{\frac{E}{F_{yr}}} = \frac{\pi(4.79) \sqrt{\frac{29,000}{0.7(50)}}}{12} = 36.1 \text{ ft} \quad \text{Eq. (6.10.8.2.3-5)}$$

Since $L_p < L_b < L_r$, use Eq. (6.10.8.2.3-2) to calculate the lateral torsional buckling resistance.

$$\begin{aligned} F_{nc} &= C_b \left[1 - \left(1 - \frac{F_{yr}}{R_h F_{yc}} \right) \left(\frac{L_b - L_p}{L_r - L_p} \right) \right] R_b R_h F_{yc} \leq R_b R_h F_{yc} \quad \text{Eq. (6.10.8.2.3-2)} \\ &= 1.0 \left[1 - \left[1 - \frac{0.7(50)}{1.0(50)} \right] \left(\frac{20.47 - 9.61}{36.1 - 9.61} \right) \right] (1.0)(1.0)(50) = 43.85 \text{ ksi} \end{aligned}$$

Therefore, check Eq. (6.10.3.2.1-2) for local buckling as follows:

$$\begin{aligned} f_{bu} + \frac{1}{3} f_\ell &= |-30.82| + \frac{1}{3} (|-12.22|) = 34.89 \text{ ksi} < \phi_t F_{nc} = 1.0(48.17) = 48.17 \text{ ksi} \quad \text{OK} \\ (\text{Ratio} &= 0.724) \end{aligned}$$

Check Eq. (6.10.3.2.1-2) for lateral torsional buckling as follows:

$$\begin{aligned} f_{bu} + \frac{1}{3} f_\ell &= |-30.82| + \frac{1}{3} (|-12.22|) = 34.89 \text{ ksi} < \phi_t F_{nc} = 1.0(43.85) = 43.85 \text{ ksi} \quad \text{OK} \\ (\text{Ratio} &= 0.796) \end{aligned}$$

Thirdly, check Eq. (6.10.3.2.1-3) since the web is slender, as shown below. The slenderness of the noncomposite section is checked according to Article 6.10.6.2.3 as follows:

$$\frac{2D_c}{t_w} \leq \lambda_{rw} \quad \text{Eq. (6.10.6.2.3-1)}$$

where:

$$4.6\sqrt{\frac{E}{F_{yc}}} \leq \lambda_{rw} = \left(3.1 + \frac{5.0}{a_{wc}}\right)\sqrt{\frac{E}{F_{yc}}} \leq 5.7\sqrt{\frac{E}{F_{yc}}} \quad \text{Eq. (6.10.6.2.3-3)}$$

$$a_{wc} = \frac{2D_c t_w}{b_{fc} t_{fc}} \quad \text{Eq. (6.10.6.2.3-4)}$$

$$\frac{2D_c}{t_w} = \frac{2(48.03)}{0.5625} = 170.8$$

$$4.6\sqrt{\frac{E}{F_{yc}}} = 4.6\sqrt{\frac{29,000}{50}} = 111$$

$$5.7\sqrt{\frac{E}{F_{yc}}} = 5.7\sqrt{\frac{29,000}{50}} = 137$$

$$a_{wc} = \frac{2(48.03)(0.5625)}{20(1.0)} = 2.70$$

$$111 < \lambda_{rw} = \left(3.1 + \frac{5.0}{2.70}\right)\sqrt{\frac{29,000}{50}} = 119.3 < 137$$

$$\therefore \lambda_{rw} = 119.3 < \frac{2D_c}{t_w} = 170.8$$

Because the web is slender, Eq. (6.10.3.2.1-3) is checked to control the out-of-plane web distortions that may occur during construction.

$$f_{bu} \leq \phi_f F_{crw} \quad \text{Eq. (6.10.3.2.1-3)}$$

where the nominal web bend-buckling resistance, F_{crw} , is taken as:

$$F_{crw} = \frac{0.9Ek}{\left(\frac{D}{t_w}\right)^2} \quad \text{Eq. (6.10.1.9.1-1)}$$

but F_{crw} cannot exceed $R_h F_{yc}$ and $F_{yw}/0.7$ per Article 6.10.1.9.1 for webs without longitudinal stiffeners.

First, compute the bend-buckling coefficient, k , in which D_c is the depth of web in compression. Since the girder is noncomposite for this check, D_c is the distance from the inner edge of the compression flange to the neutral axis.

$$k = \frac{9}{\left(\frac{D_c}{D}\right)^2} = \frac{9}{\left(\frac{48.03}{84}\right)^2} = 27.5 \quad \text{Eq. (6.10.1.9.1-2)}$$

$$F_{crw} = \frac{0.9(29,000)(27.5)}{\left(\frac{84}{0.5625}\right)^2} = 32.19 \text{ ksi} < 1.0(50) = 50 \text{ ksi} < \frac{50}{0.7} = 71.4 \text{ ksi}$$

Therefore, use $F_{crw} = 32.19$ ksi to check Eq. (6.10.3.2.1-3):

$$f_{bu} = |-30.82| \text{ ksi} < \phi_f F_{crw} = 1.0(32.19) = 32.19 \text{ ksi} \quad \text{OK (Ratio} = 0.957)$$

The compression flange proportions satisfy the criteria given in Article 6.10.3.2.1.

It should be noted that the web bend-buckling resistance (F_{crw}) is generally checked against the maximum compression flange stress due to factored loads without consideration of flange lateral bending, as shown in the previous calculation. Since web bend-buckling is a check of the web, the maximum flexural compression stress in the web could be calculated and used for comparison against the bend-buckling resistance. However, the precision associated with making the distinction between the stress in the compression flange and the maximum compressive stress in the web is typically not warranted.

7.4.2 Constructability of Bottom Flange

For critical stages of construction, the following requirement must be satisfied for discretely braced tension flanges according to Article 6.10.3.2.2.

$$f_{bu} + f_{\ell} \leq \phi_f R_h F_{yt} \quad \text{Eq. (6.10.3.2.2-1)}$$

The factored tensile flange stress due to steel self-weight and Cast #1, calculated without consideration of the lateral bending, f_{bu} , in the bottom flange due to the Special Load Combination specified in Article 3.4.2.1 was calculated previously as:

$$f_{bu} = 23.63 \text{ ksi}$$

The total lateral bending moment due to overhang brackets and curvature effects, factored for constructability, is -57.1 kip-ft as previously calculated. Therefore, the lateral bending stress in the bottom flange is as follows:

$$f_{\ell} = \frac{M_{\text{tot_lat}}}{S_{\text{bot flange}}} = \frac{|-57.1|(12)}{(1.625)(21)^2/6} = 5.74 \text{ ksi}$$

Therefore,

$$f_{\text{bu}} + f_{\ell} = 23.63 + 5.74 = 29.37 \text{ ksi} < \phi_f R_h F_{yc} = 1.0(1.0)(50) = 50 \text{ ksi OK}$$

(Ratio = 0.587)

7.4.3 Constructability Shear Strength, Web

Panels of webs with transverse stiffeners are investigated for constructability, with or without longitudinal stiffeners, and must satisfy the requirement specified in Article 6.10.3.3 during critical stages of construction; that is, the factored dead load shear, V_u , must not exceed the factored shear-yield or shear-buckling resistance, $\phi_v V_{cr}$. The use of post-buckling tension-field action is not permitted during construction. This calculation is similar to the shear strength check at the strength limit state (shown previously for end panels) and therefore is not shown.

7.4.4 Constructability of the Deck

The concrete deck is checked for constructability according to Article 6.10.3.2.4, which states that the longitudinal tensile stress in the composite concrete deck due to factored loads is not to exceed ϕf_r during critical stages of construction unless longitudinal reinforcement is provided according to Article 6.10.1.7. Article 6.10.1.7 states that whenever the tensile stress in the deck exceeds ϕf_r , longitudinal reinforcement equal to at least one percent of the total cross-sectional area of the deck must be placed in the deck. The specified deck placement sequence should be considered when evaluating deck stresses as the placement of later casts may produce controlling stress conditions in previously placed casts.

By inspection, it is observed that Cast #2 will cause negative moment near mid-span of Span 1. In practice, multiple locations would be checked to determine where the one percent longitudinal reinforcement is no longer required. For the purpose of this example, the deck tensile stress will be checked only at the location of G4-1 due to Cast #2. The major-axis moment at G4-1 due to Cast #2 is -3,035 kip-ft, as shown in Table 9. This location is appropriate to check since it lies within the Cast #1 composite section, which is 100 feet long and assumed to be hardened for Cast #2. See Figure 4 for the placement sequence diagram.

According to Article 6.10.1.1.1d, the short-term modular ratio, n , is used to calculate longitudinal flexural stresses in the concrete deck due to all permanent and transient loads.

Assume no creep: $n = 7.56$.

The Special Load Combination specified in Article 3.4.2.1 controls by inspection. Calculate the factored tensile stress at the top of the structural slab. The stress in the concrete deck is obtained by dividing the stress acting on the transformed section by the modular ratio, n :

$$f_{\text{deck}} = (1.4) \frac{(-3,035)(12)(-29.04)}{306,979} \left(\frac{1}{7.56} \right) = 0.64 \text{ ksi}$$

Assume the compressive strength of the hardened concrete from Cast #1 is 3,000 psi at the time Cast #2 is made. The modulus of rupture is:

$$f_r = 0.24\sqrt{f'_c} = 0.24\sqrt{3} = 0.42 \text{ ksi}$$

Therefore,

$$\phi f_r = 0.9(0.42) = 0.38 \text{ ksi} < 0.64 \text{ ksi}$$

where $\phi = 0.9$ from Article 6.10.1.7. Since $f_{\text{deck}} > \phi f_r$, one percent longitudinal reinforcement is required at this section. The reinforcement is to be 60.0 ksi or higher strength and should be a #6 bar or smaller spaced at not more than 12 inches according to Article 6.10.1.7. The required reinforcement should be placed in two layers uniformly distributed across the deck width, and two-thirds should be placed in the top layer. As discussed under Section Properties (see Section 7.2.3) earlier in this example, #6 bars spaced at 6 inches in the top layer and #4 bars spaced at 6 inches in the bottom layer satisfy these requirements.

The longitudinal reinforcement selected above would be continued into the “negative moment region,” over the pier, and terminated in the next span at a point where it is no longer required, determined in a similar fashion as the steps described above.

If it is desired to lower the concrete stress at a given location, the deck placement sequence could be modified.

7.5 Girder Check: Section G4-1, Service Limit State (Article 6.10.4)

Article 6.10.4 contains provisions related to the control of elastic and permanent deformations at the service limit state. For the sake of brevity, only the calculations pertaining to permanent deformations will be presented in this example.

7.5.1 Permanent Deformations (Article 6.10.4.2)

Article 6.10.4.2 contains criteria intended to control permanent deformations that would impair rideability. As specified in Article 6.10.4.2.1, these checks are to be made under the Service II load combination.

Article 6.10.4.2.2 states that flanges of composite sections must satisfy the following requirements at the service limit state:

$$\text{Top flange of composite sections: } f_f \leq 0.95R_h F_{yf} \quad \text{Eq. (6.10.4.2.2-1)}$$

$$\text{Bottom flange of composite sections: } f_f + \frac{f_\ell}{2} \leq 0.95R_h F_{yf} \quad \text{Eq. (6.10.4.2.2-2)}$$

However, according to Article C6.10.4.2.2, under the load combinations specified in Table 3.4.1-1, Eqs. (6.10.4.2.2-1) and (6.10.4.2.2-2) need only be checked for compact sections in positive flexure. For sections in negative flexure and noncompact sections in positive flexure, these two equations do not control and need not be checked. Composite sections in all horizontally curved girder systems are to be treated as noncompact sections at the strength limit state, in accordance with Article 6.10.6.2.2. Therefore, for Section G4-1, Eqs. (6.10.4.2.2-1) and (6.10.4.2.2-2) do not need to be checked but are demonstrated below for illustrative purposes only.

The term f_f is the flange stress at the section under consideration due to the Service II load combination calculated without consideration of flange lateral bending. The f_ℓ term, the flange lateral bending stress, in Eq. (6.10.4.2.2-2) is to be determined in accordance with Article 6.10.1.6. A resistance factor is not included in these equations because Article 1.3.2.1 specifies that the resistance factor be taken equal to 1.0 at the service limit state.

It should be noted that as discussed in Article C6.10.4.2.2, redistribution of negative moment due to the Service II loads at the interior-pier sections in continuous span flexural members using the procedures specified in Appendix B6 is not to be applied to horizontally curved I-girder bridges. The applicability of the Appendix B6 provisions to horizontally curved I-girder bridges has not been demonstrated; hence the procedures are not permitted for this type of bridge.

Check the flange stresses due to the Service II loads at Section G4-1. η is always specified to equal 1.0 at the service limit state (Article 1.3.2):

$$0.95R_h F_{yf} = 0.95(1.0)(50) = 47.50 \text{ ksi}$$

Top Flange:

$$f_f \leq 0.95R_h F_{yf} \quad \text{Eq. (6.10.4.2.2-1)}$$

$$f_f = 1.0 \left[\frac{1.0(661 + 2,682)}{2,504} + \frac{1.0(510 + 583)}{6,934} + \frac{1.3(5,125)}{18,015} \right] 12 = -22.35 \text{ ksi}$$

$$f_f = |-22.35| \text{ ksi} < 0.95R_h F_{yf} = 47.5 \text{ ksi} \quad \text{OK} \quad (\text{Ratio} = 0.471)$$

Bottom Flange:

$$f_f + \frac{f_\ell}{2} \leq 0.95R_h F_{yf} \quad \text{Eq. (6.10.4.2.2-2)}$$

Compute f_ℓ similarly to how it was calculated for the top flange constructability checks. First, determine the flange lateral moment, M_{lat} , due to curvature under the Service II load combination

(note that flange lateral bending due to deck overhang loads is not applicable at the service limit state):

$$M_{\text{lat}} = \frac{M\ell^2}{\text{NRD}} \quad \text{Eq. (C4.6.1.2.4b-1)}$$

$$= \frac{[1.0(661 + 2,682 + 510 + 583) + 1.3(5,125)](20.47)^2}{12(716.5)(7)} = 77.3 \text{ kip-ft}$$

The factored Service II bottom flange stress is:

$$f_{\ell} = \frac{M_{\text{lat}}}{S_{\text{bot_fl}}} = \frac{77.3(12)}{1.625(21)^2/6} = 7.77 \text{ ksi}$$

The bottom flange is in tension and so the amplification factor for the flange lateral bending stress is equal to 1.0 (Article 6.10.1.6).

Therefore:

$$f_f + \frac{f_{\ell}}{2} = 1.0 \left[\frac{1.0(661 + 2,682)}{3,266} + \frac{1.0(510 + 583)}{4,042} + \frac{1.3(5,125)}{4,412} \right] 12 + \frac{7.77}{2} = 37.53 \text{ ksi}$$

$$f_f + \frac{f_{\ell}}{2} = 37.53 \text{ ksi} < 47.50 \text{ ksi} \quad \text{OK} \quad (\text{Ratio} = 0.790)$$

7.5.2 Web Bend-Buckling

With the exception of composite sections in positive flexure in which the web satisfies the requirement of Article 6.10.2.1.1 (i.e., $D/t_w \leq 150$), web bend-buckling of all sections under the Service II load combination is to be checked as follows:

$$f_c \leq F_{\text{crw}} \quad \text{Eq. (6.10.4.2.2-4)}$$

The term f_c is the compression-flange stress at the section under consideration due to the Service II loads calculated without consideration of flange lateral bending, and F_{crw} is the nominal elastic bend-buckling resistance for webs determined as specified in Article 6.10.1.9.

At Section G4-1:

$$\frac{D}{t_w} = \frac{84}{0.5625} = 149.3 < 150$$

Because Section G4-1 is a composite section subject to positive flexure satisfying $D/t_w \leq 150$, Eq. (6.10.4.2.2-4) need not be checked. An explanation as to why these particular sections are exempt from the above web bend-buckling check is given in Article C6.10.1.9.1.

7.6 Girder Check: Section G4-1, Fatigue Limit State (Article 6.10.5)

Article 6.10.5 indicates that details in I-girder section flexural members must be investigated for fatigue as specified in Article 6.6.1. For horizontally curved I-girder bridges, the fatigue stress range due to major-axis bending plus lateral bending is to be investigated. As appropriate, the Fatigue I and Fatigue II load combinations specified in Table 3.4.1-1 and the fatigue live load specified in Article 3.6.1.4 are to be employed for checking load-induced fatigue in I-girder sections. The Fatigue I load combination is used when investigating infinite load-induced fatigue, and the Fatigue II load combination is used when investigating finite load-induced fatigue.

According to Table 3.6.2.1-1, the dynamic load allowance for the fatigue load is 15 percent. Centrifugal force effects are considered and are included in the fatigue moments. For this design example, the projected 75-year single lane ADTT is assumed to be 1,000 trucks per day.

7.6.1 Fatigue in Bottom Flange

At Section G4-1, it is necessary to check the bottom flange for the fatigue limit state. The base metal at the transverse stiffener weld terminations and interior cross-frame connection plate welds at locations subject to a net tensile stress must be checked for fatigue. This detail corresponds to Condition 4.1 in Table 6.6.1.2.3-1 and is classified as a Category C' fatigue detail. Only the bottom flange is checked herein, as a net tensile stress is not induced in the top flange by the fatigue loading at this location.

According to Eq. (6.6.1.2.2-1), the factored fatigue stress range, $\gamma(\Delta f)$, must not exceed the nominal fatigue resistance, $(\Delta F)_n$. In accordance with Article C6.6.1.2.2, the resistance factor, ϕ , and the load modifier, η , are taken as 1.0 for the fatigue limit state.

$$\gamma(\Delta f) \leq (\Delta F)_n \quad \text{Eq. (6.6.1.2.2-1)}$$

From Table 6.6.1.2.3-2, the 75-year $(ADTT)_{SL}$ equivalent to infinite fatigue life for a Category C' fatigue detail is 975 trucks per day. Therefore, since the assumed $(ADTT)_{SL}$ for this design example of 1,000 trucks per day is greater than this limit of 975 trucks per day, the detail must be checked for infinite fatigue life using the Fatigue I load combination. Per Article 6.6.1.2.5, the nominal fatigue resistance for infinite fatigue life is equal to the constant-amplitude fatigue threshold:

$$(\Delta F)_n = (\Delta F)_{TH} \quad \text{Eq. (6.6.1.2.5-1)}$$

where $(\Delta F)_{TH}$ is the constant-amplitude fatigue threshold and is taken from Table 6.6.1.2.5-3. For a Category C' fatigue detail, $(\Delta F)_{TH} = 12.0$ ksi, and therefore:

$$(\Delta F)_n = 12.0 \text{ ksi}$$

As shown in Table 9, the unfactored negative and positive moments due to fatigue, including centrifugal force effects and the 15 percent dynamic load allowance, at Section G4-1 are -603 kip-ft and 1,603 kip-ft, respectively. As shown in Table 13, the short-term composite section properties ($n = 7.56$) used to compute the stress at the bottom of the web (top of the bottom flange, where the weld in question is located) are:

$$I_{NA(n)} = 306,979 \text{ in.}^4$$

$$d_{\text{BOT OF WEB}} = d_{\text{BOT OF STEEL}} - t_{\text{BOT FLANGE}} = 69.585 \text{ in.} - 1.625 \text{ in.} = 67.96 \text{ in.}$$

Therefore, the unfactored stress range at the bottom of the web due to vertical loads only is:

$$f_{\text{range_vert}} = \left(\frac{(|-603| + 1,603)(12)(67.96)}{306,979} \right) = 5.86 \text{ ksi}$$

The flange lateral bending stress at the connection plate must also be considered according to Article C6.10.5.1. The connection plates are assumed to be 6 inches wide. To compute the flange lateral bending stress range at the top of the bottom flange due to curvature, it is first necessary to compute the flange lateral moment of inertia:

$$I_{\text{flg}} = \frac{1.625(21)^3}{12} = 1,254 \text{ in.}^4$$

Using Eq. (C4.6.1.2.4b-1), compute the range of flange lateral moment at the connection plate:

$$M_{\text{lat}} = \frac{M\ell^2}{NRD} = \frac{(|-603| + 1,603)(20.47^2)}{12(716.5)(7)} = 15.36 \text{ kip-ft}$$

Compute the distance from the centerline of the web to the edge of the connection plate (or conservatively to the flange tip if desired), and then compute the stress at this point:

$$c = 6 + \frac{0.5625}{2} = 6.3 \text{ in.}$$

$$f_{\text{lat}} = \frac{15.36(6.3)}{1,254}(12) = 0.93 \text{ ksi}$$

Per Table 3.4.1-1, the load factor, γ , for the Fatigue I load combination is 1.75. The total factored stress range at the edge of the connection plate due to both major-axis bending stress and flange lateral bending stress is therefore:

$$\gamma(\Delta f) = (1.75)(5.86 + 0.93) = 11.88 \text{ ksi}$$

Checking Eq. (6.6.1.2.2-1),

$$\gamma(\Delta f) = 11.88 \text{ ksi} < (\Delta F) = 12.00 \text{ ksi} \quad \text{OK} \quad (\text{Ratio} = 0.990)$$

7.6.2 Special Fatigue Requirement for Webs

In accordance with Article 6.10.5.3, interior panels of stiffened webs must satisfy:

$$V_u \leq V_{cr} \quad \text{Eq. (6.10.5.3-1)}$$

where: V_u = shear in the web at the section under consideration, due to unfactored permanent loads plus the factored fatigue load (Fatigue I live load)

V_{cr} = shear buckling resistance determined from Eq. (6.10.9.3.3-1)

Satisfaction of Eq. (6.10.5.3-1) is intended to control elastic flexing of the web by limiting the shear in the web to a level that will not result in shear buckling under the combined effects of permanent load and the repetitive fatigue live load. The member is assumed to be able to sustain an infinite number of smaller loadings without fatigue cracking due to this effect. The live load shear in the special requirement is supposed to represent the heaviest truck expected to cross the bridge in 75 years.

Only interior panels of stiffened webs are investigated because the shear resistance of end panels of stiffened webs and the shear resistance of unstiffened webs are limited to the shear buckling resistance at the strength limit state.

The unfactored shears at Section G4-1 are shown below. These results are taken directly from the three-dimensional analysis as reported in Table 10:

Steel Dead Load:	$V_{DC1-STEEL}$	= -5 kips
Concrete Deck Dead Load:	$V_{DC1-CONC}$	= -23.8 kips
Composite Dead Load:	V_{DC2}	= -4 kips
Future Wearing Surface Dead Load:	V_{DW}	= <u>-2.9 kips</u>
Total Permanent Load		= -35.7 kips
Fatigue Live Load + Impact:	V_{FAT}	= -20 kips

Therefore, the Fatigue I shear in the web is:

$$V_u = -35.7 + 1.75(-20) = -70.7 \text{ kips}$$

Next, compute the shear-buckling resistance:

$$V_{cr} = CV_p \quad \text{Eq. (6.10.9.3.3-1)}$$

where: C = ratio of the shear-buckling resistance to the shear yield strength

V_p = plastic shear force

Compute the plastic shear force:

$$V_p = 0.58F_{yw}Dt_w \quad \text{Eq. (6.10.9.3.3-2)}$$

$$V_p = 0.58(50)(84)(0.5625) = 1,370 \text{ kips}$$

To determine the ratio C , the shear-buckling coefficient, k , must first be computed as follows:

$$k = 5 + \frac{5}{\left(\frac{d_o}{D}\right)^2} \quad \text{Eq. (6.10.9.3.2-7)}$$

At this particular location, the transverse stiffener spacing is assumed to be 82 inches. Therefore, $d_o = 82$ in.

$$k = 5 + \frac{5}{\left[\frac{82}{84}\right]^2} = 10.2$$

Check the following relationship in order to select the appropriate equation for computing C :

$$\frac{D}{t_w} = \frac{84}{0.5625} = 149.3 > 1.40 \sqrt{\frac{Ek}{F_{yw}}} = 1.40 \sqrt{\frac{29,000(10.2)}{50}} = 108$$

Since the above relationship is true, the ratio C is computed using Eq. (6.10.9.3.2-6) as follows:

$$C = \frac{1.57}{\left(\frac{D}{t_w}\right)^2} \left(\frac{Ek}{F_{yw}}\right) \quad \text{Eq. (6.10.9.3.2-6)}$$

$$C = \frac{1.57}{\left(\frac{84}{0.5625}\right)^2} \left(\frac{29,000(10.2)}{50}\right) = 0.416$$

The shear-buckling resistance is then computed in accordance with Eq. (6.10.9.3.3-1):

$$V_{cr} = (0.416)(1,370) = 570 \text{ kips}$$

Using the above results, check the requirement of Article 6.10.5.3, $V_u \leq V_{cr}$:

$$V_u = |-70.7| \text{ kips} < V_{cr} = 570 \text{ kips} \quad \text{OK} \quad (\text{Ratio} = 0.124)$$

Therefore, the web is satisfactory for fatigue at the maximum positive moment location.

7.7 Girder Check: Section G4-1, Strength Limit State (Article 6.10.6)

7.7.1 Flexure (Article 6.10.6.2)

According to Article 6.10.6.2.2, sections in positive flexure in horizontally curved steel girder bridges are to be considered noncompact sections and are to satisfy the requirements of Article 6.10.7.2. Furthermore, both compact and noncompact sections in positive flexure must satisfy the ductility requirement specified in Article 6.10.7.3. The ductility requirement is intended to protect the concrete deck from premature crushing. The section must satisfy:

$$D_p \leq 0.42 D_t \quad \text{Eq. (6.10.7.3-1)}$$

Where D_p is the distance from the top of the concrete deck to the neutral axis of the composite section at the plastic moment, and D_t is the total depth of the composite section. Reference the section property computations in Section 7.2.1.3 for the location of the neutral axis of the composite section at the plastic moment. At Section G4-1:

$$D_p = 9.0 + 4.0 - 1.0 + 0.84 = 12.84 \text{ in.}$$

$$D_t = 1.625 + 84.0 + 4.0 + 9.0 = 98.625 \text{ in.}$$

$$0.42D_t = 0.42(98.625) = 41.42 \text{ in.} > 12.84 \text{ in.} \quad \text{OK} \quad (\text{Ratio} = 0.310)$$

Noncompact sections in positive flexure must satisfy the provisions of Article 6.10.7.2. At the strength limit state, the compression flange must satisfy:

$$f_{bu} \leq \phi_f F_{nc} \quad \text{Eq. (6.10.7.2.1-1)}$$

where:

- f_{bu} = flange stress calculated without consideration of flange lateral bending determined as specified in Article 6.10.1.6
- ϕ_f = resistance factor for flexure = 1.0 (Article 6.5.4.2)
- F_{nc} = nominal flexural resistance of the compression flange determined as specified in Article 6.10.7.2.2

As explained in Article C6.10.7.2.1, flange lateral bending is not considered for the compression flanges at the strength limit state because the flanges are continuously supported by the concrete deck.

At the strength limit state, the tension flange must satisfy:

$$f_{bu} + \frac{1}{3}f_{\ell} \leq \phi_f F_{nt} \quad \text{Eq. (6.10.7.2.1-2)}$$

where:

- f_{ℓ} = flange lateral bending stress determined as specified in Article 6.10.1.6
- F_{nt} = nominal flexural resistance of the tension flange determined as specified in Article 6.10.7.2.2

Additionally, the maximum longitudinal compressive stress in the concrete deck at the strength limit state is not to exceed $0.6f_c'$. The longitudinal compressive stress in the deck is to be determined in accordance with Article 6.10.1.1.1d, which allows the permanent and transient load stresses in the deck to be computed using the short-term section properties (i.e., modular ratio taken as n).

7.7.1.1 Strength I Flexural Stress in Top and Bottom Flange

The unfactored bending moments at Section G4-1 are shown below. These results are directly from the three-dimensional analysis as reported in Table 9. The live load moment includes the centrifugal force and dynamic load allowance effects.

Noncomposite Dead Load:	M_{DC1}	=	$661 + 2,682 = 3,343$	kip-ft
Composite Dead Load:	M_{DC2}	=	510	kip-ft
Future Wearing Surface Dead Load:	M_{DW}	=	583	kip-ft
Live Load (including IM and CF):	M_{LL+IM}	=	5,125	kip-ft

Compute the factored flange flexural stresses at Section G4-1 for the Strength I load combination, without consideration of flange lateral bending. As discussed previously, the η factor is taken equal to 1.0 in this example. Therefore:

For Strength I, the bending stresses due to vertical loads are as follows:

Top Flange (compression):

$$f_{bu} = \eta \left[\frac{(\gamma_{DC1} M_{DC1})}{S_{nc}} + \frac{[(\gamma_{DC2} M_{DC2} + \gamma_{DW} M_{DW})]}{S_{3n}} + \frac{(\gamma_{LL} M_{LL})}{S_n} \right] \quad (12)$$

$$= -(1.0) \left[\frac{1.25(3,343)}{2,504} + \frac{[1.25(510) + 1.5(583)]}{6,934} + \frac{1.75(5,125)}{18,015} \right] \quad (12) = -28.62 \text{ ksi}$$

Bottom Flange (tension):

$$f_{bu} = \eta \left[\frac{(\gamma_{DC1} M_{DC1})}{S_{nc}} + \frac{[(\gamma_{DC2} M_{DC2} + \gamma_{DW} M_{DW})]}{S_{3n}} + \frac{(\gamma_{LL} M_{LL})}{S_n} \right] \quad (12)$$

$$= (1.0) \left[\frac{1.25(3,343)}{3,266} + \frac{[1.25(510) + 1.5(583)]}{4,042} + \frac{1.75(5,125)}{4,412} \right] \quad (12) = 44.24 \text{ ksi}$$

As required to check the discretely braced tension flange, the lateral bending stress due to curvature must also be calculated for the bottom flange. Using the moments shown above, the unfactored lateral bending moment and corresponding lateral bending stress are calculated as follows:

$$M_{lat} = \frac{M \ell^2}{NRD} \quad \text{Eq. (C4.6.1.2.4b-1)}$$

$$f_{\ell} = \frac{M_{lat}}{S_{bot_flange}}, \text{ where } S_{bot_flange} = \frac{(1.625)(21)^2}{6} = 119.4 \text{ in.}^3$$

$$M_{lat_DC1} = \frac{3,343(20.47)^2}{12(716.5)(7)} = 23.27 \text{ kip-ft} \quad f_{\ell_DC1} = \frac{M_{lat_DC1}}{S_{bot_fl}} = \frac{23.27(12)}{119.4} = 2.34 \text{ ksi}$$

$$M_{lat_DC2} = \frac{510(20.47)^2}{12(716.5)(7)} = 3.55 \text{ kip-ft} \quad f_{\ell_DC2} = \frac{M_{lat_DC2}}{S_{bot_fl}} = \frac{3.55(12)}{119.4} = 0.36 \text{ ksi}$$

$$M_{lat_DW} = \frac{583(20.47)^2}{12(716.5)(7)} = 4.06 \text{ kip-ft} \quad f_{\ell_DW} = \frac{M_{lat_DW}}{S_{bot_fl}} = \frac{4.06(12)}{119.4} = 0.41 \text{ ksi}$$

$$M_{lat_LL} = \frac{5,125(20.47)^2}{12(716.5)(7)} = 35.68 \text{ kip-ft} \quad f_{\ell_LL} = \frac{M_{lat_LL}}{S_{bot_fl}} = \frac{35.68(12)}{119.4} = 3.59 \text{ ksi}$$

Therefore, the total factored lateral bending stress in the bottom flange is:

$$f_{\ell} = 1.25(2.34 + 0.36) + 1.5(0.41) + 1.75(3.59) = 10.27 \text{ ksi}$$

7.7.1.2 Top Flange Flexural Resistance in Compression

Per Article 6.10.7.2.2, the nominal flexural resistance of the compression flange of noncompact composite sections in positive flexure is to be taken as:

$$F_{nc} = R_b R_h F_{yc} \quad \text{Eq. (6.10.7.2.2-1)}$$

where:

R_b = web load-shedding factor determined as specified in Article 6.10.1.10.2

R_h = hybrid factor determined as specified in Article 6.10.1.10.1.

For a homogenous girder, the hybrid factor, R_h , is equal to 1.0. In accordance with Article 6.10.1.10.2, the web load-shedding factor, R_b , is equal to 1.0 for composite section in which the web satisfies the requirement of Article 6.10.2.1.1, such that $D/t_w \leq 150$.

$$\frac{D}{t_w} = \frac{84}{0.5625} = 149.3 < 150$$

Therefore:

$$F_{nc} = (1.0)(1.0)(50.00) = 50.00 \text{ ksi}$$

For Strength I:

$$f_{bu} \leq \phi_f F_{nc} \quad \text{Eq. (6.10.7.2.1-1)}$$

$$f_{bu} = |-28.62| \text{ ksi} < \phi_f F_{nc} = (1.0)(50) = 50 \text{ ksi} \quad \text{OK} \quad (\text{Ratio} = 0.572)$$

7.7.1.3 Bottom Flange Flexural Resistance in Tension

Article 6.10.7.2.2 states that the nominal flexural resistance of the tension flange of noncompact composite sections is to be taken as:

$$F_{nt} = R_h F_{yt} \quad \text{Eq. (6.10.7.2.2-2)}$$

Therefore:

$$F_{nt} = (1.0)(50.00) = 50.00 \text{ ksi}$$

For Strength I:

$$f_{bu} + \frac{1}{3}f_{\ell} \leq \phi_f F_{nt} \quad \text{Eq. (6.10.7.2.1-2)}$$

$$f_{bu} + \frac{1}{3}f_{\ell} = 44.24 + \frac{1}{3}(10.27) = 47.66 \text{ ksi} < \phi_f F_{nt} = (1.0)(50) = 50 \text{ ksi} \quad (\text{Ratio} = 0.953) \quad \text{OK}$$

According to the provisions of Article 6.10.1.6, lateral bending stresses in discretely braced flanges are to satisfy the following requirement:

$$f_{\ell} \leq 0.6F_{yf} \quad \text{Eq. (6.10.1.6-1)}$$

For the bottom flange in the final condition at the strength limit state:

$$f_{\ell} = 10.27 \text{ ksi} < 0.6F_{yf} = 0.6(50) = 30 \text{ ksi} \quad \text{OK} \quad (\text{Ratio} = 0.342)$$

Lateral bending stresses in the top flange are not considered at the strength limit state because the flange is continuously braced by the concrete deck.

7.7.2 Web Flexural Resistance

Article C6.10.1.9.1 states that composite sections subjected to positive flexure need not be checked for web bend-buckling in their final composite condition when the web does not require longitudinal stiffeners, as is the case for this design example.

7.7.3 Concrete Deck Stresses

According to Article 6.10.7.2.1, for noncompact sections, the maximum longitudinal compressive stress in the concrete deck at the strength limit state is not to exceed $0.6f_c'$. This limit is to verify linear behavior of the concrete, which is assumed in the calculation of steel flange stresses. The longitudinal compressive stress in the deck is to be determined in accordance with Article 6.10.1.1.1.d, which allows the permanent and transient load stresses in the deck to be computed using the short-term section properties ($n = 7.56$ composite section properties). Referring to Table 13 of the section property calculations, the section modulus to the top of the concrete deck is:

$$S_{\text{deck}} = \frac{306,979}{9.0 + 4.0 + \frac{84}{2} - 25.96} = 10,571 \text{ in.}^3$$

Calculate the Strength I factored longitudinal compressive stress in the deck at this section, noting that the concrete deck is not subjected to noncomposite dead loads. The stress in the concrete deck is obtained by dividing the stress acting on the transformed section by the modular ratio, n .

$$f_{\text{deck}} = -1.0 \left[\frac{1.25(510) + 1.5(583) + 1.75(5,125)}{10,571(7.56)} \right] (12) = -1.57 \text{ ksi}$$

$$f_{\text{deck}} = |-1.57| \text{ ksi} < 0.6f'_c = 0.6(4.0) = 2.4 \text{ ksi} \quad \text{OK}$$

7.8 Girder Check: Section G4-2, Constructability (Article 6.10.3)

Although not required, the bottom flange at Section G4-2, which is a discretely braced flange in compression, may be checked to verify that it satisfies the requirements of Eqs. (6.10.3.2.1-1), (6.10.3.2.1-2), and (6.10.3.2.1-3) for critical stages of construction, if desired. Generally, these provisions will not control because the size of the bottom flange in negative flexure regions is normally governed by the strength limit state. With regard to construction loads, the maximum negative moment reached during the deck placement analysis, plus the moment due to the self-weight, typically does not significantly exceed the calculated noncomposite negative moments assuming a single stage deck placement. Nonetheless, the constructability check is performed herein for completeness, and to illustrate the constructability checks for a negative moment region. For this constructability check, it is assumed that the concrete deck has not yet hardened at Section G4-2. The following equations are checked for the compression flange:

$$f_{\text{bu}} + f_{\ell} \leq \phi_f R_h F_{yc} \quad \text{Eq. (6.10.3.2.1-1)}$$

$$f_{\text{bu}} + \frac{1}{3} f_{\ell} \leq \phi_f F_{nc} \quad \text{Eq. (6.10.3.2.1-2)}$$

$$f_{\text{bu}} \leq \phi_f F_{crw} \quad \text{Eq. (6.10.3.2.1-3)}$$

Additionally, the top flange, which is considered discretely braced for constructability (i.e., the deck is not hardened), may be checked for the following requirement specified in Article 6.10.3.2.2.

$$f_{\text{bu}} + f_{\ell} \leq \phi_f R_h F_{yt} \quad \text{Eq. (6.10.3.2.2-1)}$$

To illustrate this constructability check, it is assumed that the unfactored major-axis bending moment due to the deck placement is -7,272 kip-ft and moment due to steel self-weight is -1,917 kip-ft at this section (see Table 9).

Calculate the factored major-axis flexural stresses in the flanges of the steel section due to the factored load resulting from the steel self-weight and the assumed deck placement sequence.

For the Strength I Load Combination:

$$\text{Top Flange: } f_{\text{bu}} = \frac{1.0(1.25)[(-1,917) + (-7,272)](12)}{6,689} = 20.61 \text{ ksi}$$

$$\text{Bot. Flange: } f_{bu} = \frac{1.0(1.25)[(-1,917) + (-7,272)](12)}{7,377} = -18.68 \text{ ksi}$$

For the Special Load Combination specified in Article 3.4.2.1:

$$\text{Top Flange: } f_{bu} = \frac{1.0(1.4)[(-1,917) + (-7,272)](12)}{6,689} = 23.08 \text{ ksi}$$

$$\text{Bot. Flange: } f_{bu} = \frac{1.0(1.4)[(-1,917) + (-7,272)](12)}{7,377} = -20.93 \text{ ksi}$$

The Special Load Combination controls in this case.

For this example and for illustration purposes, the V-load equation is used to compute the flange lateral bending moments due to curvature.

$$M_{LAT} = \frac{M\ell^2}{NRD} = \left| \frac{[(-1,917) + (-7,272)](20.47)^2}{(12)(716.5)(7)} \right| = -64.0 \text{ kip-ft} \quad \text{Eq. (C4.6.1.2.4b-1)}$$

Combine the factored flange lateral bending moment computed using the V-load equation with the lateral moment due to the overhang brackets which was computed in earlier calculations. The factored flange lateral bending moment and flange lateral bending stress are computed as:

$$M_{TOT_LAT} = (1.4)[-64.0 + (-8.8)] = -101.9 \text{ kip-ft}$$

Top Flange:

$$f_{\ell} = \frac{M_{TOT_LAT}}{S_{\ell}} = \frac{|-101.9|(12)}{(2.50)(28)^2/6} = 3.74 \text{ ksi}$$

Bot. Flange:

$$f_{\ell} = \frac{M_{TOT_LAT}}{S_{\ell}} = \frac{(-101.9)(12)}{(3.00)(27)^2/6} = -3.35 \text{ ksi}$$

7.8.1 Constructability of Top Flange

For critical stages of construction, the following requirement must be satisfied for discretely braced tension flanges according to Article 6.10.3.2.2.

$$f_{bu} + f_{\ell} \leq \phi_f R_h F_{yt} \quad \text{Eq. (6.10.3.2.2-1)}$$

The tensile flange stress for the Special Load Combination specified in Article 3.4.1.2, calculated without consideration of the lateral bending, f_{bu} , in the top flange is:

$$f_{bu} = 23.08 \text{ ksi} \quad (\text{factored, calculated previously})$$

The total lateral bending stress due to overhang brackets and curvature effects in the top flange is:

$$f_{\ell} = 3.74 \text{ ksi} \quad (\text{factored, calculated previously})$$

The resistance is calculated as follows:

$$\phi_f R_h F_{yt} = (1.0)(1.0)(50.0) = 50.0 \text{ ksi}$$

Therefore,

$$f_{bu} + f_{\ell} = 23.08 + 3.74 = 26.82 \text{ ksi} < \phi_f R_h F_{yt} = 50.0 \text{ ksi} \quad \text{OK} \quad (\text{Ratio} = 0.536)$$

7.8.2 Constructability of Bottom Flange

7.8.2.1 Bottom Flange Lateral Bending Amplification

As checked for the top flange in the positive moment region, the bottom flange in the negative moment region must also be checked to determine if a first-order or second-order analysis is appropriate for computing lateral bending stresses since the discretely braced bottom flange is in compression. According to Article 6.10.1.6, lateral bending stresses determined from a first-order analysis may be used in discretely braced compression flanges for which:

$$L_b \leq 1.2L_p \sqrt{\frac{C_b R_b}{f_{bu}/F_{yc}}} \quad \text{Eq. (6.10.1.6-2)}$$

L_p is the limiting unbraced length specified in Article 6.10.8.2.3 determined as:

$$L_p = 1.0r_t \sqrt{\frac{E}{F_{yc}}} \quad \text{Eq. (6.10.8.2.3-4)}$$

where r_t is the effective radius of gyration for lateral torsional buckling specified in Article 6.10.8.2.3 determined as:

$$r_t = \frac{b_{fc}}{\sqrt{12 \left(1 + \frac{1}{3} \frac{D_c t_w}{b_{fc} t_{fc}} \right)}} = \frac{27}{\sqrt{12 \left[1 + \frac{1}{3} \frac{(39.56)(0.625)}{27(3)} \right]}} = 7.43 \text{ in.} \quad \text{Eq. (6.10.8.2.3-9)}$$

C_b is conservatively taken as 1.0 for this computation. Article C6.10.1.10.2 indicates that the web load-shedding factor, R_b , is to be taken as 1.0 for constructability. Therefore:

$$L_p = 1.0r_t \sqrt{\frac{E}{F_{yc}}} = \frac{1.0(7.43) \sqrt{\frac{29,000}{50}}}{12} = 14.9 \text{ ft}$$

Check the relationship given in Eq. (6.10.1.6-2):

$$L_b = 20.47 \text{ ft} < 1.2(14.9) \sqrt{\frac{1.0(1.0)}{\frac{20.93}{50}}} = 27.64 \text{ ft}$$

Because Eq. (6.10.1.6-2) is satisfied, Article 6.10.1.6 allows the flange lateral bending stress to be determined directly from a first-order elastic analysis. Therefore, no amplification is required, and as computed earlier for the Special Load Combination specified in Article 3.4.1.2, the total flange stress due to lateral bending is:

$$f_\ell = -3.35 \text{ ksi}$$

7.8.2.2 Flexure in Bottom Flange (Article 6.10.3.2.1)

During construction, the bottom flange at Section G4-2 is a discretely based compression flange, so the provisions of Article 6.10.3.2.1 apply. Each of the following requirements are checked. The article indicates that if the section has a slender web, Eq. (6.10.3.2.1-1) is not checked when f_ℓ is zero, and for sections with compact or noncompact webs, Eq. (6.10.3.2.1-3) is not checked. In this case, the web is nonslender (as demonstrated later), so only the first two equations must be checked.

$$f_{bu} + f_\ell \leq \phi_f R_h F_{yc} \quad \text{Eq. (6.10.3.2.1-1)}$$

$$f_{bu} + \frac{1}{3} f_\ell \leq \phi_f F_{nc} \quad \text{Eq. (6.10.3.2.1-2)}$$

$$f_{bu} \leq \phi_f F_{crw} \quad \text{Eq. (6.10.3.2.1-3)}$$

where: ϕ_f = resistance factor for flexure = 1.0 (Article 6.5.4.2)
 R_h = hybrid factor specified in Article 6.10.1.10.1 (1.0 at homogeneous Section G4-2)
 F_{crw} = nominal elastic bend-buckling resistance for webs determined as specified in Article 6.10.1.9
 F_{nc} = nominal flexural resistance of the compression flange determined as specified in Article 6.10.8.2 (i.e., local or lateral torsional buckling resistance, whichever controls). The provisions of Article A6.3.3 are not to be used to determine the

lateral torsional buckling resistance of sections in curved I-girder bridges, per Article 6.10.3.2.1.

Check Eq. (6.10.3.2.1-1) using the previously calculated values of factored flange stresses:

$$f_{bu} + f_{\ell} = |-20.93| + |-3.35| = 24.28 \text{ ksi} < \phi_f R_h F_{yc} = 1.0(1.0)(50) = 50 \text{ ksi} \quad \text{OK (Ratio} = 0.486)$$

Secondly, check Eq. (6.10.3.2.1-2). The equation must be satisfied for both local buckling and lateral torsional buckling using the appropriate value of the nominal flexural resistance, F_{nc} , for local buckling (Article 6.10.8.2.2) or for lateral torsional buckling (Article 6.10.8.2.3), as applicable.

Determine the local buckling resistance of the compression flange. First, check the flange slenderness.

$$\lambda_f = \frac{b_{fc}}{2t_{fc}} = \frac{27}{2(3)} = 4.5$$

$$\lambda_{pf} = 0.38 \sqrt{\frac{E}{F_{yc}}} = 0.38 \sqrt{\frac{29,000}{50}} = 9.15$$

Since $\lambda_f < \lambda_{pf}$, the flange is compact and the nominal flexural resistance is determined using Eq. (6.10.8.2.2-1).

R_b is taken as 1.0 for constructability checks per Article 6.10.3.2.1, and R_h is taken as 1.0 per Article 6.10.1.10.1. Therefore, F_{nc} for the local buckling resistance is calculated as:

$$\begin{aligned} F_{nc} &= R_b R_h F_{yc} && \text{Eq. (6.10.8.2.2-1)} \\ &= (1.0)(1.0)(50) = 50.00 \text{ ksi} \end{aligned}$$

Determine the lateral torsional buckling resistance of the compression flange, noting that the critical unbraced length, L_b , at this location is 20.47 ft in Span 1. The flange transition in this unbraced length is less than 20 percent of the unbraced length from the brace point with the smaller moment and the lateral moment of inertia of the flange in the smaller section is exactly one-half of the corresponding value in the larger section; therefore, the transition may be ignored and the larger section may be used to compute the lateral torsional buckling resistance.

$$L_p = 14.9 \text{ ft (calculated previously)}$$

$$L_r = \pi r_t \sqrt{\frac{E}{F_{yr}}} = \frac{\pi(7.43) \sqrt{\frac{29,000}{0.7(50)}}}{12} = 56.0 \text{ ft.} \quad \text{Eq. (6.10.8.2.3-5)}$$

Since $L_p < L_b < L_r$, use Eq. (6.10.8.2.3-2) to calculate the lateral torsional buckling resistance.

$$\begin{aligned} F_{nc} &= C_b \left[1 - \left(1 - \frac{F_{yr}}{R_h F_{yc}} \right) \left(\frac{L_b - L_p}{L_r - L_p} \right) \right] R_b R_h F_{yc} \leq R_b R_h F_{yc} \quad \text{Eq. (6.10.8.2.3-2)} \\ &= 1.0 \left[1 - \left[1 - \frac{0.7(50)}{1.0(50)} \right] \left(\frac{20.47 - 14.9}{56.0 - 14.9} \right) \right] (1.0)(1.0)(50) = 47.97 \text{ ksi} \end{aligned}$$

For checking the lateral torsional buckling resistance, the largest major-axis bending stress within the unbraced length is to be used in conjunction with the largest flange lateral bending stress (Article 6.10.1.6). In this case, the largest stresses are at Section G4-2. For checking the local buckling resistance, the major-axis bending and flange lateral bending stress at the section under consideration may be used, which again is at Section G4-2.

Therefore, check Eq. (6.10.3.2.1-2) for local buckling as follows:

$$f_{bu} + \frac{1}{3} f_\ell = |-20.93| + \frac{1}{3} (|-3.35|) = 22.05 \text{ ksi} < \phi_f F_{nc} = 1.0(50.00) = 50.00 \text{ ksi} \quad \text{OK} \\ \text{(Ratio} = 0.441\text{)}$$

Check Eq. (6.10.3.2.1-2) for lateral torsional buckling as follows:

$$f_{bu} + \frac{1}{3} f_\ell = |-20.93| + \frac{1}{3} (|-3.35|) = 22.05 \text{ ksi} < \phi_f F_{nc} = 1.0(47.97) = 47.97 \text{ ksi} \quad \text{OK} \\ \text{(Ratio} = 0.460\text{)}$$

Third, determine if Eq. (6.10.3.2.1-3) must be checked. The slenderness is checked according to Article 6.10.6.2.3 as follows:

$$\frac{2D_c}{t_w} \leq \lambda_{rw} \quad \text{Eq. (6.10.6.2.3-1)}$$

where:

$$4.6 \sqrt{\frac{E}{F_{yc}}} \leq \lambda_{rw} = \left(3.1 + \frac{5.0}{a_{wc}} \right) \sqrt{\frac{E}{F_{yc}}} \leq 5.7 \sqrt{\frac{E}{F_{yc}}} \quad \text{Eq. (6.10.6.2.3-3)}$$

$$a_{wc} = \frac{2D_c t_w}{b_{fc} t_{fc}} \quad \text{Eq. (6.10.6.2.3-4)}$$

$$\frac{2D_c}{t_w} = \frac{2(39.56)}{0.625} = 126.6$$

$$4.6 \sqrt{\frac{E}{F_{yc}}} = 4.6 \sqrt{\frac{29,000}{50}} = 111$$

$$5.7 \sqrt{\frac{E}{F_{yc}}} = 5.7 \sqrt{\frac{29,000}{50}} = 137$$

$$a_{wc} = \frac{2(39.56)(0.625)}{27(3.0)} = 0.61$$

$$111 < \lambda_{rw} = \left(3.1 + \frac{5.0}{0.61} \right) \sqrt{\frac{29,000}{50}} = 272.1 > 137$$

$$\therefore \lambda_{rw} = 137 > \frac{2D_c}{t_w} = 126.6$$

Because the web is nonslender, Eq. (6.10.3.2.1-3) need not be checked.

7.9 Girder Check: Section G4-2, Service Limit State (Article 6.10.4)

Article 6.10.4 contains provisions related to the control of elastic and permanent deformations at the service limit state.

7.9.1 Permanent Deformations (Article 6.10.4.2)

Article 6.10.4.2 contains criteria intended to control permanent deformations that would impair rideability. As specified in Article 6.10.4.2.1, these checks are to be made using the Service II load combination.

As stated previously for the service limit state check of Section G4-1, Article 6.10.4.2.2 requires that flanges of composite sections satisfy the following relationships:

$$\text{Top flange of composite sections: } f_f \leq 0.95R_h F_{yf} \quad \text{Eq. (6.10.4.2.2-1)}$$

$$\text{Bottom flange of composite sections: } f_f + \frac{f_\ell}{2} \leq 0.95R_h F_{yf} \quad \text{Eq. (6.10.4.2.2-2)}$$

However, according to Article C6.10.4.2.2, for composite sections in negative flexure designed as slender-web sections at the strength limit state according to the provisions of Article 6.10.8, and for composite sections in positive flexure designed as noncompact sections at the strength limit state, these two equations do not control and need not be checked. Composite sections in all horizontally curved girder systems are to be treated as slender-web sections in negative flexure and as noncompact sections in positive flexure at the strength limit state, in accordance with Article 6.10.6.2.2 (regardless of their web slenderness). Therefore, for Section G4-2, Eqs. (6.10.4.2.2-1) and (6.10.4.2.2-2) do not need to be checked and are not demonstrated in this example.

7.9.2 Web Bend-Buckling

With the exception of composite sections in positive flexure in which the web satisfies the requirement of Article 6.10.2.1.1 (i.e., $D/t_w \leq 150$), web bend-buckling of all sections under the Service II load combination is to be checked as follows:

$$f_c \leq F_{crw} \quad \text{Eq. (6.10.4.2.2-4)}$$

The term f_c is the compression-flange stress at the section under consideration due to the Service II loads calculated without consideration of flange lateral bending, and F_{crw} is the nominal elastic bend-buckling resistance for webs determined as specified in Article 6.10.1.9. Because Section G4-2 is a section in negative flexure, it must be checked for Eq. (6.10.4.2.2-4).

Determine the nominal web bend-buckling resistance, F_{crw} , for Section G4-2 in accordance with Article 6.10.1.9.1, as follows:

$$F_{crw} = \frac{0.9 E k}{\left(\frac{D}{t_w}\right)^2} \quad \text{Eq. (6.10.1.9.1-1)}$$

However, F_{crw} is not to exceed the smaller of $R_h F_{yc}$ and $F_{yw}/0.7$. The bend-buckling coefficient, k , is computed as:

$$k = \frac{9}{(D_c / D)^2} \quad \text{Eq. (6.10.1.9.1-2)}$$

where:

D_c = depth of the web in compression in the elastic range (in.). For composite sections, D_c is to be determined as specified in Article D6.3.1.

In accordance with Article 6.10.4.2.1, for members with shear connectors provided throughout the entire length of the girder that also satisfy Article 6.10.1.7, the concrete deck may be assumed to be effective for both positive and negative flexure, provided that the corresponding longitudinal stresses in the concrete deck at the section under consideration are smaller than $2f_r$, where f_r is the

modulus of rupture of concrete specified in Article 6.10.1.7. Article 6.10.1.7 specifies that the minimum one percent longitudinal reinforcement provided in the concrete deck must be provided wherever the tensile stress in the deck exceeds ϕf_r at the service limit state and for constructability and is satisfied for Section G4-2 in this design example.

$$f_r = 0.24\sqrt{f'_c}$$

Therefore,

$$2f_r = 2(0.24\sqrt{4}) = 0.960 \text{ ksi}$$

In accordance with Article 6.10.1.1d, the longitudinal flexural stresses in the concrete deck due to all permanent and transient loads are to be computed using the short-term modular ratio, n . Since the deck is not subjected to noncomposite dead loads, the longitudinal stress in the deck at Section G4-2 is due to DC2, DW, and LL+I moments only. The unfactored major-axis bending moments at Section G4-2 are (see Table 9):

Noncomposite Dead Load:	$M_{DC1} = -1,917 + (-7,272) = -9,189 \text{ kip-ft}$
Composite Dead Load:	$M_{DC2} = -1,537 \text{ kip-ft}$
Future Wearing Surface Dead Load:	$M_{DW} = -1,478 \text{ kip-ft}$
Live Load (including IM and CF):	$M_{LL+IM} = -6,726 \text{ kip-ft}$

The longitudinal tensile stress in the deck is computed using the short-term section properties ($n = 7.56$ composite section properties) in accordance with Article 6.10.1.1d. Referring to Table 16 of the section property calculations and noting that the total depth of the composite Section G4-2 is 100 inches, the section modulus to the top of the concrete deck is:

$$S_{\text{deck}} = \frac{539,403}{100.00 - 63.40} = 14,738 \text{ in.}^3$$

Calculate the Service II factored longitudinal tensile stress in the deck at this section, noting that the concrete deck is not subjected to noncomposite dead loads. The stress in the concrete deck is obtained by dividing the stress acting on the transformed section by the modular ratio, n .

$$f_{\text{deck}} = 1.0 \left[\frac{1.00(1,537) + 1.00(1,478) + 1.30(6,726)}{(14,738)(7.56)} \right] 12 = 1.266 \text{ ksi}$$

$$f_{\text{deck}} = 1.266 \text{ ksi} > 2f_r = 0.960 \text{ ksi}$$

Since f_{deck} is greater than $2f_r$, for this service limit state check, the concrete deck cannot be assumed to be effective for negative flexure and the flexural stresses in the steel section caused by the Service II load combination are to be computed using the section consisting of the steel girder and the longitudinal reinforcement within the effective width of the concrete deck. Refer to Table 17 and Table 18 for the composite section properties with longitudinal steel reinforcement. The

major-axis bending stresses in the top and bottom flange for the Service II load combination are computed as follows (f_t = tension flange, f_c = compression flange):

For Service II:

Top Flange:

$$f_t = 1.0 \left[\frac{1.00(9,189)}{6,689} + \frac{1.00(1,537)}{6,944} + \frac{1.00(1,478)}{6,944} + \frac{1.30(6,726)}{7,146} \right] 12 = 36.38 \text{ ksi}$$

Bottom Flange:

$$f_c = 1.0 \left[\frac{1.00(9,189)}{7,377} + \frac{1.00(1,537)}{7,429} + \frac{1.00(1,478)}{7,429} + \frac{1.30(6,726)}{7,523} \right] 12 = -33.76 \text{ ksi}$$

To compute F_{crw} , it is first necessary to determine D_c , the depth of the web in compression. In accordance with Article D6.3.1, for composite sections in negative flexure where the concrete deck is not permitted to be considered effective in tension at the service limit state, D_c is to be computed for the section consisting of the steel girder plus the longitudinal reinforcement. As explained in Article CD6.3.1, for composite sections in negative flexure, the distance between the neutral axis locations for the steel and composite sections is small, and the location of the neutral axis for the composite section is largely unaffected by the dead-load stress. Therefore, D_c is simply computed for the section consisting of the steel girder plus the longitudinal reinforcement. In this example, the section properties from Table 18 are used to compute D_c as follows, where the thickness of the bottom flange is 3 in. (the short-term section is conservatively used):

$$D_c = 44.55 - 3.00 = 41.55 \text{ in.}$$

Compute the bend-buckling coefficient, k :

$$k = \frac{9}{(D_c / D)^2} = \frac{9}{(41.55 / 84)^2} = 36.78$$

Therefore, the nominal web bend-buckling resistance, F_{crw} , is computed as:

$$F_{crw} = \frac{0.9 E k}{\left(\frac{D}{t_w} \right)^2} = \frac{0.9 (29,000) (36.78)}{\left(\frac{84}{0.625} \right)^2} = 53.14 \text{ ksi} > \min(R_h F_{yc}, F_{yw} / 0.7) = 50.0 \text{ ksi}$$

Therefore, use $F_{crw} = 50.0$ ksi.

Verify Eq. (6.10.4.2.2-4):

$$f_c = |-33.76| \text{ ksi} < F_{crw} = 50.0 \text{ ksi} \quad \text{OK} \quad (\text{Ratio} = 0.675)$$

7.10 Girder Check: Section G4-2, Fatigue Limit State (Article 6.10.5)

Article 6.10.5 indicates that details in I-girder section flexural members must be investigated for fatigue as specified in Article 6.6.1. For horizontally curved I-girder bridges, the fatigue stress range due to major-axis bending plus lateral bending is to be considered. As appropriate, the Fatigue I and Fatigue II load combinations specified in Table 3.4.1-1 and the fatigue live load specified in Article 3.6.1.4 are to be employed for checking load-induced fatigue in I-girder sections. The Fatigue I load combination is used when investigating infinite load-induced fatigue life, and the Fatigue II load combination is used when investigating finite load-induced fatigue life.

According to Table 3.6.2.1-1, the dynamic load allowance for the fatigue load is 15%. Centrifugal force effects are considered and included in the fatigue moments. As discussed previously, the projected 75-year single lane ADTT is assumed to be 1,000 trucks per day.

7.10.1 Fatigue in Top Flange

At Section G4-2, it is necessary to check the top flange for the fatigue limit state. The base metal at the transverse stiffener weld terminations and interior cross-frame connection plate welds at locations subject to a net tensile stress must be checked as a Category C' fatigue detail per Condition 4.1 in Table 6.6.1.2.3-1. Only the top flange is checked herein, as a net tensile stress is not induced in the bottom flange by the fatigue loading at this location. Also, it should be noted that lateral bending stress in the top flange is not a concern for the fatigue limit state at this section since the deck is in place and continuously braces the top flange.

According to Eq. (6.6.1.2.2-1), the factored fatigue stress range, $\gamma(\Delta f)$, must not exceed the nominal fatigue resistance, $(\Delta F)_n$. In accordance with Article C6.6.1.2.2, the resistance factor, ϕ , and the load modifier, η , are taken as 1.0 for the fatigue limit state.

$$\gamma(\Delta f) \leq (\Delta F)_n \quad \text{Eq. (6.6.1.2.2-1)}$$

For continuous spans, the number of stress cycles per truck passage, n , is equal to 1.5 at sections near the interior pier and 1.0 elsewhere (Table 6.6.1.2.5-2). Sections 'near the interior pier' are defined as sections within a distance of one-tenth of the span on each side of the interior support. As indicated in Article C6.6.1.2.3, for values of n other than 1.0, the values of the 75-year $(ADTT)_{SL}$ Equivalent to Infinite Life given in Table 6.6.1.2.3-2 are to be modified by dividing by the appropriate value of n taken from Table 6.6.1.2.5-2.

From Table 6.6.1.2.3-2, the 75-year $(ADTT)_{SL}$ equivalent to infinite fatigue life for a Category C' fatigue detail, adjusted for $n = 1.5$, is $975/1.5 = 650$ trucks per day. Therefore, since the assumed $(ADTT)_{SL}$ for this design example of 1,000 trucks per day is greater than this limit of 650 trucks

per day, the detail must be checked for infinite fatigue life using the Fatigue I load combination. Per Article 6.6.1.2.5, the nominal fatigue resistance for infinite fatigue life is equal to the constant-amplitude fatigue threshold:

$$(\Delta F)_n = (\Delta F)_{TH} \quad \text{Eq. (6.6.1.2.5-1)}$$

where $(\Delta F)_{TH}$ is the constant-amplitude fatigue threshold and is taken from Table 6.6.1.2.5-3. For a Category C' fatigue detail, $(\Delta F)_{TH} = 12.0$ ksi, and therefore:

$$(\Delta F)_n = 12.0 \text{ ksi}$$

As shown in Table 9, the unfactored negative and positive moments due to fatigue, including centrifugal force effects and the 15 percent dynamic load allowance, at Section G4-2 are -1,315 kip-ft and 351 kip-ft, respectively.

In accordance with Article 6.6.1.2.1, for flexural members that utilize shear connectors throughout the entire length that also have concrete deck reinforcement satisfying the provisions of Article 6.10.1.7, it is permissible to compute the flexural stresses assuming the concrete deck to be effective for both positive and negative flexure at the fatigue limit state.

As required by Articles 6.10.10.1, shear connectors are necessary along the entire length of horizontally curved continuous composite bridges. Also, earlier calculations in this design example show that the deck reinforcement is in compliance with Article 6.10.1.7. Therefore, the concrete deck is assumed effective in computing the major-axis bending stresses for the fatigue limit state at Section G4-2. From Table 16, the short-term composite section properties ($n = 7.56$) used to compute the stress at the top of the web (bottom of the top flange, where the weld in question is located) are:

$$I_{NA(n)} = 539,403 \text{ in.}^4$$

$$d_{\text{TOP OF WEB}} = d_{\text{TOP OF STEEL}} - t_{f_TOP FLANGE} = 26.10 \text{ in.} - 2.50 \text{ in.} = 23.60 \text{ in.}$$

Per Table 3.4.1-1, the load factor, γ , for the Fatigue I load combination is 1.75. The factored stress range at the top of the web is computed as follows:

$$\gamma(\Delta f) = 1.75 \left(\frac{(|-1,315| + 351)(12)(23.60)}{539,403} \right) = 1.53 \text{ ksi}$$

The lateral bending stress range is neglected since the top flange is continuously braced by the composite concrete deck. Checking Eq. (6.6.1.2.2-1),

$$\gamma(\Delta f) = 1.53 \text{ ksi} < (\Delta F)_n = 12.0 \text{ ksi} \quad \text{OK} \quad (\text{Ratio} = 0.128)$$

7.10.2 Special Fatigue Requirement for Webs

In accordance with Article 6.10.5.3, interior panels of stiffened webs must satisfy:

$$V_u \leq V_{cr} \quad \text{Eq. (6.10.5.3-1)}$$

where: V_u = shear in the web at the section under consideration, due to unfactored permanent loads plus the factored fatigue load (Fatigue I live load)

V_{cr} = shear buckling resistance determined from Eq. (6.10.9.3.3-1).

Satisfaction of Eq. (6.10.5.3-1) is intended to control elastic flexing of the web, and the member is assumed to be able to sustain an infinite number of smaller loadings without fatigue cracking due to this effect. The live load shear in the special requirement is supposed to represent the heaviest truck expected to cross the bridge in 75 years.

Only interior panels of stiffened webs are investigated because the shear resistance of end panels of stiffened webs and the shear resistance of unstiffened webs are limited to the shear buckling resistance at the strength limit state.

The unfactored shears at Section G4-1 are shown below. These results are directly from the three-dimensional analysis as reported in Table 10.

Steel Dead Load:	$V_{DC1-STEEL}$	= -45 kips
Concrete Deck Dead Load:	$V_{DC1-CONC}$	= -144 kips
Composite Dead Load:	V_{DC2}	= -36 kips
Future Wearing Surface Dead Load:	V_{DW}	= <u>-28 kips</u>
Total Permanent Load		= -253 kips
Fatigue Live Load (incl. IM + CF):	V_{LL+IM}	= -55 kips

Therefore, the Fatigue I shear in the web is:

$$V_u = -253 + 1.75(-55) = -349 \text{ kips}$$

Next, compute the shear-buckling resistance:

$$V_{cr} = CV_p \quad \text{Eq. (6.10.9.3.3-1)}$$

where: C = ratio of the shear-buckling resistance to the shear yield strength

V_p = plastic shear force

Compute the plastic shear force:

$$V_p = 0.58F_{yw}Dt_w \quad \text{Eq. (6.10.9.3.3-2)}$$

$$= 0.58(50)(84)(0.625) = 1,523 \text{ kips}$$

To determine the ratio C, the shear-buckling coefficient, k, must first be computed as follows:

$$k = 5 + \frac{5}{\left(\frac{d_o}{D}\right)^2} \quad \text{Eq. (6.10.9.3.2-7)}$$

At this particular location, the transverse stiffener spacing is assumed to be 82 inches. Therefore, $d_o = 82$ in.

$$k = 5 + \frac{5}{\left[\frac{82}{84}\right]^2} = 10.2$$

Check the following relationship in order to select the appropriate equation for computing C:

$$\frac{D}{t_w} = \frac{84}{0.625} = 134.4 > 1.40 \sqrt{\frac{Ek}{F_{yw}}} = 1.40 \sqrt{\frac{29,000(10.2)}{50}} = 108$$

Since the above relationship is true, the ratio C is computed using Eq. (6.10.9.3.2-6) as follows:

$$C = \frac{1.57}{\left(\frac{D}{t_w}\right)^2} \left(\frac{Ek}{F_{yw}}\right) \quad \text{Eq. (6.10.9.3.2-6)}$$

$$C = \frac{1.57}{\left(\frac{84}{0.625}\right)^2} \left(\frac{29,000(10.2)}{50}\right) = 0.514$$

The shear-buckling resistance is then computed in accordance with Eq. (6.10.9.3.3-1):

$$V_{cr} = (0.514)(1,523) = 783 \text{ kips}$$

Using the above results, check the requirement of Article 6.10.5.3, $V_u \leq V_{cr}$:

$$V_u = |-349| \text{ kips} < V_{cr} = 783 \text{ kips} \quad \text{OK} \quad (\text{Ratio} = 0.446)$$

Therefore, the web is satisfactory for fatigue at the maximum negative moment location.

7.11 Girder Check: Section G4-2, Strength Limit State (Article 6.10.6)

7.11.1 Flexure (Article 6.10.6.2)

According to Article 6.10.6.2.3, composite sections in negative flexure in horizontally curved steel girder bridges are to be treated as slender-web sections at the strength limit state regardless of their web slenderness and must therefore satisfy the requirements of Article 6.10.8.

Composite sections in negative flexure must satisfy the provisions of Article 6.10.8.1. At the strength limit state, the compression flange must satisfy:

$$f_{bu} + \frac{1}{3}f_{\ell} \leq \phi_f F_{nc} \quad \text{Eq. (6.10.8.1.1-1)}$$

where:

- f_{bu} = flange stress calculated without consideration of flange lateral bending determined as specified in Article 6.10.1.6
- ϕ_f = resistance factor for flexure = 1.0 (Article 6.5.4.2)
- F_{nc} = nominal flexural resistance of the compression flange determined as specified in Article 6.10.8.2

Per Article 6.10.8.1.3 for continuously braced flanges, at the strength limit state, the tension flange must satisfy:

$$f_{bu} \leq \phi_f R_h F_{yf} \quad \text{Eq. (6.10.8.1.3-1)}$$

It should be noted that flange lateral bending is not considered for the tension flange at the strength limit state in this case because the flange is continuously supported by the hardened concrete deck.

7.11.1.1 Strength I Flexural Stress in Top and Bottom Flange

The unfactored bending moments at Section G4-2 from the analysis are shown below (see Table 9). The live load moment includes the centrifugal force and dynamic load allowance effects.

Noncomposite Dead Load:	$M_{DC1} = -1,917 + (-7,272) = -9,189$ kip-ft
Composite Dead Load:	$M_{DC2} = -1,537$ kip-ft
Future Wearing Surface Dead Load:	$M_{DW} = -1,478$ kip-ft
Live Load (including IM and CF):	$M_{LL+IM} = -6,726$ kip-ft

Compute the factored flange flexural stresses at Section G4-2 for the Strength I load combination, without consideration of flange lateral bending. As discussed previously, the η factor is taken equal to 1.0 in this example. In accordance with Article 6.10.1.1.1c, the flexural stresses are computed

using section properties based on a composite section consisting of the steel section and the longitudinal reinforcement within the effective width of the concrete deck (refer to Table 17 and Table 18). Therefore:

For Strength I, the bending stresses due to vertical loads are as follows:

Top Flange (tension):

$$f_{bu} = \left[\frac{(\gamma_{DC1} M_{DC1})}{S_{nc}} + \frac{[(\gamma_{DC2} M_{DC2} + \gamma_{DW} M_{DW})]}{S_{3n}} + \frac{(\gamma_{LL} M_{LL})}{S_n} \right] (12)\eta$$

$$= \left[\frac{1.25(9,189)}{6,689} + \frac{[1.25(1,537) + 1.5(1,478)]}{6,944} + \frac{1.75(6,726)}{7,146} \right] (12)(1) = 47.52 \text{ ksi}$$

Bottom Flange (compression):

$$f_{bu} = \left[\frac{(\gamma_{DC1} M_{DC1})}{S_{nc}} + \frac{[(\gamma_{DC2} M_{DC2} + \gamma_{DW} M_{DW})]}{S_{3n}} + \frac{(\gamma_{LL} M_{LL})}{S_n} \right] (12)\eta$$

$$= \left[\frac{1.25(9,189)}{7,377} + \frac{[1.25(1,537) + 1.5(1,478)]}{7,429} + \frac{1.75(6,726)}{7,523} \right] (12)(1) = -44.14 \text{ ksi}$$

As required to check the discretely braced compression flange, the lateral bending stress must also be calculated for the bottom flange. Using the moments shown above, the unfactored lateral bending moment and corresponding first-order lateral bending stress due to curvature are calculated as follows:

$$M_{lat} = \frac{M\ell^2}{NRD} \quad \text{Eq. (C4.6.1.2.4b-1)}$$

$$f_{\ell} = \frac{M_{lat}}{S_{bot_flange}}, \text{ where } S_{bot_flange} = \frac{(3.0)(27)^2}{6} = 364.5 \text{ in.}^3$$

$$M_{lat_DC1} = \frac{9,189(20.47)^2}{12(716.5)(7)} = -63.97 \text{ kip-ft}$$

$$f_{\ell_DC1} = \frac{M_{lat_DC1}}{S_{bot_fl}} = \frac{-63.97(12)}{364.5} = -2.11 \text{ ksi}$$

$$M_{lat_DC2} = \frac{1,537(20.47)^2}{12(716.5)(7)} = -10.70 \text{ kip-ft}$$

$$f_{\ell_DC2} = \frac{M_{lat_DC2}}{S_{bot_fl}} = \frac{-10.70(12)}{364.5} = -0.35 \text{ ksi}$$

$$M_{lat_DW} = \frac{1,478(20.47)^2}{12(716.5)(7)} = -10.29 \text{ kip-ft}$$

$$f_{\ell_DW} = \frac{M_{lat_DW}}{S_{bot_fl}} = \frac{-10.29(12)}{364.5} = -0.34 \text{ ksi}$$

$$M_{\text{lat_LL}} = \frac{6,726(20.47)^2}{12(716.5)(7)} = -46.83 \text{ kip-ft} \quad f_{\ell_LL} = \frac{M_{\text{lat_LL}}}{S_{\text{bot_fl}}} = \frac{-46.83(12)}{364.5} = -1.54 \text{ ksi}$$

As investigated for the bottom flange constructability checks for Section G4-2, the bottom flange for the strength limit state may be subject to lateral bending amplification. The flange lateral bending stress, f_t , may be determined directly from first-order elastic analysis if the following relation is satisfied:

$$L_b \leq 1.2L_p \sqrt{\frac{C_b R_b}{f_{bu}/F_{yc}}} \quad \text{Eq. (6.10.1.6-2)}$$

Per Article 6.10.1.10.2, R_b is to be taken as 1.0 if the web satisfies:

$$\frac{2D_c}{t_w} \leq \lambda_{rw} \quad \text{Eq. (6.10.1.10.2-1)}$$

where:

$$4.6 \sqrt{\frac{E}{F_{yc}}} \leq \lambda_{rw} = \left(3.1 + \frac{5.0}{a_{wc}} \right) \sqrt{\frac{E}{F_{yc}}} \leq 5.7 \sqrt{\frac{E}{F_{yc}}} \quad \text{Eq. (6.10.1.10.2-5)}$$

For the strength limit state and in accordance with Article D6.3.1, for composite sections in negative flexure, D_c is to be computed for the section consisting of the steel girder plus the longitudinal reinforcement (the short-term section is conservatively used). Referring to Table 18, D_c is taken as:

$$D_c = 44.55 - 3.0 = 41.55 \text{ in.}$$

Therefore,

$$\frac{2D_c}{t_w} = \frac{2(41.55)}{0.625} = 133.0$$

$$a_{wc} = \frac{2D_c t_w}{b_{fc} t_{fc}} \quad \text{Eq. (6.10.1.10.2-8)}$$

$$4.6 \sqrt{\frac{E}{F_{yc}}} = 4.6 \sqrt{\frac{29,000}{50}} = 111$$

$$5.7 \sqrt{\frac{E}{F_{yc}}} = 5.7 \sqrt{\frac{29,000}{50}} = 137$$

$$a_{wc} = \frac{2(41.55)(0.625)}{27(3.0)} = 0.64$$

$$111 < \lambda_{rw} = \left(3.1 + \frac{5.0}{0.64} \right) \sqrt{\frac{29,000}{50}} = 262.8 > 137$$

$$\therefore \lambda_{rw} = 137 > \frac{2D_c}{t_w} = 133.0$$

Eq. (6.10.1.10.2-2) is satisfied:

Therefore, $R_b = 1.0$.

$$L_p = 1.0 r_t \sqrt{\frac{E}{F_{yc}}} \quad \text{Eq. (6.10.8.2.3-4)}$$

where r_t is the effective radius of gyration for lateral torsional buckling specified in Article 6.10.8.2.3 determined as:

$$r_t = \frac{b_{fc}}{\sqrt{12 \left(1 + \frac{1}{3} \frac{D_c t_w}{b_{fc} t_{fc}} \right)}} = \frac{27}{\sqrt{12 \left[1 + \frac{1}{3} \frac{(41.55)(0.625)}{27(3)} \right]}} = 7.41 \text{ in.} \quad \text{Eq. (6.10.8.2.3-9)}$$

$$L_p = 1.0 r_t \sqrt{\frac{E}{F_{yc}}} = \frac{1.0(7.41) \sqrt{\frac{29,000}{50}}}{12} = 14.9 \text{ ft}$$

Check Eq. (6.10.1.6-2) assuming $C_b = 1.0$:

$$L_b = 20.47 \text{ ft} > 1.2(14.9) \sqrt{\frac{(1.0)(1.0)}{|-44.14|/50}} = 19.0 \text{ ft}$$

Since Eq. (6.10.1.6-2) is not satisfied, the second-order elastic compression-flange lateral bending stresses must be considered. The first-order values may be amplified as follows:

$$f_{\ell} = \left(\frac{0.85}{1 - \frac{f_{bu}}{F_{cr}}} \right) f_{\ell 1} \geq f_{\ell 1} \quad (\text{second - order analysis}) \quad \text{Eq. (6.10.1.6-4)}$$

where: f_{bu} = bottom flange stress calculated without consideration of flange lateral bending
 F_{cr} = elastic lateral torsional buckling stress for the flange under consideration determined using Eq. (6.10.8.2.3-8)

$$F_{cr} = \frac{C_b R_b \pi^2 E}{\left(\frac{L_b}{r_t} \right)^2} \quad \text{Eq. (6.10.8.2.3-8)}$$

Using Eq. (6.10.8.2.3-8), compute the elastic lateral torsional buckling stress, F_{cr} :

$$F_{cr} = \frac{1.0(1.0)\pi^2(29,000)}{\left[\frac{20.47(12)}{7.41} \right]^2} = 260.5 \text{ ksi}$$

The amplification factor (AF) is then determined as follows:

$$AF = \left(\frac{0.85}{1 - \frac{|-44.14|}{260.5}} \right) = 1.023 > 1.0 \quad \text{OK}$$

Therefore, the total factored lateral bending stress at the bottom flange, including the amplification factor, is:

$$f_{\ell} = 1.023 \left[1.25 \left[(-2.11) + (-0.35) \right] + 1.5(-0.34) + 1.75(-1.54) \right] = -6.42 \text{ ksi}$$

7.11.1.2 Top Flange Flexural Resistance in Tension

As stated previously, the continuously braced top flange must satisfy:

$$f_{bu} \leq \phi_f R_h F_{yf} \quad \text{Eq. (6.10.8.1.3-1)}$$

For Strength I:

$$f_{bu} = 47.52 \text{ ksi} < \phi_f R_h F_{yf} = 1.0(1.0)(50) = 50 \text{ ksi} \quad \text{OK (Ratio} = 0.950)$$

7.11.1.3 Bottom Flange Flexural Resistance in Compression

For discretely braced compression flanges at the strength limit state, Eq. (6.10.8.1.1-1) must be satisfied for both local buckling and lateral torsional buckling using the appropriate value of the nominal flexural resistance, F_{nc} , for local buckling (Article 6.10.8.2.2) or for lateral torsional buckling (Article 6.10.8.2.3), as applicable.

Per Article 6.10.8.2.2, if $\lambda_f \leq \lambda_{pf}$, then the local buckling resistance of the compression flange is to be taken as:

$$F_{nc} = R_b R_h F_{yc} \quad \text{Eq. (6.10.8.2.2-1)}$$

where:

R_b = web load-shedding factor determined as specified in Article 6.10.1.10.2

R_h = hybrid factor determined as specified in Article 6.10.1.10.1.

Compute the slenderness ratio for the compression flange:

$$\lambda_f = \frac{b_{fc}}{2t_{fc}} = \frac{27}{2(3.0)} = 4.50 \quad \text{Eq. (6.10.8.2.2-3)}$$

Compute the limiting slenderness ratio for a compact flange:

$$\lambda_{pf} = 0.38 \sqrt{\frac{29,000}{50}} = 9.15 \quad \text{Eq. (6.10.8.2.2-4)}$$

$$\lambda_f = 4.50 < \lambda_{pf} = 9.15$$

Therefore, $F_{nc} = R_b R_h F_{yc}$

For a homogenous girder, the hybrid factor, R_h , is equal to 1.0. As shown earlier, the web load-shedding factor, R_b , is equal to 1.0. Therefore, F_{nc} for the local buckling resistance is calculated as:

$$F_{nc} = (1.0)(1.0)(50.00) = 50.00 \text{ ksi}$$

Next, determine the lateral torsional buckling resistance of the compression flange, noting that the critical unbraced length, L_b , is 20.47 ft in Span 1. The flange transition in this unbraced length is less than 20 percent of the unbraced length from the brace point with the smaller moment and the lateral moment of inertia of the flange in the smaller section is exactly one-half of the corresponding value in the larger section; therefore, the transition may be ignored and the larger section may be used to compute the lateral torsional buckling resistance.

$L_p = 14.9$ ft (calculated previously)

$$L_r = \pi r_t \sqrt{\frac{E}{F_{yr}}} = \frac{\pi(7.41)\sqrt{\frac{29,000}{0.7(50)}}}{12} = 55.8 \text{ ft} \quad \text{Eq. (6.10.8.2.3-5)}$$

Since $L_p < L_b < L_r$, use Eq. (6.10.8.2.3-2) to calculate the lateral torsional buckling resistance. C_b is conservatively assumed as 1.0.

$$\begin{aligned} F_{nc} &= C_b \left[1 - \left(1 - \frac{F_{yr}}{R_h F_{yc}} \right) \left(\frac{L_b - L_p}{L_r - L_p} \right) \right] R_b R_h F_{yc} \leq R_b R_h F_{yc} \quad \text{Eq. (6.10.8.2.3-2)} \\ &= 1.0 \left[1 - \left[1 - \frac{0.7(50)}{1.0(50)} \right] \left(\frac{20.47 - 14.9}{55.8 - 14.9} \right) \right] (1.0)(1.0)(50) = 47.96 \text{ ksi} \end{aligned}$$

For checking the lateral torsional buckling resistance, the largest major-axis bending stress within the unbraced length is to be used in conjunction with the largest flange lateral bending stress (Article 6.10.1.6). In this case, the largest stresses are at Section G4-2. For checking the local buckling resistance, the major-axis bending and flange lateral bending stress at the section under consideration may be used, which again is at Section G4-2.

Check Eq. (6.10.8.1.1-1) for local buckling as follows:

$$f_{bu} + \frac{1}{3}f_\ell \leq \phi_f F_{nc} \quad \text{Eq. (6.10.8.1.1-1)}$$

$$f_{bu} + \frac{1}{3}f_\ell = |-44.14| + \frac{1}{3}(-6.42) = 46.28 \text{ ksi} < \phi_f F_{nc} = 1.0(50.00) = 50.00 \text{ ksi} \quad \text{OK (Ratio} = 0.926)$$

Check Eq. (6.10.8.1.1-1) for lateral torsional buckling as follows:

$$f_{bu} + \frac{1}{3}f_\ell = |-44.14| + \frac{1}{3}(-6.42) = 46.28 \text{ ksi} < \phi_f F_{nc} = 1.0(47.96) = 47.96 \text{ ksi} \quad \text{OK (Ratio} = 0.965)$$

If the ratio for lateral torsional buckling had exceeded 1.0, consideration should be given to computing the moment gradient modifier, C_b , using Eq. (6.10.8.2.3-7). Where C_b is greater than 1.0, indicating the presence of a significant beneficial moment gradient effect, the lateral-torsional buckling resistances may alternatively be calculated by the equivalent procedures specified in Article D6.4.1. These procedures can result in the plateau strength, F_{max} , for lateral-torsional buckling shown in Figure C6.10.8.2.1-1 to be reached at significantly larger unbraced lengths

under moment-gradient conditions when the effects of the moment gradient are included in determining the limits on the unbraced length, L_b . The procedures in Article D6.4.1 allow the Engineer to focus directly on the maximum unbraced length at which the flexural resistance is equal to F_{max} . The use of these equivalent procedures is strongly recommended when C_b values greater than 1.0 are utilized in the design.

7.11.2 Web Shear Strength (Article 6.10.9)

According to the provisions of Article 6.10.9.1, at the strength limit state, straight and curved web panels must satisfy:

$$V_u \leq \phi_v V_n \quad \text{Eq. (6.10.9.1-1)}$$

where:

- ϕ_v = resistance factor for shear = 1.0 (Article 6.5.4.2)
- V_n = nominal shear resistance determined as specified in Articles 6.10.9.2 and 6.10.9.3 for unstiffened and stiffened webs, respectively
- V_u = factored shear in the web at the section under consideration

Since the web at Support 1 is an interior panel (i.e., a web panel not adjacent to the discontinuous end of a girder), Article 6.10.9.3.2 applies, and the nominal shear resistance is to be taken as:

$$V_n = V_p \left[C + \frac{0.87(1-C)}{\sqrt{1 + \left(\frac{d_o}{D}\right)^2}} \right] \quad \text{Eq. (6.10.9.3.2-2)}$$

where:

- d_o = transverse stiffener spacing
- V_n = nominal shear resistance of the web panel
- V_p = plastic shear force
- C = ratio of the shear-buckling resistance to the shear yield strength

The above shear resistance includes post-buckling tension-field action, and applies provided that the following proportional requirement is satisfied:

$$\frac{2Dt_w}{(b_{fc}t_{fc} + b_{ft}t_{ft})} \leq 2.5 \quad \text{Eq. (6.10.9.3.2-1)}$$

Checking the above equation for Section G4-2:

$$\frac{2(84)(0.625)}{[(27)(3.0) + (28)(2.5)]} = 0.70 < 2.5 \quad \text{OK}$$

Therefore, the equation for V_n shown above applies for the web panel in Span 1 adjacent to Section G4-2.

7.11.2.1 Applied Shear

The unfactored shears for Girder G4 at Support 2 are shown below. These results are taken directly from the three-dimensional analysis as reported in Table 10.

Steel Dead Load:	$V_{DC1-STEEL}$	= -45 kips
Concrete Deck Dead Load:	$V_{DC1-CONC}$	= -144 kips
Composite Dead Load:	V_{DC2}	= -36 kips
Future Wearing Surface Dead Load:	V_{DW}	= -28 kips
Live Load (including IM + CF):	V_{LL+IM}	= -159 kips

The maximum Strength I factored shear is computed as:

$$V_u = 1.25(-45 - 144 - 36) + 1.50(-28) + 1.75(-159) = -602 \text{ kips}$$

7.11.2.2 Shear Resistance

Compute the plastic shear force:

$$V_p = 0.58F_{yw}Dt_w \quad \text{Eq. (6.10.9.3.2-3)}$$

$$= 0.58(50)(84)(0.625) = 1,523 \text{ kips}$$

To determine the ratio C , the shear-buckling coefficient, k , must first be computed as follows:

$$k = 5 + \frac{5}{\left(\frac{d_o}{D}\right)^2} \quad \text{Eq. (6.10.9.3.2-7)}$$

At this particular location, the transverse stiffener spacing is assumed to be 82 inches. Therefore, $d_o = 82$ in.

$$k = 5 + \frac{5}{\left[\frac{82}{84}\right]^2} = 10.2$$

Check the following relation in order to determine the appropriate equation for computing C:

$$\frac{D}{t_w} = \frac{84}{0.625} = 134.4 > 1.40 \sqrt{\frac{Ek}{F_{yw}}} = 1.40 \sqrt{\frac{29,000(10.2)}{50}} = 108$$

Since the above relation is true, the ratio C is computed using Eq. (6.10.9.3.2-6) as follows:

$$C = \frac{1.57}{\left(\frac{D}{t_w}\right)^2} \left(\frac{Ek}{F_{yw}}\right) \quad \text{Eq. (6.10.9.3.2-6)}$$

$$C = \frac{1.57}{\left(\frac{84}{0.625}\right)^2} \left(\frac{29,000(10.2)}{50}\right) = 0.514$$

The nominal shear resistance is then computed in accordance with Eq. (6.10.9.3.2-2):

$$V_n = V_p \left[C + \frac{0.87(1-C)}{\sqrt{1 + \left(\frac{d_o}{D}\right)^2}} \right] = (1,523) \left[0.514 + \frac{0.87(1-0.514)}{\sqrt{1 + \left(\frac{82}{84}\right)^2}} \right] = 1,244 \text{ kips}$$

Using the above results, check the requirement of Article 6.10.9.1, $V_u \leq \phi_v V_n$:

$$V_u = |-602 \text{ kips}| \leq \phi_v V_n = (1.0)(1,244) = 1,244 \text{ kips} \quad \text{OK (Ratio} = 0.484)$$

Therefore, the stiffened web of Section G4-2 is satisfactory for shear at Support 2.

7.12 Bolted Field Splice

7.12.1 General

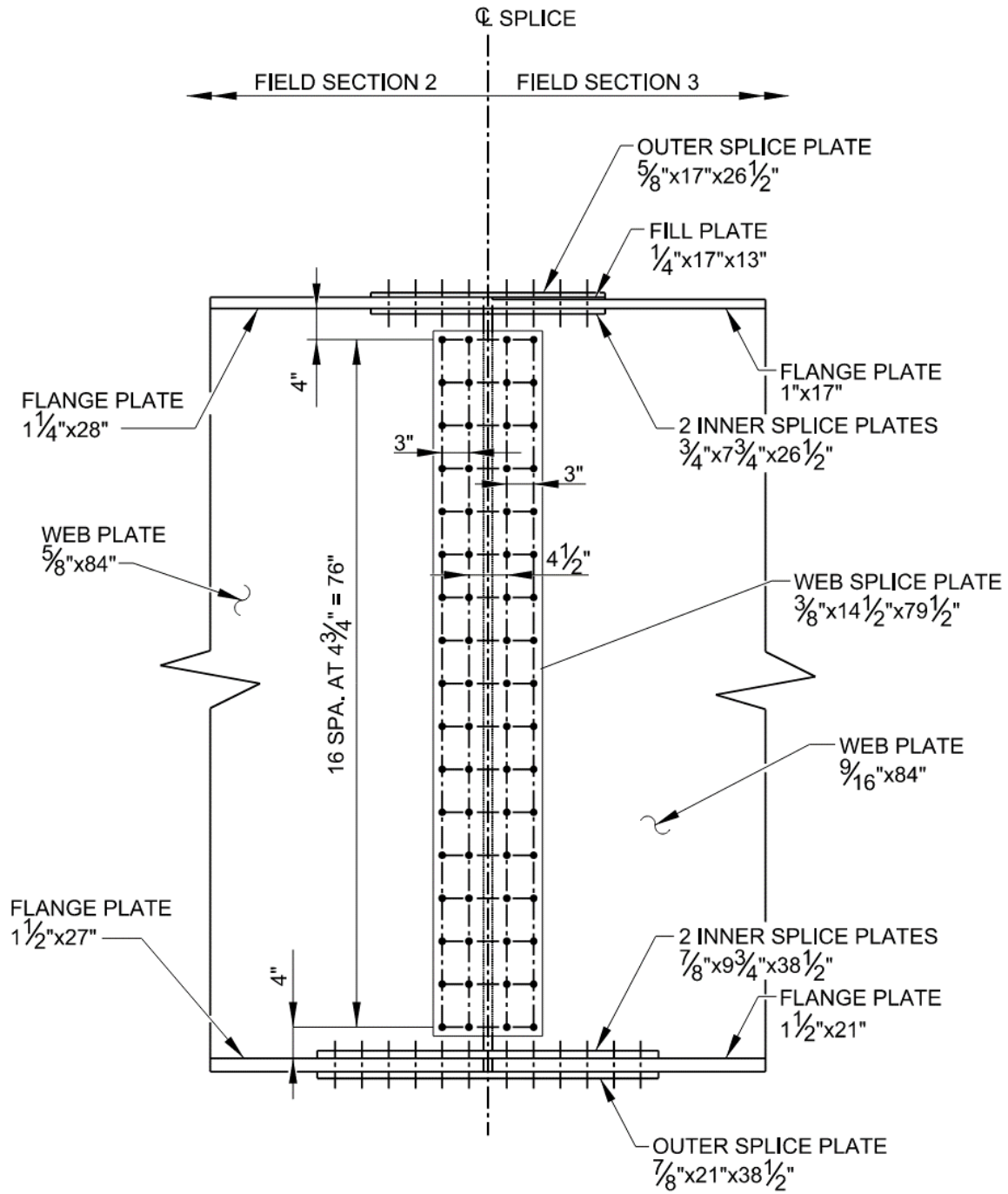
This section will show the design of a bolted field splice in accordance with the provisions of Article 6.13.6.1.3. The design computations will be illustrated for the Field Splice #2 on Girder G4. First, single bolt capacities are computed for slip resistance (Article 6.13.2.8) and shear resistance (Article 6.13.2.7), and then the bearing resistance on the connected material is computed (Article 6.13.2.9). The tensile resistance (Article 6.13.2.10) of a single bolt is also computed for completeness but is not used in this example. The field splice is then checked for constructability, the service limit state, and the strength limit state. For further information on bolted field splice

design, refer to the NSBA document *Bolted Field Splices for Steel Bridge Flexural Members – Overview and Design Examples* [19], which is available on the NSBA website (www.aisc.org/nsba), and also NSBA's *Steel Bridge Handbook Design: Splice Design* [20].

All bolts used in the field splice are 0.875-inch diameter ASTM F3125 Grade 325 bolts. Table 6.13.2.4.2-1 shows that a standard hole diameter size for a 0.875-inch diameter bolt is 0.9375 inch. The connection is designed assuming that a Class B surface condition is provided and that the surface is unpainted and blast cleaned. The threads are assumed excluded from the shear planes in the flange splices and included in the shear planes in the web splice. This will be checked later on in Sections 7.12.4.4 and 7.12.5.3.

Article 6.13.6.1.3a requires at least two rows of bolts on each side of the joint. Thus, four rows of four bolts are selected for each flange splice, and two vertical rows with 17 bolts per row are selected for the web splice on each side of the joint. Oversize or slotted holes in either the member or the splice plates are not permitted. In continuous spans, bolted splices preferably should be located in regions of lower moment at or near points of dead load contraflexure to reduce the major-axis bending moments acting on the splice. This may not always be possible in certain situations, such as in longer-span bridges or in cases where additional field splices may be needed to reduce the size of a shipping piece; for example, in a sharply curved member or where shipping lengths start to exceed a practical upper limit. Web and flange splices in areas of stress reversal are to be investigated for both positive and negative flexure to determine the governing condition.

The elevation view of the bolted field splice being investigated is shown in Figure 10, and views of the top and bottom flange splice plates are shown in Figure 11 and Figure 12, respectively.



- NOTES:
1. ALL BOLTS ARE $\frac{7}{8}$ " DIA (F3125 GRADE 325) H.S. BOLTS.
 2. A 0.50 IN. GAP IS ASSUMED BETWEEN THE EDGES OF THE FIELD PIECES.

Figure 10 Bolted Field Splice in Span 2 of G4 – Elevation View

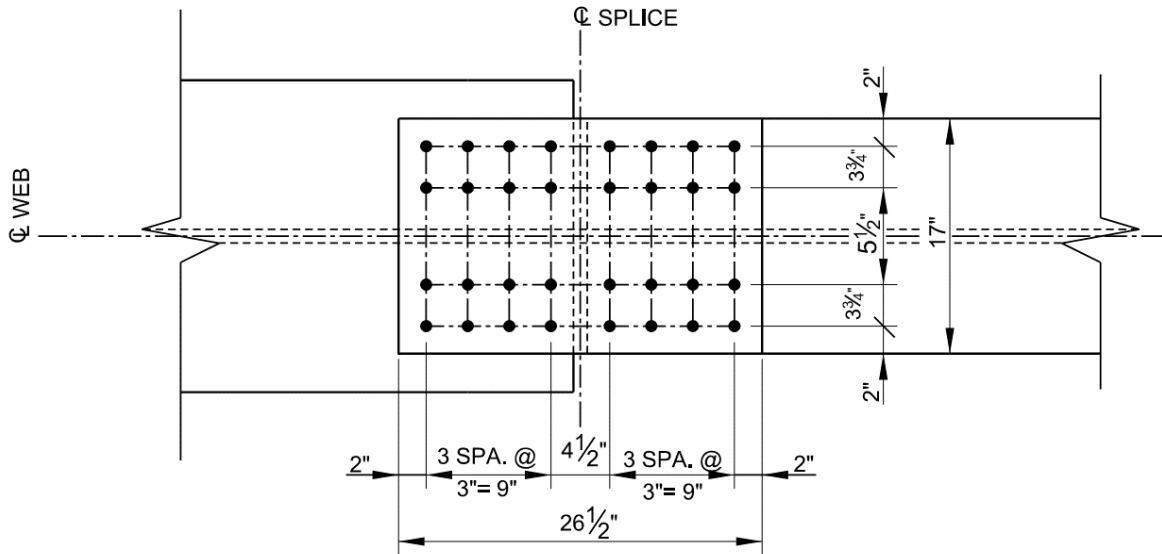


Figure 11 Bolted Field Splice in Span 2 of G4 – Top Flange

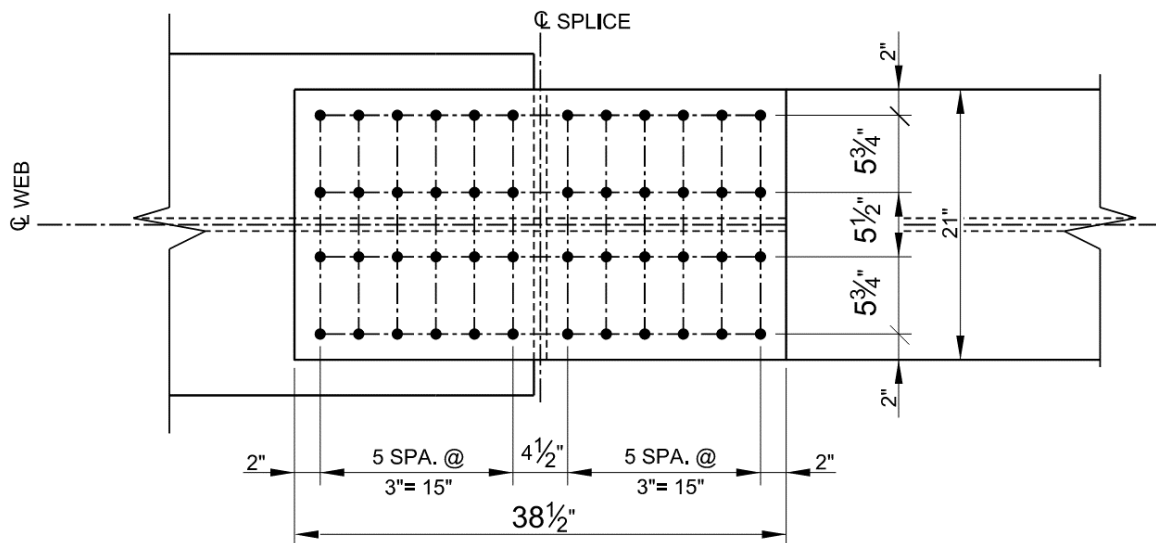


Figure 12 Bolted Field Splice in Span 2 of G4 – Bottom Flange

Referring to Table 9, the factored Strength I design bending moments at the point of splice are computed as follows:

$$\text{Positive Moment} = 0.90[(-1,967) + (-250)] + 0.65(-237) + 1.75(2,054) = +1,445 \text{ kip-ft}$$

$$\text{Negative Moment} = 1.25[(-1,967) + (-250)] + 1.5(-237) + 1.75(-2,772) = -7,978 \text{ kip-ft}$$

7.12.2 Bolt Resistance Calculation for the Service Limit State and Constructability

Article 6.13.6.1.3a specifies that bolted splices for flexural members are to be designed using slip-critical connections (Article 6.13.2.1.1). The connections are to be proportioned to prevent slip under load combination Service II and during the placement of the concrete deck. For slip-critical connections, the factored resistance, R_r , of a bolt for the Service II load combination and for constructability is taken as:

$$R_r = R_n \quad \text{Eq. (6.13.2.2-1)}$$

where: R_n = the nominal resistance as specified in Article 6.13.2.8

The nominal slip resistance of a bolt in a slip-critical connection is to be taken as:

$$R_n = K_h K_s N_s P_t \quad \text{Eq. (6.13.2.8-1)}$$

where: N_s = number of slip planes per bolt

P_t = minimum required bolt tension specified in Table 6.13.2.8-1

K_h = hole size factor specified in Table 6.13.2.8-2

K_s = surface condition factor specified in Table 6.13.2.8-3

For all bolts in this connection:

- $N_s = 2$ since each connection has two slip planes.
- $P_t = 39$ kips for ASTM F3125 Grade 325, 0.875-inch bolts.
- $K_h = 1.0$ since standard size holes are used.
- $K_s = 0.50$ since a Class B surface preparation is assumed for this design example.

Therefore, the slip resistance of a single bolt for service and constructability checks is:

$$R_r = R_n = (1.0)(0.50)(2)(39) = 39 \text{ kips/bolt}$$

7.12.3 Bolt Resistance Calculations for the Strength Limit State

The factored resistance, R_r , of a bolted connection at the strength limit state is taken as

$$R_r = \phi R_n \quad \text{Eq. (6.13.2.2-2)}$$

where: ϕ = applicable resistance factor for bolts specified in Article 6.5.4.2

The nominal resistance of the bolted connection at the strength limit state must be computed for shear, bearing, and tension, where applicable.

Article 6.13.6.1.3a states that the factored flexural resistance of the flanges at the point of the splice at the strength limit state must satisfy the applicable provisions of Article 6.10.6.2, which relate to

flexure. The girder satisfies the provisions of Article 6.10.6.2 at the splice location; however, the checks at this location are not included in this example.

7.12.3.1 Bolt Shear Resistance (Article 6.13.2.7)

The nominal shear resistance, R_n , of a high-strength bolt at the strength limit state in joints whose length between extreme fasteners measured parallel to the line of action of the force is less than or equal to 38.0 in. (which will be assumed in this design example) and where threads are excluded from the shear plane is computed as follows:

$$R_n = 0.56A_b F_{ub} N_s \quad \text{Eq. (6.13.2.7-1)}$$

where: A_b = area of bolt corresponding to the nominal diameter
 F_{ub} = specified minimum tensile strength of the bolt per Article 6.4.3
 N_s = number of shear planes per bolt

$$R_n = 0.56(0.601)(120)(2) = 80.8 \text{ kips / bolt}$$

The factored shear resistance at the strength limit state is taken as:

$$R_r = \phi_s R_n \quad \text{Eq. (6.13.2.2-2)}$$

where: ϕ_s = shear resistance factor for ASTM F3125 bolts in shear = 0.80 (Article 6.5.4.2)

$$R_r = 0.80(80.8) = 64.6 \text{ kips/bolt}$$

The nominal shear resistance in similar joints where threads are included in the shear plane is computed as:

$$R_n = 0.45A_b F_{ub} N_s \quad \text{Eq. (6.13.2.7-2)}$$

$$R_n = 0.45(0.601)(120)(2) = 64.9 \text{ kips / bolt}$$

The factored shear resistance at the strength limit state is taken as:

$$R_r = 0.80(64.9) = 51.9 \text{ kips/bolt}$$

The nominal shear resistance of a bolt in lap splice tension connections greater than 38.0 in. in length is to be taken as 0.83 times the preceding values.

7.12.3.2 Bearing Resistance of the Connected Material (Article 6.13.2.9)

The nominal bearing resistance of interior and end bolt holes at the strength limit, R_n , is taken as one of the following two terms, depending on the bolt clear distance and the clear end distance.

- (1) With bolts spaced at a clear distance between holes not less than $2.0d$ and with a clear end distance not less than $2.0d$:

$$R_n = 2.4dtF_u \quad \text{Eq. (6.13.2.9-1)}$$

- (2) If either the clear distance between holes is less than $2.0d$ or the clear end distance is less than $2.0d$:

$$R_n = 1.2L_c tF_u \quad \text{Eq. (6.13.2.9-2)}$$

where: d = nominal diameter of the bolt (in.)
 t = thickness of the connected material (in.)
 F_u = tensile strength of the connected material specified in Table 6.4.1-1 (ksi)
 L_c = clear distance between holes or between the hole and the end of the member in the direction of the applied force

For example, in the case of the web splice plates, the end distance is 1.75 inches. According to Article 6.8.3, the width of each standard bolt hole for design is to be taken as the nominal diameter of the hole = $0.9375''$, creating a clear end distance of 1.28 inches, which is less than $2.0d$. Therefore, Eq. (6.13.2.9-2) applies. Since the sum of the web splice plate thicknesses is greater than the thickness of the web on both sides of the splice, the thinner of the two webs is used for the thickness, t . The nominal bearing resistance for the end row of bolts in the web splice plate is:

$$R_n = 1.2(1.28)(0.5625)(65) = 56.16 \text{ kips/bolt}$$

The factored resistance is:

$$R_r = \phi_{bb}R_n \quad \text{Eq. (6.13.2.2-2)}$$

where: ϕ_{bb} = resistance factor for bolts bearing on material = 0.80 (Article 6.5.4.2)

$$R_r = 0.80(56.16) = 44.93 \text{ kips/bolt}$$

7.12.3.3 Bolt Tensile Resistance (Article 6.13.2.10)

The nominal tensile resistance of a bolt, T_n , independent of any initial tightening force, is to be taken as:

$$T_n = 0.76A_b F_{ub} \quad \text{Eq. (6.13.2.10.2-1)}$$

$$T_n = 0.76(0.601)(120) = 54.8 \text{ kips/bolt}$$

The tensile bolt resistance is not used in this example because a bolted field splice in a flexural member only loads the bolts in shear.

7.12.4 Flange Splice Design

7.12.4.1 General

Article 6.13.6.1.3b states that flange splice plates and their connections are to be designed to develop the smaller design yield resistance of the flanges on either side of the splice. The design yield resistance of each flange, P_{fy} , at the point of splice is taken as:

$$P_{fy} = F_{yf} A_e \quad (6.13.6.1.3b-1)$$

in which: A_e = effective area of the flange under consideration (in.²). A_e is to be taken as:

$$A_e = \left(\frac{\phi_u F_u}{\phi_y F_{yf}} \right) A_n \leq A_g \quad (6.13.6.1.3b-2)$$

where: ϕ_u = resistance factor for fracture of tension members = 0.80 (Article 6.5.4.2)
 ϕ_y = resistance factor for yielding of tension members = 0.95 (Article 6.5.4.2)
 A_n = net area of the flange under consideration determined as specified in Article 6.8.3 (in.²)
 A_g = gross area of the flange under consideration (in.²)
 F_u = specified minimum tensile strength of the flange under consideration determined as specified in Table 6.4.1-1 (ksi)
 F_{yf} = specified minimum yield strength of the flange under consideration (ksi)

The use of the effective flange area in the computation of P_{fy} accounts for the loss in section causing a reduction in the fracture resistance of the net section at the connection for loading conditions in which the flange is subject to tension. The effective flange area is conservatively used for both tension and compression flanges.

7.12.4.2 Flange Splice Bolts

For each flange, the smaller design yield resistance at the point of splice, P_{fy} , is to be divided by the factored shear resistance of the bolts, determined in Section 7.12.3.1, to determine the total number of flange splice bolts required on one side of the splice at the strength limit state. Where filler plates are required, the provisions of Article 6.13.6.1.4 apply.

Top Flange

The right side of the splice has the smaller design yield resistance (i.e., the top flange on the right side has a smaller area).

$$A_e = \left(\frac{0.80(65)}{0.95(50)} \right) [17 - 4(0.9375)](1.0) = 14.5 \text{ in.}^2 < (1.0)(17) = 17.0 \text{ in.}^2$$

$$P_{fy} = 50(14.5) = 725 \text{ kips}$$

Calculate the reduction in the bolt factored shear resistance due to the required 1/4-inch filler plate (Figure 10) from Eq. (6.13.6.1.4-1):

$$R = \left[\frac{(1 + \gamma)}{(1 + 2\gamma)} \right] \quad \text{Eq. (6.13.6.1.4-1)}$$

where: $\gamma = A_f/A_p$

A_f = sum of the area of the fillers on both sides of the connected plate (in.²)

A_p = smaller of either the connected plate area on the side of the connection with the filler or the sum of the splice plate areas on both sides of the connected plate (in.²)

The reduction factor, R, accounts for the reduction in the nominal shear resistance of the bolts due to bending of the bolts and will result in having to provide additional bolts on the side of the splice with the filler to develop the filler.

When the splice plate, filler plate and flange widths are all equal in the splice, which is typically the case, the area ratio, γ , is only a function of the thickness of the flange and the filler. Therefore:

$$R = \left[\frac{\left(1 + \frac{0.25}{1.0}\right)}{\left(1 + \frac{2(0.25)}{1.0}\right)} \right] = 0.83$$

Therefore:

$$N = \frac{725}{0.83(64.6)} = 13.5 \text{ bolts}$$

Use 4 rows with 4 bolts per row = 16 bolts on each side of the splice. For practical reasons, use the same number on bolts on both sides of the flange splice.

Bottom Flange

The right side of the splice has the smaller design yield resistance (i.e., the bottom flange on the right side has a smaller area). A filler plate is not required.

$$A_e = \left(\frac{0.80(65)}{0.95(50)} \right) [21 - 4(0.9375)](1.5) = 28.3 \text{ in.}^2 < (1.5)(21) = 31.5 \text{ in.}^2$$

$$P_{fy} = 50(28.3) = 1,415 \text{ kips}$$

$$N = \frac{1,415}{64.6} = 21.9 \text{ bolts}$$

Use 4 rows with 6 bolts per row = 24 bolts on each side of the splice.

For flanges with one web in horizontally curved girders, the effects of flange lateral bending need not be considered in the design of the bolted flange splices since the combined areas of the flange splice plates will typically equal or exceed the area of the smaller flange to which they are attached. The girder flanges are designed so that the yield stress of the flange is not exceeded at the flange tips under combined major-axis and lateral bending for constructability and at the strength limit state. Flange lateral bending is also less critical at locations in-between the cross-frames or diaphragms where bolted splices are located. The rows of bolts provided in the flange splice on each side of the web provide the necessary couple to resist the lateral bending. Flange lateral bending will increase the flange slip force on one side of the splice and decrease the slip force on the other side of the splice; slip cannot occur unless it occurs on both sides of the splice.

7.12.4.3 Moment Resistance

The moment resistance provided by the flanges at the point of splice is next to be checked against the factored moment at the strength limit state. Should the factored moment exceed the moment resistance provided by the flanges, the additional moment is to be resisted by the web as specified in Article 6.13.6.1.3c.

For composite sections subject to positive flexure, the moment resistance provided by the flanges at the strength limit state is computed as P_{fy} for the bottom flange times the moment arm taken as the vertical distance from the mid-thickness of the bottom flange to the mid-thickness of the concrete deck including the concrete haunch (Figure C6.13.6.1.3b-1). For composite sections subject to negative flexure and noncomposite sections subject to positive or negative flexure, the moment resistance provided by the flanges is computed as P_{fy} for the top or bottom flange, whichever is smaller, times the moment arm taken as the vertical distance between the mid-thickness of the top and bottom flanges (Figure C6.13.6.1.3b-2). If necessary, the moment resistance provided by the flanges can potentially be increased by staggering the flange bolts.

Positive Flexure (refer to Figure C6.13.6.1.3b-1)

Use P_{fy} for the bottom flange = 1,415 kips

Flange moment arm: $A = D + t_{ft}/2 + t_{haunch} + t_s/2 = 84 + (1.5/2) + 4.0 + (9.0/2) = 93.25 \text{ in.}$

$M_{flange} = 1,415 \times (93.25/12) = 10,996 \text{ kip-ft} > +1,445 \text{ kip-ft} \text{ OK}$

Negative Flexure (refer to Figure C6.13.6.1.3b-2)

Use the smaller value of P_{fy} for the top and bottom flanges. In this case, the top flange has the smaller value of $P_{fy} = 725 \text{ kips.}$

Flange Moment Arm: $A = D + (t_{ft} + t_{fc})/2 = 84 + (1.5 + 1.0)/2 = 85.25$ in.

$$M_{\text{flange}} = 725 \times (85.25/12) = 5,151 \text{ kip-ft} < |-7,978| \text{ kip-ft}$$

Therefore, the flanges do not have adequate capacity by themselves to resist the factored Strength I negative moment at the point of splice.

Referring to Figure C6.13.6.1.3c-2, the required horizontal web force, H_w , to satisfy the Strength I moment requirement is:

$$H_w = \frac{(\text{Strength I moment} - M_{\text{flange}})}{D/4} = \frac{(7,978 - 5,151) \times 12}{84/4} = 1,615 \text{ kips}$$

Therefore, negative moment controls the web connection design at the strength limit state, which is discussed later on in this design example (Section 7.12.5).

7.12.4.4 Flange Splice Plates

The design of the bottom-flange splice plates is illustrated in this design example. The width of the outside splice plate should be at least as wide as the width of the narrowest flange at the splice. The thickness of the outside splice plate should be at least one-half the thickness of the thinner flange at the splice plus 1/16 of an inch [19]. As a result, the flange will control the bearing and block shear rupture resistance, which is checked later on in this design example.

$$t_o \geq \frac{1.5}{2} + 0.0625 = 0.8125 \text{ in. Use } t_o = \frac{7}{8} \text{ in.}$$

The width of the inside splice plates should be such that the plates clear the flange-to-web weld on each side of the web by a minimum of 1/8 in [19]. Assuming 5/16-inch flange-to-web welds are used, the minimum clearance distance, C , between the two inner splice plates is computed as follows:

$$C \geq t_{\text{web}} + 2 \left[\text{weld size} + \frac{1}{8} \right] = 0.625 + 2 \left[0.3125 + \frac{1}{8} \right] = 1.5 \text{ in.}$$

$$b_i = \frac{(b_f - C)}{2} = \frac{(21 - 1.5)}{2} = 9.75 \text{ in.}$$

At the strength limit state, P_{fy} may be assumed equally divided to the inner and outer flange splice plates when the areas of the inner and outer plates do not differ by more than 10 percent (Article C6.13.6.1.3b). In this case, P_{fy} may be assumed equally divided to the inner and outer plates and the shear resistance of the bolted connection may be checked for P_{fy} acting in double shear. Applying the above 10 percent guideline gives:

$$0.9b_f t_o \leq 2b_i t_i \leq 1.1b_f t_o$$

Substituting the equation for b_i given above into the preceding equation and rearranging gives:

$$0.9t_o \leq \left(1 - \frac{C}{b_f}\right)t_i \leq 1.1t_o$$

$$0.9(0.875) \leq \left(1 - \frac{1.5}{21.0}\right)t_i \leq 1.1(0.875)$$

$$0.79 \leq (0.93)t_i \leq 0.96$$

$$0.85 \leq t_i \leq 1.03 \quad \text{Use } t_i = \frac{7}{8}$$

Therefore, for the bottom-flange splice, try a 7/8 in. x 21 in. outside splice plate and two 7/8 in. x 9 3/4 in. inside splice plates. A filler plate is not required. All plates are ASTM A709 Grade 50 steel.

At the strength limit state, the design force in the splice plates is not exceed the factored resistance in tension specified in Article 6.13.5.2. The factored resistance, R_r , in tension is to be taken as the least of the values given by either Eqs. 6.8.2.1-1 and 6.8.2.1-2 for yielding and fracture, respectively, or the block shear rupture resistance specified in Article 6.13.4.

Check the factored yield resistance of the splice plates in tension:

$$R_r = \phi_y F_y A_g \quad \text{Eq. (6.8.2.1-1)}$$

where: ϕ_y = resistance factor for yielding of tension members = 0.95 (Article 6.5.4.2)
 A_g = gross cross-sectional area of the connected element (in.²)

Outside splice plate:

$$R_r = 0.95(50)(21.0)(0.875) = 873 \text{ kips} > 1,415 / 2 = 708 \text{ kips} \quad \text{ok}$$

Inside splice plates:

$$R_r = 0.95(50)(2)(9.75)(0.875) = 810 \text{ kips} > 1,415 / 2 = 708 \text{ kips} \quad \text{ok}$$

Check the net section fracture resistance of the splice plates in tension. As specified in Article 6.8.3, for design calculations, the width of standard-size bolt holes is taken as the nominal diameter of the holes, or ¹⁵/₁₆ in. for a 7/8-in.-diameter bolt. According to Article 6.13.5.2, for splice plates subject to tension, the design net area, A_n , must not exceed $0.85A_g$.

Outside plate:

$$0.85(21.0)(0.875) = 15.6 \text{ in.}^2 > A_n = [21.0 - 4(0.9375)](0.875) = 15.1 \text{ in.}^2 \text{ ok}$$

Inside plates:

$$0.85(2)(9.75)(0.875) = 14.5 \text{ in.}^2 > A_n = [2(9.75) - 4(0.9375)](0.875) = 13.8 \text{ in.}^2 \text{ ok}$$

Therefore, use the lesser net area to check the net section fracture resistance of the splice plates. If A_n had been greater than or equal to $0.85A_g$, then $0.85A_g$ should be substituted for A_n to check the net section fracture resistance.

$$R_r = \phi_u F_u A_n R_p U \quad \text{Eq. (6.8.2.1-2)}$$

where: ϕ_u = resistance factor for fracture of tension members = 0.80 (Article 6.5.4.2)

F_u = tensile strength of the connected element specified in Table 6.4.1-1 (ksi)

A_n = net cross-sectional area of the connected element determined as specified in Article 6.8.3 (in.²)

R_p = reduction factor for holes taken equal to 0.90 for bolt holes punched full size, and 1.0 for bolt holes drilled full size or subpunched and reamed to size (use 1.0 for splice plates since the holes in field splices are not allowed to be punched full size)

U = reduction factor to account for shear lag (use 1.0 for splice plates since all elements are connected)

Outside plate:

$$R_r = 0.80(65)[21.0 - 4(0.9375)](0.875)(1.0)(1.0) = 785 \text{ kips} > 1,415 / 2 = 708 \text{ kips ok}$$

Inside plates:

$$R_r = 0.80(65)[2(9.75) - 4(0.9375)](0.875)(1.0)(1.0) = 717 \text{ kips} > 1,415 / 2 = 708 \text{ kips ok}$$

To check the block shear rupture resistance of the splice plates and the flange (and later on the factored bearing resistance of the bolt holes in Section 7.12.4.5), the bolt spacings and bolt edge and end distances must first be established and checked. Refer to the bolt pattern shown in Figure 12.

As specified in Article 6.13.2.6.1, the minimum spacing between centers of bolts in standard holes is not to be less than $3.0d$, where d is the diameter of the bolt. For $7/8$ -in.-diameter bolts:

$$s_{\min} = 3d = 3(0.875) = 2.63 \text{ in. use } 3.0 \text{ in.}$$

Since the length between the extreme bolts (on one side of the splice) in this lap-splice tension connection measured parallel to the line of action of the force is less than 38.0 in., no reduction in the factored shear resistance of the bolts is required, as originally assumed.

As specified in Article 6.13.2.6.2, to seal against the penetration of moisture in joints, the spacing, s , of a single line of bolts adjacent to a free edge of an outside plate or shape (when the bolts are not staggered) must satisfy the following requirement:

$$s \leq (4.0 + 4.0t) \leq 7.0 \text{ in.}$$

where t is the thickness of the thinner outside plate or shape. First, check for sealing along the edges of the outer splice plate (the thinner plate) parallel to the direction of the applied force. The bolt lines closest to the edges of the flanges are assumed to be 2.0 in. from the edges of the flanges. A ½-in. gap is assumed between the girder flanges at the splice to allow the splice to provide drainage and allow for fit-up:

$$s_{\max} = 4.0 + 4.0(0.875) = 7.50 \text{ in.} > 7.0 \text{ in.}$$

$$s_{\max} = 7.0 \text{ in.} > 4.5 \text{ in. OK}$$

Check for sealing along the free edge at the end of the splice plate:

$$s_{\max} = 4.0 + 4.0(0.875) = 7.50 \text{ in.} > 7.0 \text{ in.}$$

$$s_{\max} = 7.0 \text{ in.} > 5.75 \text{ in. OK}$$

Note that the maximum pitch requirements for stitch bolts specified in Article 6.13.2.6.3 apply only to the connection of plates in mechanically fastened built-up members and are not to be applied here in the design of the splice.

The edge distance of bolts is defined as the distance perpendicular to the line of force between the center of a hole and the edge of the component. In this example, the edge distance of 2.0 in. satisfies the minimum edge distance requirement of 1½ in. specified for 7/8-in.-diameter bolts in Table 6.13.2.6.6-1. This distance also satisfies the maximum edge distance requirement of $8.0t$ (not to exceed 5.0 in.) = $8.0(0.875) = 7.0 \text{ in.} > 5.0 \text{ in.}$ (use 5.0 in.) specified in Article 6.13.2.6.6.

The end distance of bolts is defined as the distance along the line of force between the center of a hole and the end of the component. In this example, the end distance of 2.0 in. satisfies the minimum end distance requirement of 1½ in. specified for 7/8-in.-diameter bolts. The maximum end distance requirement of 5.0 in. is also satisfied. Although not specifically required, note that the distance from the corner bolts to the corner of the splice plate, equal to $\sqrt{(2.0)^2 + (2.0)^2} = 2.8 \text{ in.}$, also satisfies the maximum end distance requirement. If desired, the corners of the plate can be clipped to meet this requirement. Although not done in this example, fabricators generally prefer that the end distance on the girder flanges at the point of splice be increased a minimum of ¼ in. from the design value to allow for girder trim.

Check the block shear rupture resistance of the splice plates in tension.

$$R_r = \phi_{bs} R_p (0.58 F_u A_{vn} + U_{bs} F_u A_{tn}) \leq \phi_{bs} R_p (0.58 F_y A_{vg} + U_{bs} F_u A_{tn}) \quad \text{Eq. (6.13.4-1)}$$

where: ϕ_{bs} = resistance factor for block shear rupture = 0.80 (Article 6.5.4.2)

A_{vg} = gross area along the plane resisting shear stress (in.²)

A_{vn} = net area along the plane resisting shear stress (in.²)

A_{tn} = net area along the plane resisting tension stress (in.²)

U_{bs} = reduction factor for block shear rupture resistance taken equal to 0.50 when the tension stress is non-uniform and 1.0 when the tension stress is uniform (use 1.0 for splice plates)

Assume the potential block shear failure planes on the outside and inside splice plates shown in Figure 13.

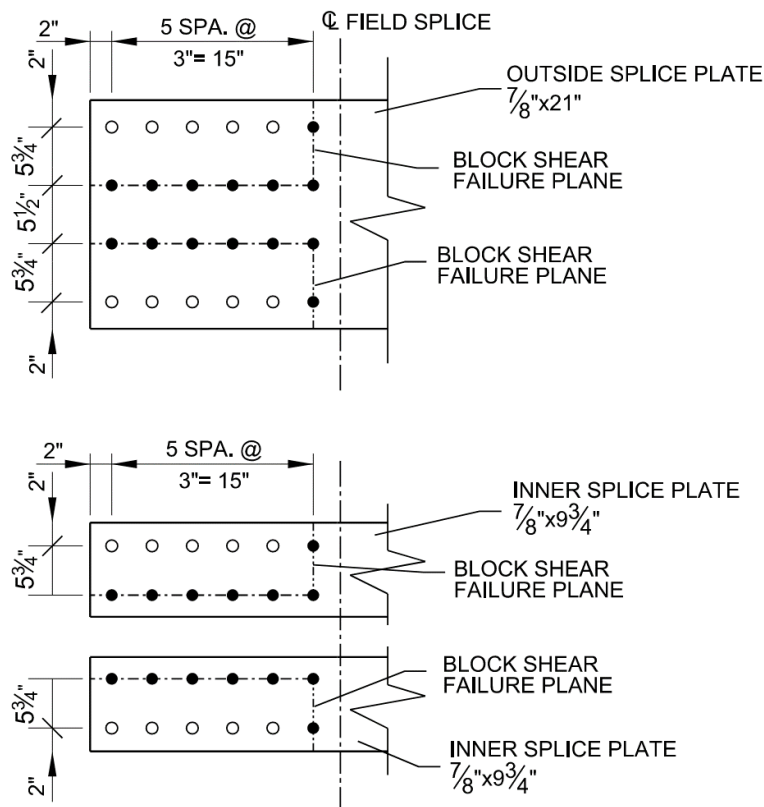


Figure 13 Bottom Flange Splice – Assumed Block Shear Failure Planes in the Splice Plates

Check the outside splice plate. A_{tn} is the net area along the place resisting the tensile stress.

$$A_{tn} = 2[5.75 + 2.0 - 1.5(0.9375)](0.875) = 11.10 \text{ in.}^2$$

A_{vn} is the net area along the plane resisting the shear stress.

$$A_{vn} = 2[5(3.0) + 2.0 - 5.5(0.9375)](0.875) = 20.73 \text{ in.}^2$$

A_{vg} is the gross area along the plane resisting the shear stress.

$$A_{vg} = 2[5(3.0) + 2.0](0.875) = 29.75 \text{ in.}^2$$

Therefore:

$$\begin{aligned} R_r &= 0.80(1.0)[0.58(65)(20.73) + 1.0(65)(11.10)] \\ &= 1,202 \text{ kips} < 0.80(1.0)[0.58(50)(29.75) + 1.0(65)(11.10)] \\ &= 1,267 \text{ kips} \\ \therefore R_r &= 1,202 \text{ kips} > \frac{1,415}{2} = 708 \text{ kips} \quad \text{OK} \end{aligned}$$

Since the inside splice plates are the same thickness as the outside splice plate in this case, the block shear rupture resistance of the inside splice plates is the same as the outside splice plate and is satisfactory.

Check the block shear rupture resistance in tension of the critical girder bottom flange at the splice. Only the calculations for the flange on the right-hand side of the splice, which is the critical flange for this check, are shown below. Two potential failure modes are investigated for the flange as shown in Figure 14.

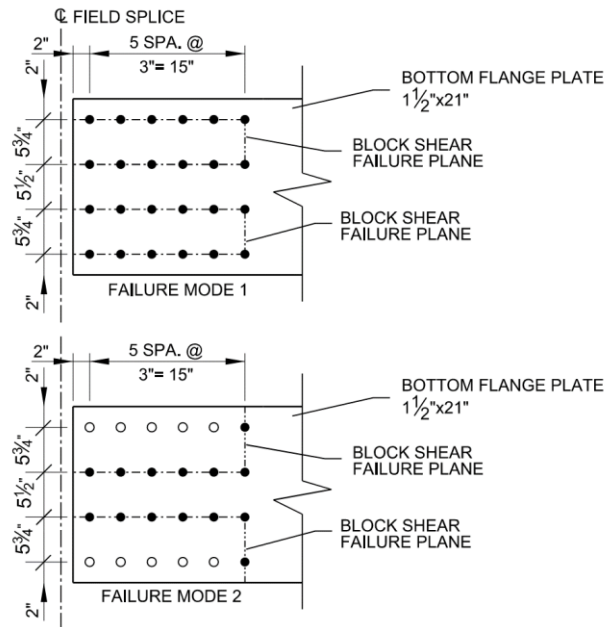


Figure 14 Bottom Flange Splice – Assumed Block Shear Failure Planes in the Flange on the Right-Hand Side of the Splice

For Failure Mode 1:

$$A_{tn} = 2[5.75 - 0.9375](1.5) = 14.44 \text{ in.}^2$$

$$A_{vn} = 4[5(3.0) + 2.0 - 5.5(0.9375)](1.5) = 71.06 \text{ in.}^2$$

$$A_{vg} = 4[5(3.0) + 2.0](1.5) = 102.0 \text{ in.}^2$$

$$\begin{aligned} R_r &= 0.80(1.0)[0.58(65)(71.06) + 1.0(65)(14.44)] \\ &= 2,894 \text{ kips} < 0.80(1.0)[0.58(50)(102.0) + 1.0(65)(14.44)] \\ &= 3,117 \text{ kips} \\ \therefore R_r &= 2,894 \text{ kips} > 1,415 \text{ kips} \quad \text{OK} \end{aligned}$$

For Failure Mode 2:

$$A_{tn} = 2[5.75 + 2.0 - 1.5(0.9375)](1.5) = 19.03 \text{ in.}^2$$

$$A_{vn} = 2[5(3.0) + 2.0 - 5.5(0.9375)](1.5) = 35.53 \text{ in.}^2$$

$$A_{vg} = 2[5(3.0) + 2.0](1.5) = 51.00 \text{ in.}^2$$

$$\begin{aligned} R_r &= 0.80(1.0)[0.58(65)(35.53) + 1.0(65)(19.03)] \\ &= 2,061 \text{ kips} < 0.80(1.0)[0.58(50)(51.00) + 1.0(65)(19.03)] \\ &= 2,173 \text{ kips} \\ \therefore R_r &= 2,061 \text{ kips} > 1,415 \text{ kips} \quad \text{OK} \end{aligned}$$

The factored yield resistance of the splice plates in compression is the same as the factored yield resistance of the splice plates in tension given by Eq. (6.8.2.1-1), and therefore, need not be checked. Buckling of the splice plates in compression is not a concern since the unsupported length of the plates is limited by the maximum bolt spacing and end distance requirements.

Since the combined area of the inside and outside flange splice plates is greater than the area of the smaller bottom flange at the point of splice, fatigue of the base metal of the bottom flange splice plates adjacent to the slip-critical bolted connections does not need to be checked. Similarly, the flexural stresses in the splice plates at the service limit state under the Service II load combination need not be checked.

Calculations similar to the above show that a $\frac{5}{8}$ in. x 17 in. outside splice plate with two $\frac{3}{4}$ in. x $7\frac{3}{4}$ in. inside splice plates are sufficient to resist the design yield resistance of the top flange, $P_{fy} =$

725 kips. Include a ¼ in. x 17 in. filler plate on the outside. All plates are again ASTM A709 Grade 50 steel.

Check that the threads are excluded from the shear planes as originally assumed. According to the 2020 RCSC Specification [21], shear planes located in the transition length of high-strength bolts should be considered shear planes with the threads included. Unless the use and position of washers and DTIs are clearly identified in the contract documents, a conservative assumption to determine whether threads are excluded from or included in the shear plane is to position one washer and one DTI under the bolt head located adjacent to the thicker outer ply. Refer to ASTM F436/F436M for washer thicknesses; the nominal thickness of the typical standard washer is 5/32 inches (the dimension “T” in the calculations below). Refer to ASME B18.2.6 [22] or manufacturer data for the appropriate DTI dimensions (for a 7/8” diameter bolt, use a DTI thickness of 0.260 inches – the dimension “F” in the calculations below). Sum the grip length of the connection, i.e., the total nominal thicknesses of the connection plies, the thicknesses of the assumed washer and DTI, plus an additional value specified in Table C-2.2 of the 2020 RCSC Specification [21] to allow for manufacturing tolerances and sufficient thread engagement with a heavy hex nut. Round up the sum to the next ¼-inch increment up to a bolt length of 6 inches and to the next ½-inch increment for longer bolts to determine the minimum nominal bolt length (the dimension “L_{NOM}” in the calculations below). Next, determine the minimum bolt body length, i.e., the distance from the head of the bolt to the beginning of the transition length (the dimension “L_{B MIN}” in the calculations below) and compare that length to the location of the furthest shear plane measured from the bolt head (the dimension “L_{SP}” in the calculations below) to determine whether the threads are excluded or included. The minimum bolt body length can either be determined directly from Table 2.1.9.2-1 of ASME B18.2.6 [22] using the calculated minimum nominal bolt length and the nominal bolt diameter or calculated indirectly by subtracting the appropriate thread length, L_T, and transition thread length, Y, found in Table C-2.1 of the 2020 RCSC Specification [21] from the calculated minimum nominal bolt length.

Short high-strength bolts with lengths indicated in Table 2.5 of the 2020 RCSC Specification [21] are fully threaded in accordance with ASME B18.2.6 [22] and thus should be designed for threads included in the shear plane. The thicknesses of the assumed washer and DTI should conservatively be subtracted from the calculated minimum nominal bolt length before making this determination.

Bottom Flange Splice:

7/8" diameter bolt

$$L_{\text{PLY}} = 0.875" + 1.5" + 0.875" = 3.25"$$

$$L_{\text{MIN}} = L_{\text{PLY}} + F + T + 1.125" \text{ (RCSC Table C-2.2)} \\ = 3.25" + 0.260" + 5/32" + 1.125" = 4.791"$$

$$L_{\text{NOM}} = 5.00" \text{ (round up to nearest } 1/4" \text{ per RCSC 2.7 Commentary)}$$

$$L_{\text{NOM}} - F - T \\ = 5.00" - 0.260" - 5/32" = 4.58" > L = 2" \text{ (RCSC Table 2.5)}$$

Therefore, bolt is not fully threaded.

$$\begin{aligned}L_{B \text{ MIN}} &= L_{\text{NOM}} - L_{\text{T}} - Y \text{ (RCSC Table C-2.1)} \\ &= 5.00" - 1.5" - 9/32" = 3.22"\end{aligned}$$

(Note: agrees with value of $L_{B \text{ MIN}}$ from Table 2.1.9.2-1 of ASME B18.2.6)

$$L_{\text{SP}} = 0.260" + 5/32" + 0.875" + 1.5" = 2.79" < L_{B \text{ MIN}} = 3.22"$$

Therefore, threads are *excluded* from the shear planes.

Top Flange Splice:

7/8" diameter bolt

$$L_{\text{PLY}} = 0.625" + 1.25" + 0.75" = 2.625"$$

$$\begin{aligned}L_{\text{MIN}} &= L_{\text{PLY}} + F + T + 1.125" \text{ (RCSC Table C-2.2)} \\ &= 2.625" + 0.260" + 5/32" + 1.125" = 4.166"\end{aligned}$$

$$L_{\text{NOM}} = 4.25" \text{ (round up to nearest } 1/4" \text{ per RCSC 2.7 Commentary)}$$

$$\begin{aligned}L_{\text{NOM}} - F - T \\ &= 4.25" - 0.260" - 5/32" = 3.83" > L = 2" \text{ (RCSC Table 2.5)}\end{aligned}$$

Therefore, bolt is not fully threaded.

$$\begin{aligned}L_{B \text{ MIN}} &= L_{\text{NOM}} - L_{\text{T}} - Y \text{ (RCSC Table C-2.1)} \\ &= 4.25" - 1.5" - 9/32" = 2.47"\end{aligned}$$

(Note: agrees with value of $L_{B \text{ MIN}}$ from Table 2.1.9.2-1 of ASME B18.2.6)

$$L_{\text{SP}} = 0.260" + 5/32" + 0.75" + 1.25" = 2.42" < L_{B \text{ MIN}} = 2.47"$$

Therefore, threads are *excluded* from the shear planes.

If the threads had been included in the shear planes in either case, check with the Owner to see if the use of DTIs is permitted. If not, the DTI may be removed from the above calculations.

7.12.4.5 Bearing Resistance Check

The bearing resistance of the connection at the strength limit state is taken as the sum of the smaller of the shear resistance of the individual bolts and the bearing resistance of the individual bolt holes parallel to the line of the design force.

The bearing resistance of connected material in the bottom flange splice will be checked herein. The sum of the inner and outer splice plate thicknesses exceeds the thickness of the thinner flange

at the point of splice, and the splice plate areas satisfy the 10 percent rule described previously. Therefore, the smaller flange on the right-hand side of the splice controls the bearing resistance of the connection.

For standard-size holes, the nominal bearing resistance, R_n , parallel to the applied bearing force is given by Eq. (6.13.2.9-1) or (6.13.2.9-2), as applicable.

For the four bolt holes adjacent to the end of the flange, the end distance is 2.0 in. Therefore, the clear distance, L_c , between the edge of the hole and the end of the flange is:

$$L_c = 2.0 - \frac{0.9375}{2} = 1.53 \text{ in.} < 2.0d = 2.0(0.875) = 1.75 \text{ in.}$$

Therefore, use Eq. (6.13.2.9-2):

$$R_n = 4(1.2L_c t F_u) = 4[1.2(1.53)(1.5)(65)] = 716 \text{ kips}$$

Since:

$$R_r = \phi_{bb} R_n$$

$$R_r = 0.80(716) = 573 \text{ kips}$$

The total factored shear resistance of the bolts in the four holes adjacent to the end of the flange, acting in double shear is $4(64.6) = 258 \text{ kips} < 573 \text{ kips}$. Therefore, the factored shear resistance of the bolts controls and bearing does not control for the four end holes.

For the other twenty bolt holes, the center-to-center distance between the bolt holes in the direction of the applied force is 3.0 in. Therefore, the clear distance, L_c , between the edges of the adjacent holes is:

$$L_c = 3.0 - 0.9375 = 2.0625 \text{ in.} > 2.0d = 1.75 \text{ in.}$$

Therefore, use Eq. (6.13.2.9-1):

$$R_n = 20(2.4d t F_u) = 20[2.4(0.875)(1.5)(65)] = 4,095 \text{ kips}$$

Since:

$$R_r = \phi_{bb} R_n$$

$$R_r = 0.80(4,095) = 3,276 \text{ kips}$$

The total factored shear resistance of the bolts in the twenty interior bolt holes is $20(64.6) = 1,292$ kips $< 3,276$ kips. Therefore, the factored shear resistance of the bolts controls and bearing does not control for the twenty interior bolt holes.

The total factored shear resistance of the bolts in the twenty-four holes is:

$$R_r = 258 + 1,292 = 1,550 \text{ kips} > P_{fy} = 1,415 \text{ kips} \quad \text{OK}$$

Calculations similar to the above show that the bearing resistance of the connected material in the top flange splice does not control, and that the total factored shear resistance of the bolts in the sixteen bolt holes in the top flange splice is sufficient.

7.12.4.6 Slip Resistance Check

The moment resistance provided by the nominal slip resistance of the flange splice bolts that are required to satisfy the strength limit state is to be checked against the factored moment for checking slip. The nominal slip resistance of the flange splice bolts was determined previously in Section 7.12.2. The nominal slip resistance of a bolt need not be adjusted for the effect of a filler; the resistance to slip between either connected part and the filler is comparable to that which would exist between the connected parts if the filler were not present.

Should the factored moment exceed the moment resistance provided by the nominal slip resistance of the flange splice bolts, the additional moment is to be resisted by the web as specified in Article 6.13.6.1.3c. The factored moments for checking slip are to be taken as the moment at the point of splice under Load Combination Service II, as specified in Table 3.4.1-1, and also the factored moment at the point of splice due to the deck placement sequence as specified in Article 3.4.2.1.

The moment resistance provided by the nominal slip resistance of the flange splice bolts is calculated as shown in Figures C6.13.6.1.3b-1 and C6.13.6.1.3b-2, with the appropriate nominal slip resistance of the flange splice bolts substituted for P_{fy} . For checking slip due to the factored deck casting moment, the moment resistance of the noncomposite section is used.

Service II Positive Moment (refer to Figure C6.13.6.1.3b-1)

$$\text{Service II Positive Moment} = 1.0(-1,967 + -250) + 1.0(-237) + 1.3(+2,054) = +216.2 \text{ kip-ft}$$

Use the nominal slip resistance of the bottom flange splice bolts.

$$\text{Nominal slip resistance of the bottom flange splice with 24 bolts: } P_t = 24(39.0 \text{ kips/bolt}) = 936 \text{ kips}$$

$$\text{Flange Moment Arm: } A = D + t_{ft}/2 + t_{haunch} + t_s/2 = 84 + 1.5/2 + 4.0 + 9.0/2 = 93.25 \text{ in.}$$

$$M_{\text{flange}} = 936 \text{ kips} \times (93.25/12) = 7,274 \text{ kip-ft} > 216.2 \text{ kip-ft} \quad \text{OK}$$

Service II Negative Moment (refer to Figure C6.13.6.1.3b-2)

$$\text{Service II Negative Moment} = 1.0(-1,967 + -250) + 1.0(-237) + 1.3(-2,772) = -6,058 \text{ kip-ft}$$

Use the nominal slip resistance of the top or bottom flange splice bolts, whichever is smaller.

Nominal slip resistance of the top flange splice with 16 bolts: $P_t = 16(39.0 \text{ kips/bolt}) = 624 \text{ kips} < 936 \text{ kips}$

$$\text{Flange moment arm: } A = D + (t_{ft} + t_{fc})/2 = 84 + (1.5 + 1.0)/2 = 85.25 \text{ in.}$$

$$M_{\text{flange}} = 624 \times (85.25/12) = 4,433 \text{ kip-ft} < |-6,058| \text{ kip-ft}$$

Therefore, the flanges do not have adequate capacity by themselves to prevent slip under the factored Service II negative moment at the point of splice.

Referring to Figure C6.13.6.1.3c-2, the required horizontal web force, H_w , to satisfy the Service II moment requirement is:

$$H_w = \frac{(\text{Service II moment} - M_{\text{flange}})}{D/4} = \frac{(6,058 - 4,433) \times 12}{84/4} = 929 \text{ kips}$$

Therefore, negative moment controls the Service II web connection design for slip, which is discussed later on in this design example (Section 7.12.5.5).

In cases where the moment resistance provided by the flange splice bolts is sufficient at the strength limit state (which is not the case in this design example), but a moment contribution from the web is required to resist slip, the number of flange splice bolts may be increased to increase the moment resistance provided by the nominal slip resistance of the flange splice bolts to prevent having to add an additional row of web splice bolts to resist the resultant web slip force.

Deck Placement (refer to Figure C6.13.6.1.3b-2)

$$M_{\text{deck placement}} = 1.4(-1,910 + -169) = -2,911 \text{ kip-ft}$$

The deck-placement moment is applied to the noncomposite section. Use the nominal slip resistance of the top or bottom flange splice bolts, whichever is smaller.

Nominal slip resistance of the top flange splice with 16 bolts: $P_t = 16(39.0 \text{ kips/bolt}) = 624 \text{ kips} < 936 \text{ kips}$

$$\text{Flange moment arm: } A = D + (t_{ft} + t_{fc})/2 = 84 + (1.5 + 1.0)/2 = 85.25 \text{ in.}$$

$$M_{\text{flange}} = 624 \times (85.25/12) = 4,433 \text{ kip-ft} > |-2,911| \text{ kip-ft} \text{ OK}$$

7.12.4.7 Article 6.10.1.8 – Tension Flanges with Holes

When checking flexural members at the strength limit state or for constructability, the following additional requirement shall be satisfied at all cross-sections containing holes in the tension flange:

$$f_t \leq 0.84 \left(\frac{A_n}{A_g} \right) F_u \leq F_{yt} \quad \text{Eq. (6.10.1.8-1)}$$

where: A_n = net area of the tension flange determined as specified in Article 6.8.3 (in.²)
 A_g = gross area of the tension flange (in.²)
 f_t = stress on the gross area of the tension flange due to the factored loads calculated without consideration of flange lateral bending (ksi)
 F_u = specified minimum tensile strength of the tension flange determined as specified in Table 6.4.1-1 (ksi)

Separate calculations show that the tensile stress in the top flange at the strength limit state controls. Calculate the factored Strength I tensile stress in the top flange at the point of splice:

$$f_t \text{ (top flange)} = 1.0 \left[\frac{1.25(-1,967)}{2,262} + \frac{1.25(-250) + 1.5(-237)}{2,507} + \frac{1.75(-2,772)}{3,002} \right] (12) = 35.63 \text{ ksi (T)}$$

$$A_n = [17.0 - 4(0.9375)](1.0) = 13.25 \text{ in.}^2$$

$$A_g = (17.0)(1.0) = 17.0 \text{ in.}^2$$

$$0.84 \left(\frac{A_n}{A_g} \right) F_u = 0.84 \left(\frac{13.25}{17.0} \right) (65) = 42.56 \text{ ksi} < F_{yt} = 50 \text{ ksi}$$

$$f_t = 35.63 \text{ ksi} < 42.56 \text{ ksi} \quad \text{OK}$$

7.12.5 Web Splice Design

7.12.5.1 General

As a minimum, web splice plates and their connections are to be designed at the strength limit state for a design web force taken equal to the smaller factored shear resistance of the web, $V_r = \phi_v V_n$, on either side of the splice determined according to the provisions of Article 6.10.9 or 6.11.9, as applicable.

Should the moment resistance provided by the flanges at the point of splice, determined as specified in Article 6.13.6.1.3b, not be sufficient to resist the factored moment at the strength limit state (which is the case in this design example), the web splice connections are to instead be designed for a design web force taken equal to the vector sum of the smaller factored shear

resistance and a horizontal force in the web that provides the necessary moment resistance in conjunction with the flanges.

The horizontal force in the web is to be computed as the portion of the factored moment at the strength limit state at the point of splice that exceeds the moment resistance provided by the flanges divided by the appropriate moment arm. For composite sections subject to positive flexure, the moment arm is taken as the vertical distance from the mid-depth of the web to the mid-thickness of the concrete deck including the concrete haunch (Figure C6.13.6.1.3c-1). For composite sections subject to negative flexure and noncomposite sections subject to positive or negative flexure, the moment arm is taken as one-quarter of the web depth (Figure C6.13.6.1.3c-2).

7.12.5.2 Web Splice Bolts

The computed design web force is to be divided by the factored shear resistance of the bolts, determined in Section 7.12.3.1, to determine the total number of web splice bolts required on one side of the splice at the strength limit state. The factored shear resistance of the bolts should be based on threads included in the shear planes, unless the web splice-plate thickness exceeds 0.5 in. As a minimum, two vertical rows of bolts spaced at the maximum spacing for sealing bolts specified in Article 6.13.2.6.2 should be provided, with a closer spacing and/or additional rows provided only as needed. For bolted web splices with thickness differences of 1/16 in. or less (which is the case in this example), filler plates should not be provided.

Since the moment resistance provided by the flange splices is not sufficient to resist the factored moment at the strength limit state at the point of splice in this case, the web splice bolts are designed at the strength limit state for a design web force taken equal to the vector sum of the smaller factored shear resistance of the web on either side of the splice and the horizontal web force, $H_w = 1,615$ kips, computed in Section 7.12.4.3.

The factored shear resistance of the 0.5625 in. web at the splice (i.e., the smaller web) is determined to be 617 kips according to the provisions of Article 6.10.9.1. Although not shown, the calculations are similar to the calculations shown earlier for computing the shear resistance of the web at Sections G4-2 and G4-3.

$$V_r = \phi_v V_n = 617 \text{ kips}$$

$$R = \sqrt{(V_r)^2 + (H_w)^2} = \sqrt{(617)^2 + (1,615)^2} = 1,729 \text{ kips}$$

Number of Bolts Required (threads included in the shear plane): $N = 1,729/51.9 = 33.3$ bolts

Use 34 bolts in two vertical rows (17 bolts per row) on each side of the splice.

Note that the greater than 38.0 in. length reduction for the shear resistance of the bolts only applies to lap-splice tension connections (Article 6.13.2.7) and is not to be applied in the design of the web splice.

The *AASHTO LRFD BDS* requires at least two rows of bolts in the web over the depth of the web (Article 6.13.6.1.3a). The maximum permitted spacing of the bolts for sealing is $s \leq (4.0 + 4.0t) \leq 7.0$ in., where t is the thickness of the splice plate (Article 6.13.2.6.2). Assuming the splice plate thickness will be one-half the smaller web thickness at the point of splice plus 1/16 in. gives a splice plate thickness of:

$$t = \frac{1}{2} \times \frac{5}{16} + \frac{1}{16} = 0.22 \text{ in. Use } t = \frac{3}{8} \text{ in.}$$

The splice-plate thickness satisfies the minimum thickness requirement for steel specified in Article 6.7.3.

The maximum bolt spacing for the $\frac{3}{8}$ in. splice plate is:

$$s \leq 4.0 + (4.0 \times 0.375) = 5.5 \text{ in.} < 7.0 \text{ in.}$$

The minimum bolt spacing is $3d = 3(0.875) = 2.625$ in.

Use a spacing = $4\frac{3}{4}$ in. $< 5\frac{1}{2}$ in. Using a 4.0 in. gap from the top and bottom of the web to the top and bottom web splice bolts so as to not impinge on bolt assembly clearances [refer to Table 7-15 of the *AISC Manual of Steel Construction* – use $H2 + \max(C1, C2) = 2\frac{3}{4}$ in. minimum clearance for a 7/8-in. diameter bolt] [23].

7.12.5.3 Web Splice Plates

The web splice plates are $\frac{3}{8}$ in. x $79\frac{1}{2}$ in. The plates are ASTM A709 Grade 50 steel.

The factored shear resistance of the web at the strength limit state, V_r , is not to exceed the factored shear yielding or factored shear rupture resistance of the web splice plates (Article 6.13.6.1.3c).

For shear yielding, the factored resistance of the web splice plates is determined as specified in Article 6.13.5.3 as follows:

$$R_r = \phi_v 0.58 F_y A_{vg} \quad \text{Eq. (6.13.5.3-1)}$$

where: A_{vg} = gross area of the connection element subject to shear (in.²)
 F_y = specified minimum yield strength of the connection element (ksi)
 ϕ_v = resistance factor for shear = 1.0 (Article 6.5.4.2)

$$R_r = 1.0(0.58)(50)2(0.375)(79.50) = 1,729 \text{ kips}$$

$$R_r = 1,729 \text{ kips} > V_r = 617 \text{ kips} \quad \text{OK}$$

For shear rupture, the factored resistance of the web splice plates is determined as specified in Article 6.13.5.3 as follows:

$$R_r = \phi_{vu} 0.58 R_p F_u A_{vn} \quad \text{Eq. (6.13.5.3-2)}$$

where: A_{vn} = net area of the connection element subject to shear (in.²)
 F_u = tensile strength of the connection element (ksi)
 R_p = reduction factor for holes taken equal to 0.90 for bolt holes punched full size and 1.0 for bolt holes drilled full size or subpunched and reamed to size (use 1.0 for splice plates since the holes in field splices are not allowed to be punched full size)
 ϕ_{vu} = resistance factor for shear rupture of connection elements = 0.80 (Article 6.5.4.2)

$$R_r = 0.80(0.58)(1.0)(65)(2)[79.50 - 17(0.9375)](0.375) = 1,438 \text{ kips}$$

$$R_r = 1,438 \text{ kips} > V_r = 617 \text{ kips} \quad \text{OK}$$

The factored shear resistance of the web, V_r , is also not to exceed the block shear rupture resistance of the web splice plates. To check the block shear rupture resistance of the web splice plates (and the factored bearing resistance of the bolt holes in Section 7.12.5.4), the bolt edge and end distances must first be established and checked.

The edge distance of bolts is defined as the distance perpendicular to the line of force between the center of a hole and the edge of the component. In this example, the edge distance from the center of the vertical line of holes in the web plate to the edge of the field piece of 2.0 in. satisfies the minimum edge distance requirement of $1\frac{1}{8}$ in. specified for $\frac{7}{8}$ -in.-diameter bolts in Table 6.13.2.6.6-1. This distance also satisfies the maximum edge distance requirement of $8.0t$ (not to exceed 5.0 in.) = $8.0(0.375) = 3.0$ in. specified in Article 6.13.2.6.6. The edge distance for the outermost vertical row of holes on the web splice plates is set at 2.0 in. Although not done in this example, fabricators generally prefer that the edge distance on the web at the point of splice be increased a minimum of $\frac{1}{4}$ in. from the design value to allow for girder trim.

The end distance of bolts is defined as the distance along the line of force between the center of a hole and the end of the component. In this example, the end distance of $1\frac{3}{4}$ in. at the top and bottom of the web splice plates satisfies the minimum end distance requirement of $1\frac{1}{8}$ in. specified for $\frac{7}{8}$ -in.-diameter bolts. The maximum end distance requirement of 3.0 in. is also satisfied. Although not specifically required, note that the distance from the corner bolts to the corner of the web splice plate, equal to $\sqrt{(2.0)^2 + (1.75)^2} = 2.7$ in., also satisfies the maximum end distance requirement.

Block shear rupture resistance normally does not govern for typical web splice plates, but the check is illustrated here for completeness. The assumed block shear failure plane for the web splice plate is shown in Figure 15.

According to Article 6.13.4, the factored resistance of the combination of parallel and perpendicular planes is to be taken as:

$$R_r = \phi_{bs} R_p (0.58 F_u A_{vn} + U_{bs} F_u A_{tn}) \leq \phi_{bs} R_p (0.58 F_y A_{vg} + U_{bs} F_u A_{tn}) \quad \text{Eq. (6.13.4-1)}$$

where: R_p = reduction factor for holes taken equal to 1.0 for bolt holes drilled full size
 A_{vg} = gross area along the plane resisting shear stress (in.²)
 A_{vn} = net area along the plane resisting shear stress (in.²)
 U_{bs} = reduction factor for block shear rupture resistance taken equal to 1.0 when the tension stress is uniform
 A_{tn} = net area along the plane resisting tension stress (in.²)
 ϕ_{bs} = resistance factor for block shear = 0.80 (Article 6.5.4.2)

First, compute the area terms, based on the assumed block shear failure planes shown in Figure 15:

$$A_{vg} = 2[79.50 - 1.75](0.375) = 58.31 \text{ in.}^2$$

$$A_{vn} = 2[79.50 - 1.75 - 16.5(0.9375)](0.375) = 46.71 \text{ in.}^2$$

$$A_{tn} = 2[3.0 + 2.0 - 1.5(0.9375)](0.375) = 2.70 \text{ in.}^2$$

Compute the factored resistance as follows:

$$R_{r1} = 0.80(1.0)[0.58(65)(46.71) + (1.0)(65)(2.70)] = 1,549 \text{ kips}$$

$$R_{r2} = 0.80(1.0)[0.58(50)(58.31) + 1.0(65)(2.70)] = 1,493 \text{ kips (controls)}$$

$$R_r = 1,493 \text{ kips} > V_r = 617 \text{ kips} \quad \text{OK}$$

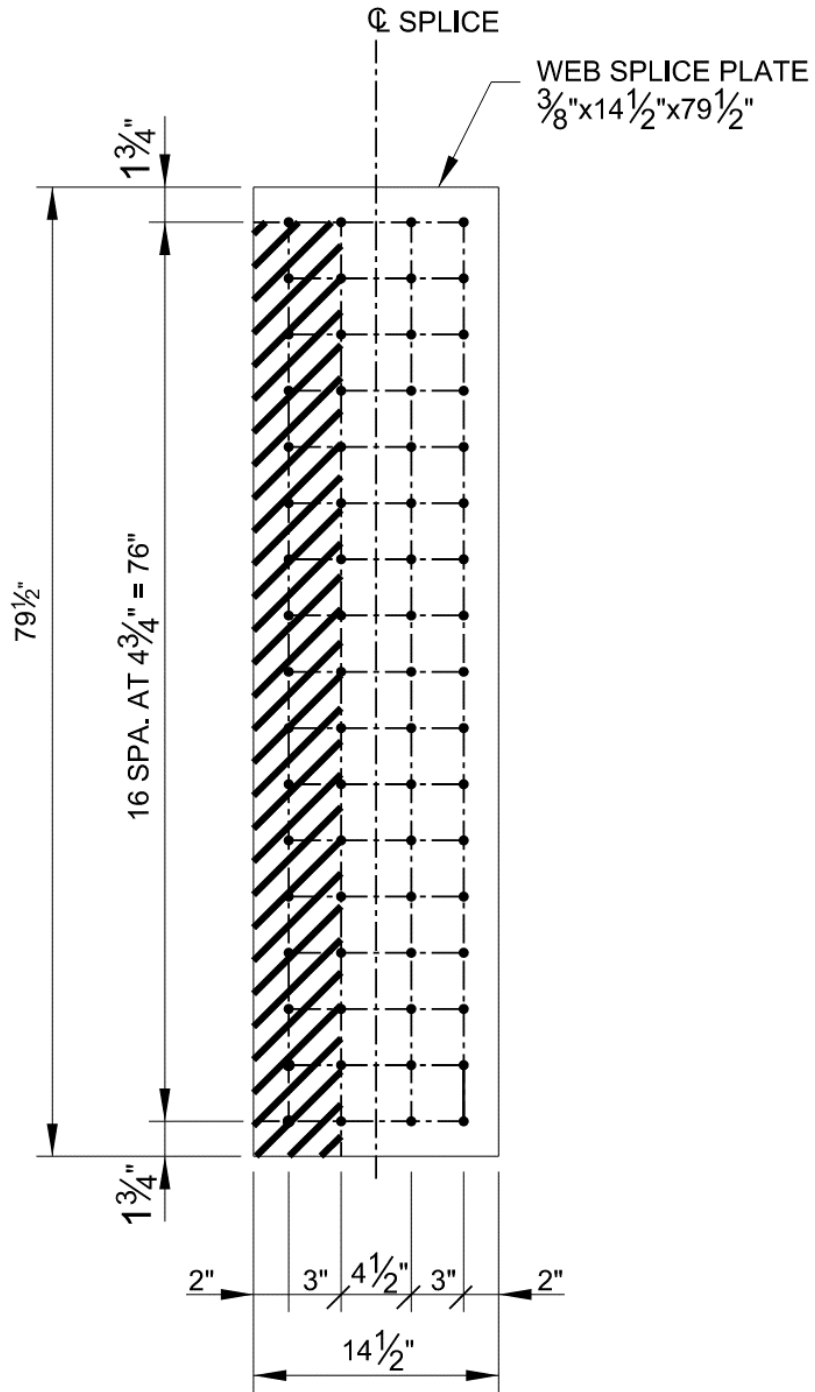


Figure 15 Assumed Block Shear Failure Planes for the Web Splice Plates

Since the combined area of the web splice plates is greater than the area of the web at the point of splice, the fatigue stresses in the base metal of the web splice plates adjacent to the slip-critical bolted connections need not be checked. Also, the flexural stresses in the splice plates at the service limit state under the Service II load combination need not be checked.

Check that the threads are included in the shear planes as originally assumed. Refer to the discussion near the end of Section 7.12.4.4 regarding this check.

Web Splice:

7/8" diameter bolt

$$L_{PLY} = 0.375" + 0.625" + 0.375" = 1.375"$$

$$L_{MIN} = L_{PLY} + F + T + 1.125" \text{ (RCSC Table C-2.2)}$$

$$= 1.375" + 0.260" + 5/32" + 1.125" = 2.916"$$

$$L_{NOM} = 3.00" \text{ (round up to nearest } 1/4" \text{ per RCSC 2.7 Commentary)}$$

$$L_{NOM} - F - T$$

$$= 3.00" - 0.260" - 5/32" = 2.58" > L = 2" \text{ (RCSC Table 2.5)}$$

Therefore, bolt is not fully threaded.

$$L_{B MIN} = L_{NOM} - L_T - Y \text{ (RCSC Table C-2.1)}$$

$$= 3.00" - 1.5" - 9/32" = 1.22"$$

(Note: agrees with value of $L_{B MIN}$ from Table 2.1.9.2-1 of ASME B18.2.6)

$$L_{SP} = 0.260" + 5/32" + 0.375" + 0.625" = 1.42" > L_{B MIN} = 1.22"$$

Therefore, threads are *included* in the shear planes.

7.12.5.4 Bearing Resistance

Check the bearing resistance of the web splice bolt holes at the strength limit state. The assumption is that at the strength limit state, the bolts have slipped and gone into bearing. The bearing resistance of the smaller web controls in this case since the web thickness is less than the sum of the two splice plate thicknesses.

When a moment contribution from the web is required at the strength limit state (which is the case in this example), the resultant forces causing bearing on the web bolt holes are inclined. The bearing resistance of each bolt hole in the web can conservatively be calculated in this case using the clear edge distance, as shown on the left of Figure C6.13.6.1.3c-3. This calculation is conservative since the resultant forces act in the direction of inclined distances that are larger than the clear edge distance. This calculation is also likely to be a conservative calculation for the bolt holes in the adjacent rows. Should the bearing resistance be exceeded, it is recommended that the

edge distance be increased slightly in lieu of increasing the number of bolts or thickening the web. Another option would be to calculate the bearing strength based on the inclined distance or resolve the resultant force in the direction parallel to the edge distance. In cases where the bearing strength of the web splice plate controls, the smaller of the clear edge or end distance on the splice plates can be used to compute the bearing strength of the outermost hole.

Based on the edge distance from the center of the hole to the edge of the field section of 2.0 in., the clear edge distance, L_c , is computed as:

$$L_c = 2.0 - \frac{0.9375}{2} = 1.53 \text{ in.} < 2.0d = 2.0(0.875) = 1.75 \text{ in.}$$

Therefore, use Eq. (6.13.2.9-2):

$$R_n = 34[1.2L_c t F_u] = 34[1.2(1.53)(0.5625)(65)] = 2,282 \text{ kips}$$

Since:

$$R_r = \phi_{bb} R_n$$

$$R_r = 0.80(2,282) = 1,826 \text{ kips}$$

The total factored shear resistance of the 34 bolts in the web splice, acting in double shear, is $34(51.9) = 1,765 \text{ kips} < 1,826 \text{ kips}$. Therefore, the factored shear resistance of the bolts controls and bearing does not control.

The total factored shear resistance of the bolts in the 34 holes is:

$$R_r = 1,765 \text{ kips} > R = 1,729 \text{ kips} \quad \text{OK}$$

7.12.5.5 Slip Resistance

At a minimum, bolted connections for web splices are to be checked for slip under a web slip force taken equal to the factored shear in the web at the point of splice.

Should the moment resistance provided by the nominal slip resistance of the flange splice bolts, determined as specified in Article 6.13.6.1.3b, not be sufficient to resist the factored moment for checking slip at the point of splice (which is the case in this example), the web splice bolts are instead to be checked for slip under a web slip force taken equal to the vector sum of the factored shear and a horizontal force in the web that provides the necessary slip resistance in conjunction with the flange splices. The horizontal force in the web is computed as the portion of the factored moment for checking slip at the point of splice that exceeds the moment resistance provided by the nominal slip resistance of the flange splice bolts divided by the appropriate moment arm (see Figure C6.13.6.1.3c-1 or C6.13.6.1.3c-2, as applicable).

The factored shear for checking slip is taken as the shear in the web at the point of splice under Load Combination Service II, as specified in Table 3.4.1-1, or the factored shear in the web at the point of splice due to the deck placement sequence as specified in Article 3.4.2.1, whichever governs.

Since the moment resistance provided by the nominal slip resistance of the flange splice bolts is not sufficient to resist the factored Service II negative moment for checking slip at the point of splice in this case, the web splice bolts are checked for slip under a resultant web slip force taken equal to the vector sum of the governing factored Service II shear in the web at the point of splice and the horizontal force in the web for the Service II negative moment case, $H_w = 929$ kips computed in Section 7.12.4.6, that provides the necessary slip resistance in conjunction with the flanges. The computed resultant force, R , for the Service II load combination governs over the factored deck casting shear as illustrated below.

The unfactored shears at the point of splice are as follows (Table 10):

V_{DC1}	=	139 kips
V_{DC2}	=	19 kips
V_{DW}	=	22 kips
V_{+LL+IM}	=	139 kips
$V_{deck\ placement}$	=	99 kips

Service II Shear = $1.0(139 + 19) + 1.0(22) + 1.3(139) = 361$ kips

$$R = \sqrt{(361)^2 + (929)^2} = 997 \text{ kips} > V_{deck\ placement} = 1.4(99) = 139 \text{ kips}$$

Slip resistance of web splice w/ 34 bolts: $P_t = 34(39.0 \text{ kips/bolt}) = 1,326 \text{ kips} > R = 997 \text{ kips}$ OK

7.13 Cross-Frame Member and Connection

7.13.1 Cross-Frame Diagonal Design

Evaluation of the cross-frame analysis results shows that the diagonal member between G4 and G3 at Support 2 has the largest force. The largest factored load of the Load Combinations examined is -88 kips (compression). Compression members are designed according to Article 6.9. According to Table 6.6.2.1-1, cross-frames in horizontally curved bridges are considered primary members.

Using the girder spacing and web height, determine the effective length of the diagonal member:

$$\ell = \sqrt{11^2 + 7^2} = 13 \text{ ft}$$

Use a L8x8x3/4 single angle with a yield stress of 50 ksi and with the following properties taken from the AISC *Steel Construction Manual* [23].

$$r_x = r_y = 2.46 \text{ in.}$$

$$r_z = 1.57 \text{ in.}$$

$$A_s = 11.5 \text{ in.}^2$$

To determine if the effects of local buckling of the outstanding angle legs on the nominal compressive resistance of the member need to be considered, check the width-to-thickness ratio provision of Article 6.9.4.2.1 for the cross-frame bottom strut member:

$$\frac{b}{t} \leq \lambda_r \quad \text{Eq. (6.9.4.2.1-1)}$$

where:

- λ_r = width-to-thickness ratio limit specified in Table 6.9.4.2.1-1
- b = the full width of the outstanding leg for a single angle (in.)
- t = element thickness (in.)

$$\frac{b}{t} = \frac{8}{0.75} = 10.7 < 0.45 \sqrt{\frac{29,000}{50}} = 10.8 \quad \text{Angle legs are nonslender.}$$

Check the limiting slenderness ratio of Article 6.9.3. As a primary compression member, the angle must satisfy the following:

$$\frac{K\ell}{r} \leq 120$$

- where: K = effective length factor specified in Article 4.6.2.5 as 1.0 for single angles regardless of end connection (in.)
- ℓ = unbraced length (in.)
- r = minimum radius of gyration (in.)

$$\frac{K\ell}{r} = \frac{1.0(13)(12)}{1.57} = 99 < 120 \quad \text{OK}$$

In an actual design, an additional iteration of the analysis may be necessary since the cross-frame member area used in the model was 5.0 in.² and the design area is 11.5 in.². Since the cross-frames are truss members in the 3D analysis, the area of the cross-frame elements affects the structure rigidity, which in turn alters the girder moments and shears as well as cross-frame forces.

Having satisfied the basic slenderness provisions, the angle is then checked for the strength limit state in accordance with Article 6.9.4.4 regarding single-angle members.

Single angles are commonly used as members in cross-frames of steel girder bridges. Since the angle is typically connected through one leg only, the member is subjected to combined axial load and flexure. In other words, the eccentricity of the applied axial load induces moments about both principal axes of the angle. As a result, it is difficult to predict the nominal compressive resistance of these members. The provisions of Article 6.9.4.4 provide a simplified approach by permitting

the effect of the eccentricities to be neglected when the single angles are evaluated as axially loaded compression members for flexural buckling only using an appropriate specified effective slenderness ratio, $(K\ell/r)_{\text{eff}}$, in place of $(K\ell/r_s)$ in Eq. (6.9.4.1.2-1). By following this approach, the single angles are designed as axially loaded compression members for flexural buckling only according to the provisions of Articles 6.9.2.1, 6.9.4.1.1, and 6.9.4.1.2. It should be noted that according to Article 6.9.4.4, the actual maximum slenderness ratio of the angle, not the effective slenderness ratio, is not to exceed the limiting slenderness ratio specified in Article 6.9.3 as checked above. Also, per Article 6.9.4.4, single angles designed using $(K\ell/r)_{\text{eff}}$ need not be checked for flexural-torsional buckling.

Compute the effective slenderness ratio per Article 6.9.4.4 based on the criteria for equal-leg angles. The length, ℓ , is defined as the distance between the work points of the joints measured along the length of the angle, which is conservatively assumed to be equal to the full diagonal distance of 13 feet in this example. First, check the ℓ/r_x limit of 80:

$$\frac{\ell}{r_x} = \frac{(13)(12)}{2.46} = 63.4 < 80$$

where: r_x = radius of gyration about the geometric axis of the angle parallel to the connected leg (Although not relevant for equal-leg angles, the term r_x should be taken as the smaller value of the radius of gyration about the angle geometric axes, which is r_y when unequal-leg angles are used and are connected through the longer leg .)

Therefore, compute the effective slenderness ratio as follows:

$$\left(\frac{K\ell}{r}\right)_{\text{eff}} = 72 + 0.75 \frac{\ell}{r_x} \quad \text{Eq. (6.9.4.4-1)}$$

$$\left(\frac{K\ell}{r}\right)_{\text{eff}} = 72 + 0.75 \frac{(13)(12)}{2.46} = 120$$

In accordance with the provisions for single-angle members in Article 6.9.4.4 and using the effective slenderness ratio, $(k\ell/r)_{\text{eff}}$, the factored compressive resistance of the angle is to be taken as:

$$P_r = \phi_c P_n \quad \text{Eq. (6.9.2.1-1)}$$

where: P_n = nominal compressive resistance determined using the provisions of Article 6.9.4.1.1
 ϕ_c = resistance factor for axial compression = 0.95(Article 6.5.4.2)

To compute P_n , first compute P_e and P_o . P_e is the elastic critical buckling resistance determined as specified in Article 6.9.4.1.2 for flexural buckling, which is the applicable buckling mode for single angles. P_o is the nominal yield resistance equal to $F_y A_g$

$$P_e = \frac{\pi^2 E}{\left(\frac{K\ell}{r_s}\right)^2} A_g \quad \text{Eq. (6.9.4.1.2-1)}$$

where $(K\ell/r)_{\text{eff}}$ is used in place of $(K\ell/r_s)$ in the denominator.

$$P_e = \frac{\pi^2 E}{\left(\frac{K\ell}{r}\right)_{\text{eff}}^2} A_g = \frac{\pi^2 (29,000)}{(120)^2} (11.5) = 229 \text{ kips}$$

$$P_o = F_y A_g = (50)(11.5) = 575 \text{ kips}$$

Since

$$\frac{P_o}{P_e} = \frac{575}{229} = 2.51 > 2.25,$$

the nominal axial resistance in compression for a member composed only of nonslender longitudinally unstiffened elements satisfying the width-to-thickness ratio limits specified in Article 6.9.4.2.1 (checked above) is computed as:

$$P_n = 0.877P_e \quad \text{Eq. (6.9.4.1.1-2)}$$

$$P_n = 0.877(229) = 201 \text{ kips}$$

Compute the factored compressive resistance of the angle as follows:

$$P_r = \phi_c P_n = 0.95(201) = 191 \text{ kips}$$

$$P_u = |-88 \text{ kips}| < P_r = 191 \text{ kips} \quad \text{OK}$$

7.13.2 Cross-Frame Fatigue Check

Fatigue of the cross-frame member is checked assuming that the diagonal is connected to a gusset plate with fillet welds. From the analysis, the maximum range of unfactored fatigue force due to one cycle of stress in any diagonal in the bridge that is subject to a net applied tensile force as specified in Article 6.6.1.2.1 is 22.7 kips. To determine the maximum range of force in a cross-frame or diaphragm member from a refined analysis, the single fatigue truck should be positioned as specified in Article 3.6.1.4.3a, with the truck confined to a single transverse position during each passage of the truck along the bridge (per Article C6.6.1.2.1).

Condition 7.2 from Table 6.6.1.2.3-1 applies, which corresponds to the base metal in an angle section connected to a gusset or connection plate by longitudinal fillet welds along both sides of the connected element of the member cross-section. Therefore, Detail Category E' applies. From Table 6.6.1.2.3-2, the 75-year $(ADTT)_{SL}$ equivalent to infinite fatigue life for a Category E' fatigue detail is 8,485 trucks per day. Therefore, since the assumed $(ADTT)_{SL}$ for this design example of 1,000 trucks per day is less than this limit of 8,485 trucks per day, the detail should be checked for finite fatigue life using the Fatigue II load combination. Table 3.4.1-1 requires that a load factor of 0.80 be applied to the force range for checking Fatigue II.

$$\text{Factored fatigue force range} = (0.80)(22.7) = 18.2 \text{ kips}$$

(Note that the *National Cooperative Highway Research Project Report 962: Proposed Modification to AASHTO Cross-Frame Analysis and Design* [11] is recommending that the Fatigue I and Fatigue II load factors be multiplied by an additional factor of 0.65 when evaluating load-induced fatigue in cross-frame and diaphragm members based on weigh-in-motion data and an analytical evaluation of cross-frames. As of this writing, this recommendation has been adopted for inclusion into the next edition of the *AASHTO LRFD BDS*.)

To account for shear lag effects in the single angle cross-frame member, the factored fatigue force range should be divided by the effective area. The effective area is calculated in accordance with Table 6.6.1.2.3-1, Description 7.2, where the effective area is computed as:

$$A_{\text{eff}} = \left(1 - \frac{\bar{x}}{L}\right) A_g$$

where: \bar{x} = connection eccentricity (in.) – see Condition 7.2 in Table 6.6.1.2.3-1

L = maximum length of the longitudinal welds (in.)

The length of the longitudinal weld on each side of the angle is taken as 7.0 inches, based on calculations in the following section. Therefore, the effective area and factored fatigue stress range are computed as:

$$A_{\text{eff}} = \left(1 - \frac{2.26}{7.0}\right)(11.5) = 7.79 \text{ in.}^2$$

$$\text{Factored fatigue stress range} = \frac{18.2}{7.79} = 2.34 \text{ ksi}$$

Per Article 6.6.1.2.5, the nominal fatigue resistance for finite fatigue life is equal to:

$$(\Delta F)_n = \left(\frac{A}{N}\right)^{\frac{1}{3}}$$

in which:

$$N = (365)(75)n(\text{ADTT})_{\text{SL}}$$

The values of n specified for “Transverse Members” in Table 6.6.1.2.5-2 are intended to apply only to floorbeams. Research has shown that the number of cycles per truck passage, n , for cross-frames and diaphragms should be taken as 1.0, per guidance from the *National Cooperative Highway Research Project Report 962: Proposed Modification to AASHTO Cross-Frame Analysis and Design* [11]. Secondary stress cycles in cross-frames and diaphragms are generally small in magnitude and do not significantly contribute to the load-induced fatigue damage of the detail. Therefore:

$$N = (365)(75)(1.0)(1,000) = 27.38 \times 10^6 \text{ cycles}$$

From Table 6.6.1.2.5-1, the detail category constant, A , for a Category E' detail is $3.9 \times 10^8 \text{ ksi}^3$. Therefore,

$$(\Delta F)_n = \left(\frac{3.9 \times 10^8}{27.38 \times 10^6} \right)^{\frac{1}{3}} = 2.42 \text{ ksi} > 2.34 \text{ ksi} \quad \text{OK}$$

7.13.3 Cross-Frame Welded Connection

As specified in Article 6.13.3.2.4, the resistance of fillet welds which are made with matched or undermatched weld metal is to be taken as the smaller of the factored shear rupture resistance of the connected material adjacent to the weld leg (Article 6.13.5.3) and the product of the effective area of the weld and the factored resistance of the weld metal. For a fillet weld, the effective area is defined in Article 6.13.3.3 as the effective weld length multiplied by the effective throat. The effective throat is the shortest distance from the root of the joint to the face of the fillet weld (equal to 0.707 times the weld leg size for welds with equal leg sizes). As specified in Article 6.13.3.5, the effective length of a fillet weld is to be at least four times its nominal size, or 1½ inches, whichever is greater.

As described in Article C6.13.3.1, matching weld metal has the same or a slightly higher minimum specified tensile strength compared to the minimum specified properties of the base metal. Matching weld metal is generally to be used for fillet welds. Undermatched weld metal may be specified by the Engineer (and is encouraged) for fillet welds connecting steels with specified minimum yield strengths greater than 50.0 ksi; in such cases, the welding procedure and weld metal must be selected to achieve sound welds. For ASTM A 709 Grade 50 steel, the specified minimum tensile strength is 65.0 ksi (Table 6.4.1-1). Thus, assume the classification strength of the weld metal is 70.0 ksi. The classification strength of the weld metal is the minimum specified tensile strength of the weld metal in ksi, which is reflected in the classification designation of the electrode.

The factored resistance of the weld metal is:

$$R_r = 0.6\phi_{e2}F_{\text{exx}} \quad \text{Eq. (6.13.3.2.4-1)}$$

where: ϕ_{e2} = resistance factor for shear in the throat of the weld metal = 0.8 (Article 6.5.4.2)
 F_{exx} = classification strength of the weld metal = 70.0 ksi in this case

$$R_r = 0.6(0.80)(0.70) = 33.6 \text{ ksi}$$

The factored resistance of a 5/16-inch fillet weld in shear in kips/inch is then computed as:

$$v = 33.6(0.707)(0.3125) = 7.42 \text{ kips/in.}$$

The factored shear rupture resistance of the connected material adjacent to the weld leg is computed as follows (Article 6.13.5.3) substituting the thickness of the connected material, t , for A_{vn} in the equation to express the factored resistance in units of kips/in.:

$$R_r = \phi_{\text{vu}} 0.58R_p F_u t \quad \text{Eq. (6.13.5.3-2)}$$

where: ϕ_{vu} = resistance factor for shear rupture of connection elements = 0.8 (Article 6.5.4.2)
 F_u = tensile strength of the connected element (ksi)
 R_p = reduction factor for punched holes taken equal to 1.0 for a welded connection

$$R_r = 0.80(0.58)(1.0)(65)(0.75) = 22.62 \text{ kips / in.}$$

The factored shear rupture resistance of the connected material does not control.

Therefore, the minimum length of weld required to resist the Strength I factored axial load is computed as:

$$\frac{|-88|}{7.42} = 11.9 \text{ in. use 7.0 in. longitudinal welds on each side of the angle}$$

Additional weld length is provided because equal-length welds on a single angle result in an unbalanced weld condition where the centroid of the weld group is offset from the centroid of the member, producing an eccentricity in the plane of the connection. In the case of single angles, the member itself is unsymmetrical and an eccentricity is created unless the weld group is balanced to align with the member centroid. Detailing excessively oversized or odd-shaped gusset plates solely to allow for the unequal length longitudinal welds necessary to achieve a balanced weld configuration in this case is generally impractical and is discouraged. Instead, consider evaluating the connection as an eccentrically loaded weld group, which causes additional shear loading of the welds [24]. This evaluation is not included in this design example.

It is generally preferable to weld the angle all around to the gusset plate to provide a seal against moisture. The sealing weld, wrapping the end of the angle should not be considered in determining

the resistance of the connection. The gusset plate must be sized appropriately to allow for the minimum required weld length to be provided.

The gusset plate should be of at least the same thickness as the angle, have at least the same equivalent net area, and have sufficient capacity to transfer resultant cross-frame forces to the girder. The design of the gusset plate is not covered in this design example. However, the gusset plate should be designed for shear, compression, tension, or a combination thereof, as applicable (refer to Articles 6.14.2.8.3 through 6.14.2.8.5 and Article 6.14.2.8.7, as applicable).

The gusset plate is bolted to the connection plate, which is welded to the girder web and flanges. The diagonal is attached near the bottom flange of G4. The bottom chord carries 40 kips out of the connection. The resultant force from the bottom chord and diagonal forces, and moment due to any eccentricity must be considered in the design of the bolt group connecting the gusset plate to the connection plate. Also, the welds between the connection plate and bottom flange must be able to transfer the resultant force. The design of the bolt group and the welded connection of the connection plate to the girder are not covered in this design example.

7.14 Shear Connector Design

Shear connectors are to be provided throughout the entire length of a curved continuous composite bridge according to the provisions of Article 6.10.10.1. To demonstrate the design of shear connectors, the required number of shear connectors will be determined for Girder 4 of Span 1. The following calculations illustrate the design for the strength and the fatigue limit states.

7.14.1 Shear Connector Design for Strength – Girder G4, Span 1

Compute the number of shear connectors required for the strength limit state in Span 1 according to the provisions of Article 6.10.10.4.

The factored shear resistance of a single connector, Q_r , at the strength limit state is taken as:

$$Q_r = \phi_{sc} Q_n \quad \text{Eq. (6.10.10.4.1-1)}$$

where: Q_n = nominal shear resistance of a single shear connector determined as specified in Article 6.10.10.4.3 (kips)

ϕ_{sc} = resistance factor for shear connectors = 0.85 (Article 6.5.4.2)

Shear connectors that are 6 in. long by 7/8 in. in diameter are selected for the design. Compute the nominal resistance of one shear connector embedded in the concrete deck according to the provisions of Article 6.10.10.4.3.

$$Q_n = 0.5A_{sc}\sqrt{f'_c E_c} \leq A_{sc}F_u \quad \text{Eq. (6.10.10.4.3-1)}$$

where: A_{sc} = cross-sectional area of a stud shear connector (in.²)

E_c = modulus of elasticity of the deck concrete = 3,834 ksi (calculated previously)

F_u = specified minimum tensile strength of a stud shear connector determined as

specified in Article 6.4.4 = 60 ksi

$$A_{sc} = \frac{\pi(0.875)^2}{4} = 0.60 \text{ in.}^2$$

$$Q_n = 0.5(0.60)\sqrt{(4)(3,834)} = 37.2 \text{ kips}$$

$$A_{sc}F_u = 0.60(60) = 36 \text{ kips (controls)}$$

Therefore, use $Q_n = 36$ kips.

Compute the nominal shear force, P , according to the provisions of Article 6.10.10.4.2. For the shear connector design, Span 1 is divided into two regions: 1) the portion between the end of the span and the location of maximum positive live load moment, and 2) the portion between the location of maximum positive live load moment and the adjacent interior support.

7.14.1.1 End of Span to Maximum Positive Live Load Moment Location

Between the end of Span 1 and the location of maximum positive live load plus impact moment, Eq. (6.10.10.4.2-1) is applicable. For this portion of Span 1, the total nominal shear force and required pitch are computed in the following calculations.

The total nominal shear force in this portion of the span is computed as follows:

$$P = \sqrt{P_p^2 + F_p^2} \quad \text{Eq. (6.10.10.4.2-1)}$$

where: P_p = total longitudinal force in the concrete deck at the point of maximum positive live load plus impact moment (kips) taken as the lesser of either:

$$P_{lp} = 0.85f'_c b_s t_s \quad \text{Eq. (6.10.10.4.2-2)}$$

or

$$P_{2p} = F_{yw}Dt_w + F_{yt}b_{ft}t_{ft} + F_{yc}b_{fc}t_{fc} \quad \text{Eq. (6.10.10.4.2-3)}$$

F_p = total radial force in the concrete deck at the point of maximum positive live load plus impact moment (kips) taken as:

$$F_p = P_p \frac{L_p}{R} \quad \text{Eq. (6.10.10.4.2-4)}$$

b_s = effective width of the concrete deck (in.)

- L_p = arc length between an end of the girder and an adjacent point of maximum positive live load plus impact moment (ft)
 R = minimum girder radius over the length, L_p (ft)

The effective width of the concrete deck, b_s , is calculated according to Article 4.6.2.6.1 for an exterior girder, and was calculated previously as 111 in. Conservatively, since G4 is an exterior girder with an overhang less than half of the girder spacing, the width of the deck could have been assumed to be equal to the interior girder effective width so that all girders would have the same stud spacing. That approach is not taken here.

$$P_{1p} = 0.85(4)(111)(9) = 3,397 \text{ kips}$$

$$P_{2p} = 50(84)(0.5625) + 50(21)(1.625) + 50(20)(1.0) = 5,069 \text{ kips}$$

The total longitudinal force in the deck, P_p , is the lesser of P_{1p} or P_{2p} ; therefore, P_p is taken to be 3,397 kips.

The arc length, L_p , between the end of the girder and the point of maximum positive live load plus impact moment is 73 feet. The total radial shear force in the concrete deck, F_p , at the point of maximum positive live load plus impact moment is computed as follows.

$$F_p = (3,397) \left(\frac{73}{716.5} \right) = 346.1 \text{ kips}$$

Therefore, the total nominal shear force in this portion of the span is:

$$P = \sqrt{3,397^2 + 346.1^2} = 3,415 \text{ kips}$$

The minimum number of shear connectors, n , over the region under consideration is taken as:

$$n = \frac{P}{Q_r} = \frac{P}{\phi_{sc} Q_n} \quad \text{Eq. (6.10.10.4.1-2)}$$

$$n = \frac{3,415}{0.85(36)} = 112$$

Compute the required pitch, p , with 3 studs per row.

$$\text{No. of rows} = \frac{112}{3} = 37.3, \text{ say } 38 \text{ rows}$$

$$p = \frac{73(12)}{(38-1)} = 23.7 \text{ in.}$$

The shear connector pitch for strength is less critical than for fatigue in this region, which is demonstrated later in this example.

7.14.1.2 Maximum Positive Live Load Moment Location to Adjacent Interior Support

Between the location of maximum positive live load plus impact moment and the adjacent interior support, Eq. (6.10.10.4.2-5) is applicable. For this portion of Span 1, the total nominal shear force and required pitch are computed in the following calculations.

The total nominal shear force in this portion of the span is computed as follows:

$$P = \sqrt{P_T^2 + F_T^2} \quad \text{Eq. (6.10.10.4.2-5)}$$

where: P_T = total longitudinal force in the concrete deck between the point of maximum positive live load plus impact moment and the centerline of an adjacent interior support (kips) taken as:

$$P_T = P_p + P_n \quad \text{Eq. (6.10.10.4.2-6)}$$

P_n = total longitudinal force in the concrete deck over an interior support (kips) taken as the lesser of either:

$$P_{1n} = F_{yw} D t_w + F_{yt} b_{ft} t_{ft} + F_{yc} b_{fc} t_{fc} \quad \text{Eq. (6.10.10.4.2-7)}$$

or

$$P_{2n} = 0.45 f'_c b_s t_s \quad \text{Eq. (6.10.10.4.2-8)}$$

F_T = total radial force in the concrete deck between the point of maximum positive live load plus impact moment and the centerline of an adjacent interior support (kips) taken as:

$$F_T = P_T \frac{L_n}{R} \quad \text{Eq. (6.10.10.4.2-9)}$$

L_n = arc length between the point of maximum positive live load plus impact moment and the centerline of an adjacent interior support (ft)

R = minimum girder radius over the length, L_n (ft)

The following two terms were computed previously and are applicable here as well:

$$P_p = 3,397 \text{ kips}$$

$$b_s = 111 \text{ in.}$$

Using the plate girder dimensions at Support 2 (Field Section 2), compute P_{1n} as follows:

$$P_{1n} = 50(84)(0.625) + 50(28)(2.5) + 50(27)(3) = 10,175 \text{ kips}$$

$$P_{2n} = 0.45(4)(111)(9) = 1,798 \text{ kips}$$

The total longitudinal force in the deck over the interior support, P_n , is the lesser of P_{1n} or P_{2n} ; therefore, P_n is taken to be 1,798 kips.

Therefore, the total longitudinal force in the concrete deck in the region under consideration is:

$$P_T = 3,397 + 1,798 = 5,195 \text{ kips}$$

Next, compute the arc length, L_n , and the total radial force in the concrete deck, F_T , in the region under consideration. The total arc length along girder G4 in Span 1 is 163.8 ft.

$$L_n = 163.8 - 73 = 90.8 \text{ ft}$$

$$F_T = 5,195 \left(\frac{90.8}{716.5} \right) = 658 \text{ kips}$$

The total nominal shear force in this portion of the span is:

$$P = \sqrt{5,195^2 + 658^2} = 5,237 \text{ kips}$$

The minimum number of shear connectors, n , over the region under consideration is taken as:

$$n = \frac{P}{Q_r} = \frac{P}{\phi_{sc} Q_n} \quad \text{Eq. (6.10.10.4.1-2)}$$

$$n = \frac{5,237}{0.85(36)} = 171.1, \text{ say } 172$$

Compute the required pitch, p , with 3 studs per row.

$$\text{No. of rows} = \frac{172}{3} = 57.3, \text{ say } 58 \text{ rows}$$

$$p = \frac{90.8(12)}{(58-1)} = 19.1 \text{ in.}$$

The shear connector pitch for strength is less critical than for fatigue in this region, which is demonstrated later in this example.

7.14.2 Shear Connector Design for Fatigue – Girder G4, Span 1

To demonstrate the fatigue requirements for shear connectors, fatigue will be checked at the maximum positive moment location and at the first interior support (Support 2).

7.14.2.1 Maximum Positive Moment Location

Determine the required pitch of the shear connectors for fatigue at this section according to the provisions of Article 6.10.10.1.2. The pitch, p , of shear connectors must satisfy the following:

$$p \leq \frac{nZ_r}{V_{sr}} \quad \text{Eq. (6.10.10.1.2-1)}$$

where: n = number of shear connectors in a cross-section

Z_r = shear fatigue resistance of an individual shear connector determined as specified in Article 6.10.10.2 (kips)

V_{sr} = horizontal fatigue shear range per unit length (kips/in.)

The projected 75-year single lane Average Daily Truck Traffic (ADTT)_{SL} is assumed to be 1,000 trucks per day. Where the projected 75-year (ADTT)_{SL} is less than 1,090 trucks per day, the fatigue resistance for an individual stud shear connector, Z_r , for finite life is defined in Article 6.10.10.2 as follows:

$$Z_r = \alpha d^2 \quad \text{Eq. (6.10.10.2-2)}$$

where: $\alpha = 34.5 - 4.28 \log N$ Eq. (6.10.10.2-3)

N = number of cycles = $365(75)n(\text{ADTT})_{\text{SL}}$

d = diameter of the stud (in.)

The Fatigue II load combination is to be used for this case according to Article 6.10.10.2. As stated earlier, shear connectors that are 6 in. long by 7/8 in. in diameter are selected for design, with 3 studs per row. The fatigue resistance of one shear connector is computed as follows:

$$N = 365(75)(1.0)(1,000) = 27.38 \times 10^6 \text{ cycles}$$

$$\alpha = 34.5 - 4.28 \log(27.38 \times 10^6) = 2.67$$

$$Z_r = 2.67(0.875)^2 = 2.04 \text{ kips}$$

The fatigue resistance for 3 shear connectors is:

$$nZ_r = 3(2.04) = 6.12 \text{ kips / row}$$

From Table 10, the unfactored shear force range at this location due to one fatigue truck is:

$$20 + |-20| = 40 \text{ kips}$$

The Fatigue I factored shear force range is:

$$V_f = 0.80(40) = 32 \text{ kips}$$

According to the provisions of Article 6.6.1.2.1, the live load stress range may be calculated using the short-term composite section assuming the concrete deck to be effective for both positive and negative flexure. The structural deck thickness, t_s , is 9.0 inches; the modular ratio, n , equals 7.56; and the effective flange width is 111 inches (calculated previously).

To compute the longitudinal shear range, first compute the transformed deck area as follows:

$$\text{Transformed deck area} = \frac{\text{Area}}{n} = \frac{(111)(9)}{7.56} = 132.1 \text{ in.}^2$$

Compute the first moment of the transformed short-term area of the concrete deck, Q , with respect to the neutral axis of the uncracked live load short-term composite section. Determine the distance from the center of the deck to the neutral axis. Section properties are taken from Table 13. The neutral axis of the short-term composite section is 17.04 in. measured from the top of the top flange.

$$\text{Moment arm of the deck} = \text{Neutral axis} - t_{flg} + haunch + t_s/2$$

$$\text{Moment arm of the deck} = 17.04 - 1.0 + 4.0 + \frac{9.0}{2} = 24.54 \text{ in.}$$

$$Q = 132.1(24.54) = 3,242 \text{ in.}^3$$

Compute the factored longitudinal fatigue shear range per unit length, V_{fat} :

$$V_{fat} = \frac{V_f Q}{I} = \frac{32(3,242)}{306,979} = 0.34 \text{ kips / in.}$$

It is also necessary to compute F_{fat} , the radial fatigue shear range per unit length. Article 6.10.10.1.2 directs the designer to compute F_{fat} by taking the larger of two computed values from Eqs.

(6.10.10.1.2-4) and (6.10.10.1.2-5). The first equation is an approximation based on the stress in the flange and the radius of curvature. The second equation is a more exact calculation based on the actual cross-frame force from the analysis. As explained in Article C6.10.10.1.2, the first equation typically governs unless torsion is caused by effects other than curvature, such as skew. In this example, the two equations are expected to yield similar results since all the torsion is due to curvature. As permitted in Article 6.10.10.1.2, for straight or horizontally curved bridges with skew not exceeding 20 degrees, the radial fatigue shear range from Eq. (6.10.10.1.2-5) may be taken equal to zero. Therefore, in this case, $F_{fat2} = 0$ and $F_{fat} = F_{fat1}$.

$$F_{fat1} = \frac{A_{bot} \sigma_{flg} \ell}{wR} \quad \text{Eq. (6.10.10.1.2-4)}$$

where: σ_{flg} = range of longitudinal fatigue stress in the bottom flange without consideration of flange lateral bending (ksi)
 ℓ = distance between brace points (ft)
 w = effective length of deck (in.) taken as 48.0 in.

The stress range σ_{flg} is based on the range of fatigue moment taken from Table 9:

$$\text{Unfactored fatigue moment range} = |-603| + 1,603 = 2,206 \text{ kip} \cdot \text{ft}$$

The section properties are again taken from Table 13. Using the load factor of 0.80 for Fatigue II, the range of longitudinal fatigue stress in the bottom flange is computed as follows:

$$\sigma_{flg} = (0.80) \left(\frac{2,206}{4,412} \right) (12) = 4.80 \text{ ksi}$$

$$A_{bot} = (21)(1.625) = 34.1 \text{ in.}^2$$

$$F_{fat1} = \frac{34.1(4.80)(20.47)}{48(716.5)} = 0.10 \text{ kips / in.}$$

$$F_{fat} = F_{fat1} = 0.10 \text{ kips/in. (factored)}$$

The positive and negative longitudinal shears due to major-axis bending are due to the fatigue vehicle located in Span 1 with the back axle on the left and then on the right of the point under consideration. This means that the truck actually has to turn around to produce the computed longitudinal shear range. The positive and negative radial shear ranges are produced by loading first in Span 1 and then in Span 2. Again, this is not a realistic loading case to combine with the longitudinal shear case but has been done to be practical and to be conservative. Combining the longitudinal and radial fatigue shear ranges vectorially, the total horizontal fatigue shear range per unit length is computed as follows:

$$V_{sr} = \sqrt{(V_{fat})^2 + (F_{fat})^2} \quad \text{Eq. (6.10.10.1.2-2)}$$

$$V_{sr} = \sqrt{(0.34)^2 + (0.10)^2} = 0.35 \text{ kips / in.}$$

Compute the required shear connector pitch for fatigue for 3 studs per row.

$$p \leq \frac{nZ_r}{V_{sr}} \quad \text{Eq. (6.10.10.1.2-1)}$$

$$p \leq \frac{6.12}{0.35} = 17.5 \text{ in./row}$$

As shown earlier, the number of shear connectors was also checked for the strength limit state according to the provisions of Article 6.10.10.4. The required pitch for fatigue, 17.5 in./row, governs.

7.14.2.2 Interior Support Location (Support 2)

Using the same procedure illustrated at the maximum positive moment location, fatigue requirements for shear connectors are investigated at the first interior support (Support 2).

Determine the required pitch of the shear connectors for fatigue at this section according to the provisions of Article 6.10.10.1.2. As before, the pitch, p , of shear connectors must satisfy the following:

$$p \leq \frac{nZ_r}{V_{sr}} \quad \text{Eq. (6.10.10.1.2-1)}$$

For continuous spans, the number of stress cycles per truck passage, n , is equal to 1.5 at sections near the interior pier and 1.0 elsewhere (Table 6.6.1.2.5-2). Sections ‘near the interior pier’ are defined as sections within a distance of one-tenth of the span on each side of the interior support. As indicated in Article C6.6.1.2.3, for values of n other than 1.0, the values of the 75-year $(ADTT)_{SL}$ Equivalent to Infinite Life given in Table 6.6.1.2.3-2 are to be modified by dividing by the appropriate value of n taken from Table 6.6.1.2.5-2.

The projected 75-year single lane Average Daily Truck Traffic $(ADTT)_{SL}$ is assumed to be 1,000 trucks per day. Where the projected 75-year $(ADTT)_{SL}$ is greater than $1,090/1.5 = 727$ trucks per day, adjusted for $n = 1.5$, the fatigue resistance for an individual stud shear connector, Z_r , for infinite life is defined in Article 6.10.10.2 as follows:

$$Z_r = 5.5d^2 \quad \text{Eq. (6.10.10.2-1)}$$

where: d = diameter of the stud (in.)

The Fatigue I load combination is to be used for this case according to Article 6.10.10.2. As stated earlier, shear connectors that are 6 in. long by 7/8 in. in diameter are selected for design, with 3 studs per row. The fatigue resistance of one shear connector is computed as follows:

$$Z_r = 5.5(0.875)^2 = 4.21 \text{ kips}$$

The fatigue resistance for 3 shear connectors is:

$$nZ_r = 3(4.21) = 12.63 \text{ kips/row}$$

From Table 10 at Section G4-2, the unfactored shear force range at this location due to one fatigue truck is:

$$3 + |-55| = 58 \text{ kips}$$

The Fatigue I factored shear force range is:

$$V_f = 1.75(58) = 101.5 \text{ kips}$$

According to the provisions of Article 6.6.1.2.1, the live load stress range may be calculated using the short-term composite section assuming the concrete deck to be effective for both positive and negative flexure. The structural deck thickness, t_s , is 9.0 inches; the modular ratio, n , equals 7.56; and the effective flange width is 111 inches (calculated previously).

Compute the first moment of the transformed short-term area of the concrete deck, Q , with respect to the neutral axis of the uncracked live load short-term composite section. Determine the distance from the center of the deck to the neutral axis. Section properties are taken from Table 16. The neutral axis of the short-term composite section is 26.10 in. measured from the top of the top flange.

$$\text{Moment arm of the deck} = \text{Neutral axis} - t_{flg} + \text{haunch} + t_s/2$$

$$\text{Moment arm of the deck} = 26.10 - 2.5 + 4 + \frac{9}{2} = 32.10 \text{ in.}$$

$$\text{Transformed deck area} = 132.1 \text{ in.}^2 \text{ (computed previously)}$$

$$Q = 132.1(32.10) = 4,240 \text{ in.}^3$$

Compute the factored longitudinal fatigue shear range per unit length, V_{fat} :

$$V_{fat} = \frac{V_f Q}{I} = \frac{101.5(4,240)}{539,403} = 0.80 \text{ kips / in.}$$

Compute the radial shear range, F_{fat} , based on Eq. (6.10.10.1.2-4). As explained previously, per Article 6.10.10.1.2 the radial fatigue shear range from Eq. (6.10.10.1.2-5) may be taken equal to zero in this case. Therefore, in this case, $F_{fat2} = 0$ and $F_{fat} = F_{fat1}$.

$$F_{fat1} = \frac{A_{bot} \sigma_{flg} \ell}{wR} \quad \text{Eq. (6.10.10.1.2-4)}$$

The stress range σ_{flg} is based on the range of fatigue moment taken from Table 9:

$$\text{Unfactored fatigue moment range} = |-1,315| + 351 = 1,666 \text{ kip - ft}$$

The section properties are again taken from Table 16. Using the load factor of 1.75 for Fatigue I, the range of longitudinal fatigue stress in the bottom flange is computed as follows:

$$\sigma_{flg} = (1.75) \left(\frac{1,666}{8,508} \right) (12) = 4.11 \text{ ksi}$$

$$A_{bot} = (27)(3.0) = 81.0 \text{ in.}^2$$

$$F_{fat1} = \frac{81.0(4.11)(20.47)}{48(716.5)} = 0.20 \text{ kips / in.}$$

$$F_{fat} = F_{fat1} = 0.20 \text{ kips/in. (factored)}$$

Combining the longitudinal and radial fatigue shear ranges vectorially, the total horizontal fatigue shear range per unit length is computed as follows:

$$V_{sr} = \sqrt{(V_{fat})^2 + (F_{fat})^2} \quad \text{Eq. (6.10.10.1.2-2)}$$

$$V_{sr} = \sqrt{(0.80)^2 + (0.20)^2} = 0.82 \text{ kips / in.}$$

Compute the required shear connector pitch for fatigue for 3 studs per row.

$$p \leq \frac{nZ_r}{V_{sr}} \quad \text{Eq. (6.10.10.1.2-1)}$$

$$p \leq \frac{12.63}{0.82} = 15.4 \text{ in. / row}$$

As shown earlier, the number of shear connectors was also checked for the strength limit state according to the provisions of Article 6.10.10.4. The required pitch for fatigue, 15.4 in./row, governs.

7.15 Bearing Stiffener Design

Bearing stiffeners are designed as columns to resist the reactions at bearing locations. According to Article 6.10.11.2.1, bearing stiffeners must be placed on the webs of built-up sections at all bearing locations. At bearing locations on rolled shapes and at other locations on built-up sections or rolled shapes subjected to concentrated loads, where the loads are not transmitted through a deck or deck system, either bearing stiffeners must be provided or else the web must be investigated for the limit states of web crippling or web local yielding according to the provisions of Article D6.5 (Appendix D6). It should be noted that the provisions of Article D6.5 should be checked whenever girders are incrementally launched over supports.

Bearing stiffeners must extend the full depth of the web and as closely as practical to the outer edges of the flanges. Each stiffener is to be either finished-to-bear against the flange through which it receives its load (i.e., the bottom flange at supports) and attached with fillet welds (which is required if the stiffener also serves as a connection plate) or attached to that flange by a full penetration groove weld. The Guidelines recommend using finish-to-bear plus fillet welds to connect the bearing stiffeners to the appropriate flange, allowing the option to use fillet welds even if not required for the connection. For connection to the top flange, finish-to-bear is not necessary, and fillet welding of the stiffener to the top flange is only necessary if the stiffener also serves as a connection plate. Full penetration groove welds are costly and often result in welding deformation of the flange.

The design of bearing stiffeners at Support 1 for Girder G4 is illustrated in this example. Grade 50 ($F_{ys} = 50$ ksi) steel is selected for the bearing stiffeners. The design of the bearing stiffener-to-web welds is not illustrated in this example; refer to Section 10.6.1.4 of NSBA's *Steel Bridge Handbook Design: Example 1: Three-Span Continuous Straight Composite Steel I-Girder Bridge* [6] for an illustration of these calculations.

Girder G4 has the largest total reaction at the simple end support (Support 1). Unfactored reactions are shown below. These results are directly from the three-dimensional analysis as presented in Table 10.

Steel Dead Load:	$R_{DC1-STEEL}$	= 23 kips
Concrete Deck Dead Load:	$R_{DC1-CONC}$	= 92 kips
Composite Dead Load:	R_{DC2}	= 23 kips
Future Wearing Surface Dead Load:	R_{DW}	= 19 kips
Live Load (including IM + CF):	R_{LL+IM}	= 143 kips

The Strength I factored reaction is computed as:

$$R_u = 1.25(23 + 92 + 23) + 1.50(19) + 1.75(143) = 451 \text{ kips}$$

7.15.1 Minimum Thickness

The thickness, t_p , of each projecting stiffener element must satisfy:

$$t_p \geq \frac{b_t}{0.48 \sqrt{\frac{E}{F_{ys}}}} \quad \text{Eq. (6.10.11.2.2-1)}$$

Try two 7.0-inch-wide bars welded to each side of the web.

$$(t_p)_{\min.} = \frac{7.0}{0.48 \sqrt{\frac{29,000}{50.0}}} = 0.61 \text{ in.}$$

Try two 7.0-inch wide by 0.75-inch thick stiffeners, one stiffener on each side of the web.

7.15.2 Bearing Resistance

According to Article 6.10.11.2.3, the factored bearing resistance for the fitted ends of bearing stiffeners is taken as:

$$(R_{sb})_r = \phi_b (R_{sb})_n \quad \text{Eq. (6.10.11.2.3-1)}$$

where: $(R_{sb})_n$ = nominal bearing resistance for the fitted ends of the bearing stiffeners (kips)

$$(R_{sb})_n = 1.4 A_{pn} F_{ys} \quad \text{Eq. (6.10.11.2.3-2)}$$

ϕ_b = resistance factor for bearing = 1.0 (Article 6.5.4.2)

A_{pn} = area of the projecting elements of the stiffener outside of the web-to-flange fillet welds but not beyond the edge of the flange (in.^2)

F_{ys} = specified minimum yield strength of the stiffener (ksi)

$$A_{pn} = 2(7-1)(0.75) = 9.0 \text{ in.}^2 \quad (\text{Assume 1 in. for the stiffener clip.})$$

The nominal bearing resistance is:

$$(R_{sb})_n = 1.4(9)(50) = 630 \text{ kips}$$

The factored bearing resistance is:

$$(R_{sb})_r = 1.0(630) = 630 \text{ kips} > R_u = 451 \text{ kips} \quad \text{OK}$$

7.15.3 Axial Resistance

Determine the axial resistance of the bearing stiffener according to Article 6.10.11.2.4. This article directs the Engineer to Article 6.9.2.1 for calculation of the factored axial resistance, P_r . The yield strength is F_{ys} , the radius of gyration is computed about the midthickness of the web, and the effective length is 0.75 times the web depth ($K\ell = 0.75D$).

$$P_r = \phi_c P_n \quad \text{Eq. (6.9.2.1-1)}$$

where: P_n = nominal compressive resistance determined using the provisions of Article 6.9.4

ϕ_c = resistance factor for compression = 0.95 (Article 6.5.4.2)

As indicated in Article C6.9.4.1.1, only the limit state of flexural buckling is applicable for bearing stiffeners. Based on the above width-to-thickness ratio limit, bearing stiffeners are also composed only of nonslender elements; therefore, local buckling effects on the overall compressive resistance of the stiffeners need not be considered.

To compute P_n , first compute P_e and P_o . P_e is the elastic critical buckling resistance determined as specified in Article 6.9.4.1.2 for flexural buckling. P_o is the nominal yield resistance equal to $F_y A_g$

$$P_e = \frac{\pi^2 E}{\left(\frac{K\ell}{r_s}\right)^2} A_g \quad \text{Eq. (6.9.4.1.2-1)}$$

Compute the effective length of the bearing stiffener according to Article 6.10.11.2.4.

$$K\ell = 0.75(84) = 63 \text{ in.}$$

Compute the radius of gyration about the midthickness of the web.

$$r_s = \sqrt{\frac{I_s}{A_s}}$$

According to the provisions of Article 6.10.11.2.4b, for stiffeners welded to the web, a portion of the web is to be included as part of the effective column section. For stiffeners consisting of two plates welded to the web, the effective column section is to consist of the two stiffener elements, plus a centrally located strip of web extending $9t_w$ on each side of the outer projecting elements of the group. The area of the web that is part of the effective section is computed as follows:

$$A_w = 2(9)(0.5625)(0.5625) = 5.7 \text{ in.}^2$$

Use the full area of the stiffeners to compute the axial resistance.

$$A = 2(7)(0.75) = 10.5 \text{ in.}^2$$

The total area of the effective section is therefore:

$$A_s = 5.7 + 10.5 = 16.2 \text{ in.}^2$$

Next, compute the moment of inertia of the effective section, conservatively neglecting the web strip:

$$I = \frac{0.75(7.0 + 0.5625 + 7.0)^3}{12} = 193 \text{ in.}^4$$

Compute the radius of gyration:

$$r_s = \sqrt{\frac{193}{16.2}} = 3.45 \text{ in.}$$

The elastic critical buckling resistance is computed as follows:

$$P_e = \frac{\pi^2(29,000)}{\left(\frac{63}{3.45}\right)^2}(16.2) = 13,905 \text{ kips}$$

The nominal yield resistance is computed as follows, with A_s used for A_g :

$$P_o = F_y A_g = (50)(16.2) = 810 \text{ kips}$$

Since,

$$\frac{P_o}{P_e} = \frac{810}{13,905} = 0.06 < 2.25,$$

the nominal axial compression resistance is computed as:

$$P_n = \left[0.658^{\left(\frac{P_o}{P_e}\right)} \right] P_o \tag{Eq. (6.9.4.1.1-1)}$$

$$P_n = \left[0.658^{\frac{1}{17.2}} \right] (810) = 790 \text{ kips}$$

The factored resistance of the bearing stiffeners is computed as follows:

$$P_r = \phi_c P_n = 0.95(790) = 750 \text{ kips}$$

$$P_u = 451 \text{ kips} < P_r = 750 \text{ kips OK}$$

The bearing stiffeners selected for Girder G4 at Support 1 satisfy the requirements for design.

8.0 SUMMARY OF DESIGN CHECKS AND PERFORMANCE RATIOS

The results for this design example at each limit state are summarized below for the maximum positive moment and maximum negative moment locations and the end support in Span 1. The results for each limit state are expressed in terms of a performance ratio, defined as the ratio of a calculated value to the corresponding resistance.

8.1 Maximum Positive Moment Region, Span 1 (Section G4-1)

Constructability

Flexure (STRENGTH I)

Eq. (6.10.3.2.1-1) – Top Flange, yielding	0.861
Eq. (6.10.3.2.1-2) – Top Flange, local buckling	0.724
Eq. (6.10.3.2.1-2) - Top Flange, lateral torsional buckling	0.796
Eq. (6.10.3.2.1-3) – Top Flange, web bend buckling	0.957
Eq. (6.10.3.2.2-1) – Bottom Flange, yielding	0.587

Service Limit State

Permanent Deformations (SERVICE II)

Eq. (6.10.4.2.2-1) – Top Flange	0.471
Eq. (6.10.4.2.2-2) – Bottom Flange	0.790

Fatigue Limit State

Flexure (FATIGUE I)

Eq. (6.6.1.2.2-1) – Bottom Flange	0.990
Special Fatigue Requirement for Webs – Eq. (6.10.5.3-1)	0.124

Strength Limit State

Ductility Requirement – Eq. (6.10.7.3-1)	0.310
Flexure (STRENGTH I)	
Eq. (6.10.7.2.1-1) – Top Flange	0.572
Eq. (6.10.7.2.1-2) – Bottom Flange	0.953
Eq. (6.10.1.6-1) – Bottom Flange	0.342

8.2 Interior Support, Maximum Negative Moment (Section G4-2)

Constructability

Flexure (STRENGTH I)

Eq. (6.10.3.2.2-1) – Top Flange, yielding	0.536
Eq. (6.10.3.2.1-1) – Bottom Flange, yielding	0.486
Eq. (6.10.3.2.1-2) – Bottom Flange, local buckling	0.441
Eq. (6.10.3.2.1-2) – Bottom Flange, lat. torsional buckling	0.460

Service Limit State (SERVICE II)

Web Bend-Buckling - Eq. (6.10.4.2.2-4)	0.675
--	-------

Fatigue Limit State	
Flexure (FATIGUE I)	
Eq. (6.6.1.2.2-1) – Top Flange	0.128
Special Fatigue Requirement for Webs – Eq. (6.10.5.3-1)	0.446

Strength Limit State	
Flexure (STRENGTH I)	
Eq. (6.10.8.1.1-1) – Bottom Flange, local buckling	0.926
Eq. (6.10.8.1.1-1) – Bottom Flange, lat. torsional buckling	0.965
Eq. (6.10.8.1.3-1) – Top Flange, yielding	0.950
Shear (STRENGTH I) – Eq. (6.10.9.1-1)	0.484

8.3 End Support (Section G4-3)

Strength Limit State (STRENGTH I)	
Shear – Eq. (6.10.9.1-1)	0.791

9.0 REFERENCES

1. AASHTO. *AASHTO LRFD Bridge Design Specifications*, 9th Edition, American Association of State Highway and Transportation Officials, Washington, DC, 2020.
2. Kulicki, J., Wassef, W., Smith, C, and Johns, K. “AASHTO-LRFD Design Example: Horizontally Curved Steel I-Girder Bridge, Final Report,” National Cooperative Highway Research Project 12-52, Transportation Research Board, Washington, DC, 2005.
3. AASHTO/NSBA. *G1.4: Guidelines for Design Details*, 1st Edition, NSBAGDD-1-OL, American Association of State Highway and Transportation Officials, Washington, DC, 2006.
4. Texas Department of Transportation (TxDOT). *Preferred Practices for Steel Bridge Design, Fabrication, and Erection*, Texas Steel Quality Council, 2009.
5. AASHTO/NSBA. *G12.1: Guidelines to Design for Constructability and Fabrication*, 4th Edition, NSBAGDC-4-OL, American Association of State Highway and Transportation Officials, Washington, DC, 2020.
6. NSBA. *Steel Bridge Design Handbook: Design Example 1: Three-Span Continuous Straight Composite Steel I-Girder Bridge*. National Steel Bridge Alliance, 2022.
7. NSBA. *Steel Bridge Design Handbook: Design Example 2A: Two-Span Continuous Straight Composite Steel I-Girder Bridge*. National Steel Bridge Alliance, 2022.
8. NSBA. *Steel Bridge Design Handbook: Structural Analysis*. National Steel Bridge Alliance, 2022.
9. FHWA. *Manual for Refined Analysis in Bridge Design and Evaluation*. Federal Highway Administration, Washington, DC, 2019.
10. NSBA. *Steel Bridge Design Handbook: Bracing System Design*. National Steel Bridge Alliance, 2022.
11. NCHRP. *National Cooperative Highway Research Project Report 962: Proposed Modification to AASHTO Cross-Frame Analysis and Design*, National Cooperative Highway Research Program, Transportation Research Board, Washington, DC, 2021.
12. NHI. *Analysis and Design of Skewed and Curved Steel Bridges with LRFD. Reference Manual for NHI Course No. 130095*. FHWA-NHI-10-087. National Highway Institute, Federal Highway Administration, U.S. Department of Transportation, Washington, DC, 2011.
13. AASHTO. *Guide Specifications for Wind Loads on Bridges During Construction*. American Association of State Highway and Transportation Officials, Washington, DC, 2017

14. NSBA. *Skewed and Curved Steel I-Girder Bridge Fit*. NSBA Technical Subcommittee Fit Task Force, Stand-Alone Summary, National Steel Bridge Alliance, Chicago, IL, 2016.
15. NSBA. *Skewed and Curved Steel I-Girder Bridge Fit*. NSBA Technical Subcommittee Fit Task Force, Guide Document, National Steel Bridge Alliance, Chicago, IL, 2016.
16. White, D. W., Nguyen T. V., Coletti, D. A., Chavel, B. W., Grubb, M. A., and Boring, C. G. “Guidelines for Reliable Fit-Up of Steel I-Girder Bridges”. NCHRP 20-07/Task 355, National Cooperative Highway Research Program, Transportation Research Board, Washington, DC, 2015.
17. AASHTO/NSBA. *S10.1: Steel Bridge Erection Guide Specification*, NSBASBEGS-3, American Association of State Highway and Transportation Officials, Washington, DC, 2019.
18. NHI. Engineering for Structural Stability in Bridge Construction. *Reference Manual for NHI Course No. 130102*. FHWA-NHI-15-044. National Highway Institute, Federal Highway Administration, U.S. Department of Transportation, Washington, DC, 2015.
19. NSBA. (2021). *Bolted Field Splices for Steel Bridge Flexural Members – Overview and Design Examples*, National Steel Bridge Alliance, Chicago, IL, 2021.
20. NSBA. *Steel Bridge Design Handbook: Splice Design*. National Steel Bridge Alliance, 2022.
21. RCSC. *Specification for Structural Joints Using High-strength Bolts*. Research Council on Structural Connections, Chicago, IL, 2020.
22. ASME. *Fasteners for Use in Structural Applications*, ASME B18.2.6. American Society of Mechanical Engineers, New York, NY, 2019.
23. AISC. *Steel Construction Manual*, 15th Edition, American Institute of Steel Construction, Chicago, IL, 2017.
24. Salmon, C. G., Johnson, J. E., and Malhas, F. A. *Steel Structures: Design and Behavior*, Fifth Edition. Pearson Prentice Hall, Upper Saddle River, NJ, 2009.



Smarter. Stronger. Steel.

National Steel Bridge Alliance
312.670.2400 | aisc.org/nsba